U.PORTO

FEUP FACULDADE DE ENGENHARIA
UNIVERSIDADE DO PORTO

STEEL COLUMN BASES UNDER BIAXIAL LOADING CONDITIONS

PATRÍCIA MEDEIROS AMARAL

A Dissertation submitted in partial fulfillment of the requirements for the degree of

MASTER IN CIVIL ENGINEERING — SPECIALIZATION IN STRUCTURAL ENGINEERING

Supervisor: Prof. José Miguel de Freitas Castro

Co-supervisors: Ing. Zdeněk Sokol and Prof. Ing. František Wald

JULY 2014

INTEGRATED MASTER IN CIVIL ENGINEERING 2013/2014

DEPARTMENT OF CIVIL ENGINEERING

Tel. +351-22-508 1901

Fax +351-22-508 1446

✉ miec@fe.up.pt

Edited by

FACULTY OF ENGINEERING OF THE UNIVERSITY OF PORTO

Rua Dr. Roberto Frias

4200-465 PORTO

Portugal

Tel. +351-22-508 1400

Fax +351-22-508 1440

✉ feup@fe.up.pt

http://www.fe.up.pt

Partial reproductions of this document are allowed on the condition that the Author is mentioned and that the reference is made to Integrated *Masters in Civil Engineering – 2013/2014 – Department of Civil Engineering, Faculty of Engineering of the University of Porto, Porto, Portugal, 2014*.

The opinions and information included in this document represent solely the point of view of the respective Author, while the Editor cannot accept any legal responsibility or other with respect to errors or omissions that may exist.

This document was produced from an electronic version supplied by the respective Author.

To my family

The only limit to our realization of tomorrow will be our doubts of today.

Franklin D. Roosevelt

ACKNOWLEDGMENTS

I want to thank Dr. Miguel Castro that, not only, accepted to be my tutor immediately but also helped me to take care of everything so that I could go abroad. Indeed, he always helped me to find the best solution and kept me interested in going further.

I would like also to thank Prof. František Wald who allowed doing my dissertation at the Czech Technical University in Prague. Without him this amazing opportunity would not be possible and, for that, I will never forget him. Moreover, he provided me many resources that allowed me to understand the topic and to put everything together.

A special thanks belongs to Ing. Zdeněk Sokol that was always available to help me. He transmitted the knowledge I needed to fully understand the subject and took care of me the whole time I was in Prague.

I am much grateful for the support that Nuno and António gave me with ABAQUS. Without them I would not be able to finish my model.

Thanks to Lukas, who I shared my desk the time that I was working in Prague and always tried to help me even when he didn't know how.

I am also thankful to Norberto, the one who was always there for me, especially in the worst times.

To my family who supported me the whole time I was studying and always made an effort so I would have everything that I merited. They are one big part of my life and I want to thank them, not just for my studies, but for everything. Without them I would not be who I am and would never get to where I am.

To all the friends that crossed my way during my journey at the university, they made these five years become unforgettable.

ABSTRACT

The main goal of this work is the development of a procedure that would allow obtaining the moment capacity of a column base under combined biaxial bending and axial force.

The component method prescribed in EN 1993-1-8 for the design of column base connections is firstly described. The method allows the calculation of moment capacity and initial stiffness of the joint under combined axial force and bending about the major axis.

A numerical model is developed in ABAQUS and validated with data obtained from experiments carried out at Brno University of Technology. The tests included strong axis bending and biaxial bending of a simple column base. Then, the column base model is subjected to bending about the strong axis, with a proportional loading, and the obtained results (moment capacity and initial stiffness) are compared with the component method results.

Afterwards, an analytical model for the design of column bases subjected to weak axis bending is introduced. A moment-moment interaction curve is proposed that allows obtaining the resistance of column bases under out-of-plane bending.

The procedure for obtaining the resistance and stiffness of the column base subjected to weak axis bending is achieved by modifying the existing component method so that it is suitable for this type of loading. The interaction curve is created based on the resistances for bending about the main axes. The validity of the proposed model is checked against the results obtained from nonlinear analysis performed in ABAQUS.

KEYWORDS: steel structures, column bases, component method, weak axis bending, biaxial bending.

RESUMO

O objetivo principal deste trabalho é o desenvolvimento de um procedimento que permite a obtenção do momento resistente da base de um pilar metálico quando sujeita a flexão desviada composta.

Em primeiro lugar, o método das componentes proposto na norma EN 1993-1-8 para o dimensionamento bases de pilares é descrito. O método permite o cálculo do momento resistente e da rigidez inicial da ligação carregada segundo o eixo principal de maior rigidez (i.e., força axial e flexão segundo o eixo forte). Este analisa os componentes principais separadamente e, em seguida, procede à assemblagem das suas características para obter o comportamento da ligação.

Apresenta-se o desenvolvimento de um modelo numérico no programa ABAQUS, o qual é validado com resultados obtidos através de ensaios experimentais realizados na *Brno University of Technology*. Os ensaios incluíram flexão segundo o eixo principal e flexão desviada de uma base de pilar simples. Posteriormente, a base do pilar deste modelo é sujeita a flexão segundo o eixo forte e os resultados obtidos (momento resistente e rigidez inicial) são comparados com os resultados do método das componentes.

De seguida desenvolve-se um modelo analítico para o dimensionamento de bases de pilares sujeitas a flexão segundo o eixo fraco. Propõem-se também uma curva de interação que permite obter a resistência da ligação quando sujeita a flexão desviada.

O modelo analítico baseia-se na modificação do método das componentes proposto na norma EN1993-1-8, de modo a ser adequado para este tipo de carregamento. A curva de interação é criada com base nos momentos resistentes da flexão segundo os eixos principais. O modelo é validado com resultados obtidos de análises não lineares efetuadas no programa ABAQUS.

PALAVRAS-CHAVE: estruturas metálicas, bases de pilares, método das componentes, flexão segundo o eixo fraco, flexão desviada.

INDEX OF CONTENTS

ACKNOWLEDGMENTS i
RESUMO iii
ABSTRACT v

1. INTRODUCTION 1
1.1 SCOPE OF THE DISSERTATION 1
1.2 OBJECTIVES 1
1.3 CHAPTERS OVERVIEW 2
2. STATE OF THE ART 3
2.1 INTRODUCTION 3
2.2 DESIGN OF COLUMN BASES 3
2.2.1 BASE PLATE 4
2.2.2 MORTAR LAYER 5
2.2.3 CONCRETE BLOCK 5
2.2.4 ANCHOR BOLTS 6
2.3 COMPONENT METHOD FOR COLUMN BASES UNDER STRONG AXIS BENDING 6
2.3.1 BASE PLATE IN BENDING AND ANCHOR BOLTS IN TENSION 8
2.3.1.1 Component resistance 11
2.3.1.2 Effective length of the T-stub 14
2.3.1.3 Component stiffness 17
2.3.2 BASE PLATE IN BENDING AND CONCRETE IN COMPRESSION 17
2.3.2.1 Component resistance 18
2.3.2.2 Component stiffness 21
2.3.3 COLUMN FLANGE AND WEB IN COMPRESSION 24
2.3.4 ANCHOR BOLTS IN SHEAR 24
2.3.5 COLUMN BASE ONLY SUBJECTED TO COMPRESSION 26
2.3.6 ASSEMBLY 26
2.3.6.1 Bending resistance 26
2.3.6.2 Stiffness 29
2.4 CLASSIFICATION OF COLUMN BASE JOINTS 33
2.4.1 ACCORDING TO RESISTANCE 33
2.4.2 ACCORDING TO STIFFNESS 34

3. NUMERICAL MODEL 35

3.1 INTRODUCTION 35

3.2 MODEL DESCRIPTION 35

3.2.1 MATERIAL PROPERTIES 36

3.2.2 ASSEMBLY 37

3.2.3 CONTACT INTERACTIONS 38

3.2.4 BOUNDARY CONDITIONS 38

3.2.5 LOADING AND ANALYSIS STEPS 38

3.2.6 ELEMENT TYPE AND MESHING 39

3.3 VALIDATION OF THE NUMERICAL MODEL 39

3.3.1 EXPERIMENT ON A COLUMN BASE 40

3.3.1.1 Description of specimen 40

3.3.1.2 Test results 41

3.4 COMPARISON WITH THE COMPONENT METHOD DESCRIBED IN EUROCODE 3 45

4. ANALYTICAL MODEL 47

4.1 INTRODUCTION 47

4.2 COMPONENT METHOD FOR WEAK AXIS BENDING 48

4.2.1 BASE PLATE IN BENDING AND ANCHOR BOLTS IN TENSION 49

4.2.1.1 Component resistance 49

4.2.1.2 Effective length of the T-stub 50

4.2.1.3 Component stiffness 52

4.2.2 BASE PLATE IN BENDING AND CONCRETE IN COMPRESSION 52

4.2.2.1 Component resistance 52

4.2.2.2 Component stiffness 54

4.2.3 COLUMN FLANGE IN COMPRESSION 54

4.2.4 ASSEMBLY OF THE COMPONENTS 55

4.2.4.1 Bending resistance 55

4.2.4.2 Stiffness 56

4.3 M_Z-M_Y INTERACTION CURVE 57

4.4 VALIDATION OF THE ANALYTICAL MODEL 59

4.4.1 WEAK AXIS BENDING 59

4.4.2 INTERACTION CURVE 60

4.5 WORKED EXAMPLE 62

4.5.1 DATA OF THE JOINT 62

4.5.2 COLUMN BASE UNDER STRONG AXIS BENDING 64
4.5.2.1 Bending resistance 64
4.5.2.2 Initial Stiffness 67
4.5.3 COLUMN BASE UNDER WEAK AXIS BENDING 69
4.5.3.1 Bending resistance 69
4.5.3.2 Initial Stiffness 71
4.5.4 M_Z-M_Y INTERACTION CURVE 73
5. CONCLUSION 75

INDEX OF FIGURES

Figure 2.1 - Column bases: a) Exposed column base, b) Embedded column [2] 3

Figure 2.2 – Elements of exposed column base [3] 4

Figure 2.3 - Outstand width (c) representation [5] 4

Figure 2.4 - Base plates types of behavior [3] 5

Figure 2.5 – Types of anchor bolts: a) cast-in-situ anchor bolts, b) hooked bars, c) undercut anchor bolts, d)bonded anchor bolts, e) grouted anchor bolts, f) anchoring to grillage beams [5] 6

Figure 2.6 - Components of column base with anchored base plate [5] 7

Figure 2.7 - Characteristics of the component [9] 8

Figure 2.8 - Moment-Rotation curve of the joint [9] 8

Figure 2.9 – a) Tensile zone and equivalent T-stub for bending moment in strong axis [9]; b) Schematic representation a T-stub [10] 9

Figure 2.10 - T-stub separated from the concrete block [10] 9

Figure 2.11 – Beam model of T-stub and prying force Q [7] 10

Figure 2.12 - Equivalent length of anchor bolt [2] 11

Figure 2.13 - Failure modes of the T-stub in contact with the concrete foundation [2] 11

Figure 2.14 - T-stub without contact with the concrete foundation [2] 12

Figure 2.15 - The design resistance of the T-stub [10] 13

Figure 2.16 - The yield line patterns: a) circular patterns, b) non-circular patterns [7] 14

Figure 2.17 - Geometry and distances of the tension zone 15

Figure 2.18 - Stress distribution in the grout [5] 18

Figure 2.19 - Design distribution for concentrated forces, adapted from [12] 20

Figure 2.20 – Distribution of forces in the compressed T-stub [11] 20

Figure 2.21 - Area of the equivalent T-stub in compression: a)short projection; b) Large projection [12] 21

Figure 2.22 - Flange of a flexible T-stub [11] 22

Figure 2.23 - Behavior of an anchor bolt loaded by shear [14] 25

Figure 2.24 - T-stubs under compression [1] 26

Figure 2.25 – Mechanical models of resistance for bending about the strong axis [1] 26

Figure 2.26 - Equilibrium of forces on the base plate in case of a dominant bending moment 28

Figure 2.27 - Mechanical models of stiffness for bending about the strong axis, adapted from [1] 30

Figure 2.28 - Mechanical model in the case of a dominant bending moment 30

Figure 2.29 - Moment-rotation curves for non-proportional loadings and proportional loadings [15] ... 33

Figure 2.30 - Proposed classification system according to the initial stiffness [16] 34

Figure 3.1 - Components of the model: a) column welded to the base plate; b) concrete block; c) bolt and head of the bolt 36

Figure 3.2 - Material behavior used in FEM analysis for column, base plate and anchor bolts [18] 37

Figure 3.3 - Assembly of the column base connection 37

Figure 3.4 - Mesh of the column base assembly 39

Figure 3.5 - Test set-up [17] 41

Figure 3.6 - Bending moment-rotation diagram of specimens 1 and 2 subjected to axial force and in-plane bending moment and calculation according to EC3 [17] 42

Figure 3.7 - Bending moment-rotation diagram of specimens 3 and 4 subjected to axial force and out-of-plane bending moment [17] 42

Figure 3.8 - Force on anchor bolts measured with force washers (FW) and straing gauges (SG) [17] 43

Figure 3.9 - Comparison of moment-rotation diagrams for strong axis bending 44

Figure 3.10 - Comparison of moment-rotation diagrams for out-of-plane bending (26,56º) 44

Figure 3.11 - Moment-rotation diagram for strong axis bending with proportional loading (e=-0,250m) 46

Figure 4.1 - Applied moment in the column base 47

Figure 4.2 - Components of column bases under bending about weak axis 48

Figure 4.3- Tension zones and equivalent T-stub for bending moment in turn of the weak axis, adapted from [9] 49

Figure 4.4 - Group yield lines [9] 50

Figure 4.5 - Straight yield line [9] 50

Figure 4.6 – Effective area of the compressed T-stub 53

Figure 4.7 - Column flange in compression 54

Figure 4.8 – Loading cases for calculation of the moment capacity about the weak axis 55

Figure 4.9 - Mechanical models of stiffness for bending about the weak axis 56

Figure 4.10 - Linear M_z-M_y Interaction curve 57

Figure 4.11 – Elliptical M_z-M_y interaction curve 58

Figure 4.12 - Determination of the moment capacity 58

Figure 4.13 - Moment-rotation diagram for weak axis bending with proportional loading (e= -0,250m) 59

Figure 4.14 - M_z-M_y interaction curves for e=-0,250m 60

Figure 4.15 - M_z-M_y interaction curves for e=+0,250m 61

Figure 4.16 - M_z-M_y interaction curves for e=infinite 61

Figure 4.17 - Design of the column base 63

Figure 4.18 – Compressed T-stub 68

Figure 4.19- Mz-My Interaction curve (worked example) 73

INDEX OF TABLES

Table 2.1 - Effective length of a T-stub in case of bending about the strong axis [7] 16

Table 2.2 -Factor α and its approximation for concrete [11] 22

Table 2.3 - Design moment capacity $M_{j,Rd}$ of column bases [1] 29

Table 2.4 - Rotational stiffness for column bases [1] 32

Table 3.1 - Comparison of numerical results with experimental results for strong axis bending 45

Table 3.2 - Comparison of numerical results with experimental results for out-of-plane bending (26,56º) 45

Table 3.3 - Comparison between numerical results and analytical results for strong axis bending with proportional loading (e=-0,25m) 46

Table 4.1 - Effective length of a T-stub in case of bending is weak axis 51

Table 4.2 - Comparison between numerical results and analytical results for weak axis bending with proportional loading (e=-0,25m) 60

Table 4.3 - Data of the joint 63

SYMBOLS

Upper case

- A - Cross section Area [mm^2]
- A_{c0} - Loaded area [mm^2]
- A_{c1} - Maximum spread area [mm^2]
- A_{eff} - Effective area [mm^2]
- A_s - Tensile stress area of bolt [mm^2]
- $C_{f,d}$ - Coefficient of friction between the base plate and the grout layer
- E - Modules of elasticity of steel [GPa]
- E_c - Modules of elasticity of concrete [GPa]
- F - Tensile force applied on the T-stub [KN]
- $F_{C,Rd}$ - Compressed part resistance [KN]
- $F_{f,rd}$ - Design friction resistance [KN]
- $F_{T,Rd}$ - Tension part resistance [KN]
- $F_{t,Rd}$ - Design tension resistance of a single bolt [KN]
- I - Moment of inertia [mm^4]
- L - Length [mm]
- L_b - Active length of the anchor bolt [mm]
- M_{Rd} - Design moment capacity [KN.m]
- $M_{N,Rd}$ - Interaction bending resistance with compression [KN.m]
- $M_{pl,Rd}$ - Plastic moment capacity [KN.m]
- $N_{c,Ed}$ - Design value of the normal compressive force in the column [KN]
- N_{Ed} - Design axial load [KN]
- $N_{pl,Rd}$ - Design capacity in tension/compression [KN]
- N_{Rd} - Design resistance [KN]
- Q - Prying force [KN]
- W_{pl} - Plastic section modulus [mm^3]

Lower case

- a - Length [mm]
- b - Length [mm]
- c - Effective width [mm]
- d - Bolt diameter [mm]

e - Eccentricity [mm]

f_{ck} - Characteristic strength of concrete [Mpa]

f_{cd} - Design strength of concrete [Mpa]

f_{ub} - Ultimate tensile strength of the bolt [Mpa]

f_u - Ultimate tensile strength of structural steel [Mpa]

f_y - Nominal value of the yield strength of structural steel [Mpa]

h - Height [mm]

k_b - Stiffness of bolt [mm]

k_c - Stiffness of compressed part [mm]

k_p - Stiffness of plate [mm]

k_t - Stiffness of tension part [mm]

l_{eff} - Effective length of T-stub [mm]

m - Distance between threaded bolt and headed stud [mm]

m_{pl} Plastic moment capacity per unit [mm]

n - Distance between bolts and location of the prying [mm]

$s_{j,ini}$ - Initial stiffness [MN.m/rad]

t - Material thickness [mm]

t_f - Thickness of T-stub flange [mm]

t_w - Thickness of T-stub web [mm]

z - Lever arm of tension/compressed part [mm]

Latin symbols

θ_j - Material coefficient

γ_c - Partial safety coefficient for concrete

γ_{M0} - Partial safety coefficient for resistance of any cross section

γ_{M2} - Partial safety coefficient for resistance for steel

δ - Deformation [mm]

ε - Strain

ν - Poisson's ratio

σ - Stress [MPa]

Φ - Rotation [rad]

1
INTRODUCTION

1.1 SCOPE OF THE DISSERTATION

One of the biggest problems in steel structures is the connection between the various elements, namely beam-to-column joints or column bases joints. The mechanical properties of these joints are known to have big influence on the behavior of the structure, thus, their characterization is very important for the structural frame analyses and design process.

Regarding column bases, they are one of the most important structural components since their function is to transfer the acting loads of the superstructure to the foundation system. However, they are still one of the least studied structural elements. Compared to the beam-to column joints, where there are more than thousands of published tests, the number of tests on column bases is very small. Furthermore, within the existing studies concerning column bases, most of them focused on strong axis bending, very few about weak axis bending and almost none about biaxial bending.

The analytical method that is currently used for studying column bases is the component method which is described in EN 1993-1-88[1]. It analyses the behavior of the joint when subjected to in-plane-bending (strong axis bending). However, there is no method that provides the mechanical properties of the joint when subjected to weak axis bending or biaxial bending.

Consequently, it is very difficult or almost impossible to predict the behavior of column bases in out-of-plane bending. The accurate way would be to model the joint by a Finite Element Method (FEM). However, models based on FEM are very complicated and, consequently, very time consuming. Therefore, the main objective of this work is to provide an analytical method for obtaining the resistance of column bases under biaxial bending.

1.2 OBJECTIVES

The primary objective of this dissertation is to evaluate the structural behavior of column bases under biaxial loading conditions. Therefore, there was an effort for obtaining a procedure, based on the component method described in EN 1993-1-8[1], which would allow the designers to get the joint's moment capacity for biaxial bending. Thus, the work presented in this dissertation was divided into the following tasks:

- Literature review about column bases and the component method (for bending about the strong axis);
- Searching for existing experiments on column bases that are suitable for comparing with the component method;

- Development of a numerical model, validated against experimental results, and compare numerical results with the ones provided by the component method (which is described in EN 1993-1-8 [1]);
- Development of a method that studies the behavior of column bases under weak axis bending;
- Generation of an interaction curve between the moment capacities for bending about the main axis ($M_{y,Rd}$ and $M_{z,Rd}$), which provides the resistance of the column base for any type of bending;
- Validation of the analytical model based on comparisons with numerical results.

1.3 CHAPTERS OVERVIEW

The current dissertation is organized in five chapters.

The introduction of the topic of the work as well as the objective and organization of the thesis are presented in the first chapter.

The second chapter contains the literature review about column bases and the method that is in current use for studying its behavior when subjected to strong axis bending. This method corresponds to the component method which is in accordance with EN 1993-1-8 [1]. This chapter also contains the classification of column bases according to that standard.

The third chapter introduces a numerical model which is created through the Finite Element program ABAQUS. This model is validated with test results, obtained by an experiment carried out on a simple column base, by Brno University of Technology. These tests included in-plane bending (strong axis bending) and out-of-plane bending (biaxial bending). The numerical model is then subjected to strong axis bending with a proportional loading and the results are compared with the ones provided by the component method.

In the forth chapter, an analytical model is proposed including not only a method that studies the behavior of column bases subjected to weak axis bending, but also a moment-moment interaction curve. This curve allows the calculation of the moment capacity of column bases under any type of bending. Afterwards, the method is validated by the comparison with numerical results. The chapter closes with a presentation of a worked example.

The fifth and final chapter presents the conclusion of the work and some aspects that should be improved in further works on this topic.

2
STATE OF THE ART

2.1 INTRODUCTION

One of the most important structural elements in steel structures is the column base, especially when it is designed for resisting bending moments. The loads applied in the column have to be transferred by the anchor bolts and the base plate to the corresponding foundation.

Despite its important role, there is not much concern about their design. This normally leads to expensive and often inappropriate solutions. Bad solutions could also lead to a big risk for the safety of the structure.

This chapter presents the most common design of column bases as well as the main elements of it. Besides that, the most significant characteristics of these elements are also described.

Regarding the study of the behavior of column bases under strong axis bending, the method that is currently in use is the component method which is described in Eurocode 3 [1]. This method will be fully described at the current section of the work. The classification of these joints according to resistance and stiffness is also introduced.

2.2 DESIGN OF COLUMN BASES

A column base connection is a special type of joint that connects the steel column to its foundation which function is to transfer the loading from the supported member to the supporting member. The most common type of connection is the exposed base plate (see Figure 2.1a), but they can also be embedded in the concrete, as shown in Figure 2.1b). This dissertation is only going to focus on the exposed ones, since the embedded ones are much less common and demand a different study.

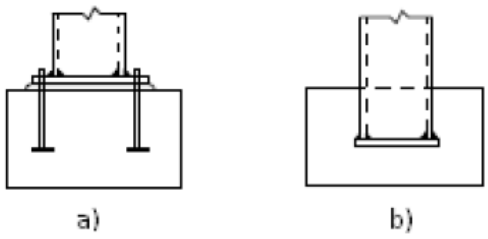


Figure 2.1 - Column bases: a) Exposed column base, b) Embedded column [2]

The main elements of exposed column base plates, also known as anchored base plate, are (see Figure 2.2):

- column foot;
- base plate welded to the column foot;
- mortar layer;
- anchored bolts;
- concrete block (foundation).

Sometimes the joint can be reinforced using stiffeners. In addition, if necessary, the joint could be added with a shear resisting key (shear lug).

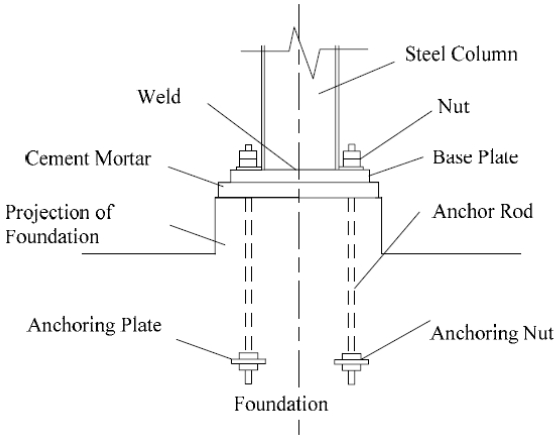


Figure 2.2 – Elements of exposed column base [3]

2.2.1 BASE PLATE

A base plate is a steel sheet that is welded to the column. Its main purpose is to increase the contact area between the column and the concrete block, which will decrease the stress in case of compression and prevent crushing of the concrete. Another function is to transfer the possible tension in the column to the anchor bolts.

The welds are made around the whole cross section of the column and they can be designed according to EN 1993-1-8 [1].

The most common shape of base plates is rectangular and its dimensions are determined by the effective area method. The method takes into account the area required to transmit the compressive forces under the base plate at the appropriate strength of the concrete [4]. The calculation of the area is based on estimation of the effective width or outstand width, *c* (see Figure 2.3).

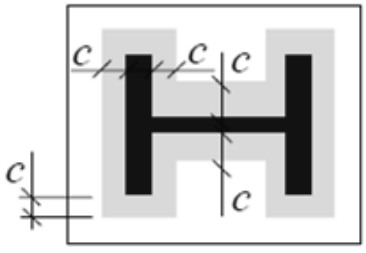


Figure 2.3 - Outstand width (c) representation [5]

Regarding their strength, base plates are roughly sorted according to whether the thickness is smaller, equal to, or greater than that required to form a plastic hinge in the plate [3]. In Figure 2.4, the three types of base plates and their expected deformed shapes are illustrated.

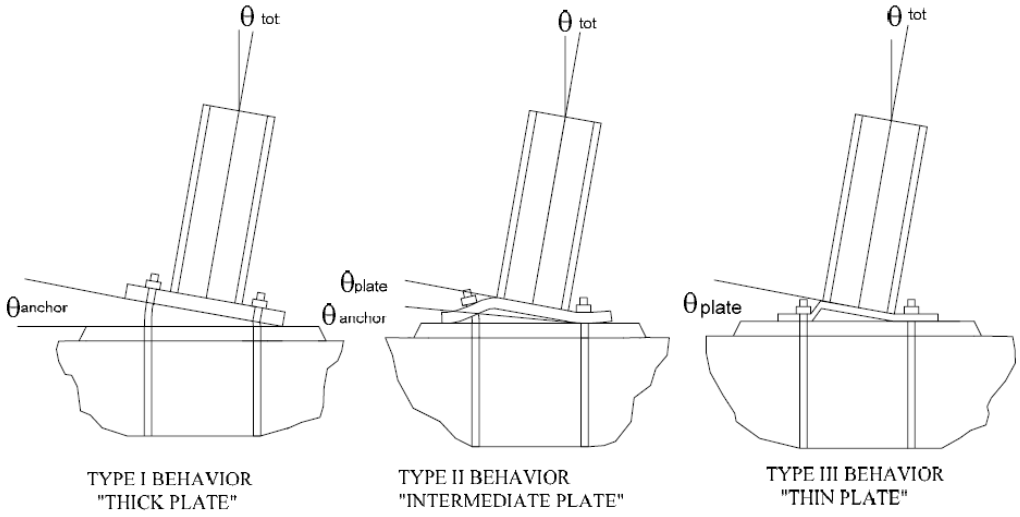


Figure 2.4 - Base plates types of behavior [3]

Rigid plates, or thick plates, are the strongest ones but the most likely to present a non-ductile behavior due to fracture of anchor bolts or the development of crushing and spalling failure of the grout for large rotations [3]. Flexible plates, or thin plates, have a ductile behavior, in which the inelasticity is concentrated in the base plate itself. In the case of semi-rigid plates, the failure is due to the anchor bolts as well as the base plate.

2.2.2 MORTAR LAYER

The contact between the steel plate and the concrete block is provided by the mortar layer allowing the transition of shear forces from the column to the concrete footing by the friction between themselves. Its thickness is usually taken as 0.1 (max 0.2) the width of the plate [2].

In the construction process of exposed column bases, this element is the last to be materialized. A specific space between the base plate and the concrete block is left to be later filled with the mortar. Sometimes, the base plate has holes so that the air stuck in the process of inserting the grout can escape, usually when the base plate is thick [6].

2.2.3 CONCRETE BLOCK

The concrete block is the foundation of the column which function is to transfer the loads to the ground and they are dimensioned according to specific soil conditions.

The method for their design is based on calculation of the effective rigid area under the flexible plate. The bearing strength of concrete is recalculated into the design value of compressive strength, f_{cd} [2].

2.2.4 ANCHOR BOLTS

The main purpose of the anchor bolts is to hold down the column by transferring the tensile loads to the corresponding foundation. These loads may appear in form of pure tension or tension in one side of the column caused by a bending moment.

There are various types of anchor bolts, as shown in Figure 2.5, and they should be chosen according to the appropriate conditions. The most common ones are the cast-in-situ anchor bolts and hooked bars, since they are the most economic ones. Anchoring to grillage beams embedded in the concrete foundation is designed only for column bases loaded by large bending moment, because it is very expensive.

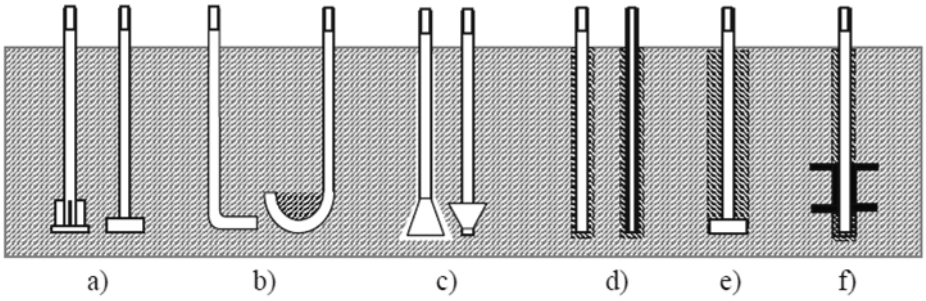


Figure 2.5 – Types of anchor bolts: a) cast-in-situ anchor bolts, b) hooked bars, c) undercut anchor bolts, d)bonded anchor bolts, e) grouted anchor bolts, f) anchoring to grillage beams [5]

To avoid brittle failure, the collapse of the anchoring should be avoided and the collapse of anchor bolts is preferred. For seismic areas, the failure of the column base should occur in base plate rather than in the anchor bolts because the plastic mechanism in the plate ensures ductile behavior and dissipation of energy [7].

The bolt resistance is easy to estimate (can be found in EN 1993-1-8 [1]) but the anchoring resistance calculation is very complicated and not convenient for practical design. Each anchoring has a different failure mode and consequently a different type way of calculating the resistance. This essay will not focus on this matter.

The concrete block failure for the in-situ-cast anchors is prevented by concrete reinforcement or by limited pitch p_{min}=5d (minimum value is 50 mm) and the edge distance e_{min}=3d (minimum value is also 50mm) [2].

2.3 COMPONENT METHOD FOR COLUMN BASES UNDER STRONG AXIS BENDING

Nowadays, the most common method for analyzing steel and composite joints is the component method. This method basic principle consists in determining the complex non-linear joint response through the subdivision into basic joint components and each one contributes to its structural behavior by means of resistance and stiffness.

The component method also allows the designers to take options more efficiently where the contribution of each component can be optimized. Thus, the main advantage of the component method is the possibility to analyze an individual component no matter the type of joint [8].

The procedure of this method consists on the following steps:

1) Identification of the basic components;
2) Characterization of the mechanical properties of each component;
3) Assembly of the component properties to obtain the properties of the connection;
4) Classification of the joint;
5) Modeling.

The joint components are usually independent of each other and their behavior is easy to describe. They are generally divided by the type of loading (tension, compression and shear), obtaining the following main components (see Figure 2.6):

- Base plate in bending and anchor bolts in tension;
- Base plate in bending and concrete block in compression;
- The anchor bolts in shear;
- Column web and flange in compression.

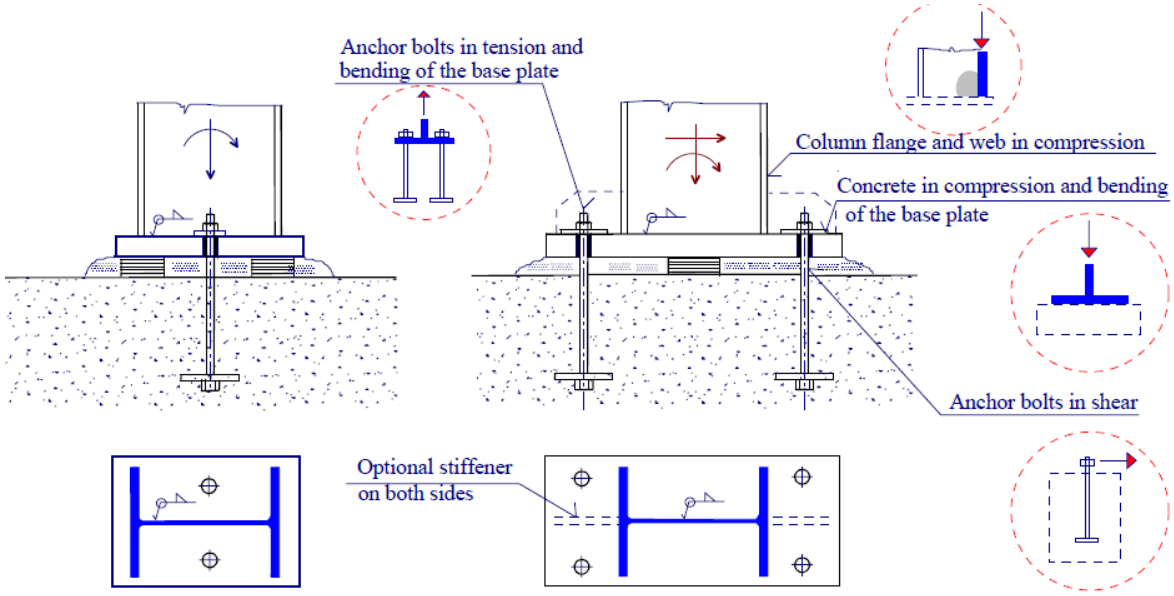


Figure 2.6 - Components of column base with anchored base plate [5]

These components are related to the column bases with open sections and anchored base plates, however the component method is also applicable for other types of column bases if the right components are chosen.

The most relevant mechanical properties of the components are: resistance, F_{rd}, stiffness, K, and deformation capacity, δ_{Cd}. With these parameters it is possible to obtain a curve that reproduces the component behavior, see Figure 2.7.

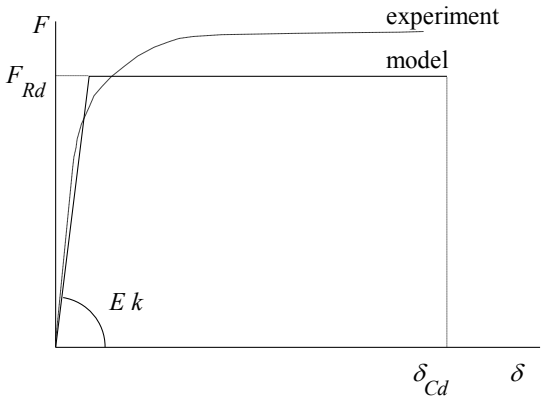


Figure 2.7 - Characteristics of the component [9]

The assembly procedure consists of combining the mechanical properties of each component to obtain the joint behavior, which can be reproduced by the moment-rotation curve. As it is shown in Figure 2.8, the rotational stiffness, s_j, corresponds to a secant stiffness in the moment-rotation curve and the initial stiffness, $s_{j,ini}$, corresponds to the initial slope of the curve (elastic phase) [10].

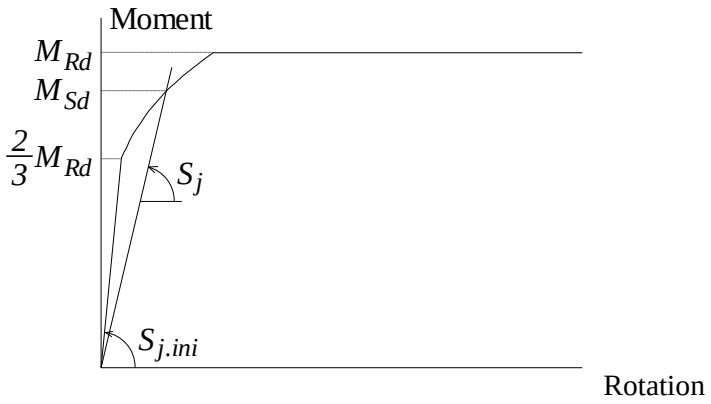


Figure 2.8 - Moment-Rotation curve of the joint [9]

The joint is classified in terms of resistance and stiffness with the purpose of simplification of the joint behavior under the frame analysis.

The final step is the modeling, which is required to determine how the mechanical properties of the joint are taken into account in the frame analysis.

2.3.1 BASE PLATE IN BENDING AND ANCHOR BOLTS IN TENSION

When the column base is loaded with a bending moment, the anchor bolts in the tensile zone are activated to transfer the applied force and the column base is deformed. This deformation consists of the elongation of the anchor bolts and bending of the base plate. The failure of the tensile zone can be caused by: the yielding of the base plate, the failure of the anchor bolts or a combination of both phenomena [7].

The behavior of this component is described by the help of a T-stub model based on similar assumptions as used in beam-to-column connections. However, there are some differences between

their properties and behavior that have to be taken into account. The column base plate has different requirements from the base plate in the beam-to-column connections since it is designed primarily for the transmission of compressive forces, which leads to a thicker base plate and longer anchor bolts. The influence of pad and bolt head might be higher.

In this procedure, the tension part is replaced by a T-stub with a width corresponding to the effective length, l_{eff}, see Figure 2.9, so that the loading capacity of the T-section is identical to the resistance of the corresponding component.

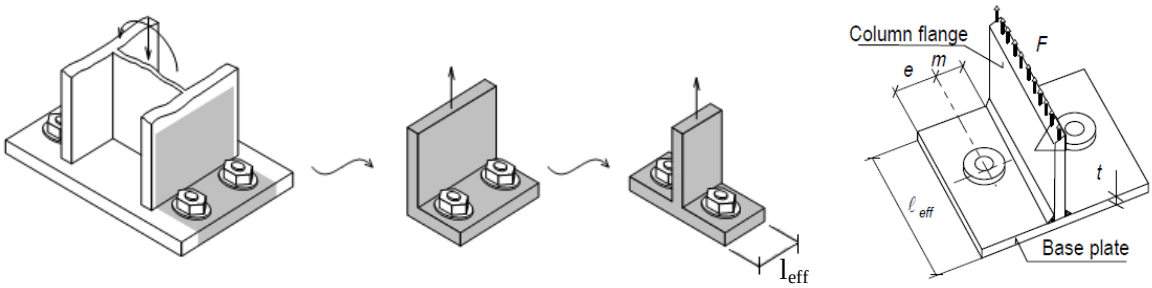


Figure 2.9 – a) Tensile zone and equivalent T-stub for bending moment in strong axis [9]; b) Schematic representation a T-stub [10]

When analyzing this model, two cases should be considered according to the presence of prying action. In the first case, the bolts are considered as flexible and the base plate as stiff. When loaded in tension, the plate is separated from the concrete foundation (see Figure 2.10). In the other case, the edge of the plate is in contact with the concrete and prying occurs, which means that the bolts are loaded by additional prying force, Q.

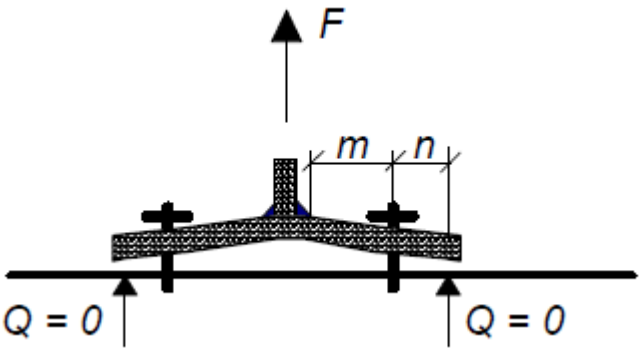


Figure 2.10 - T-stub separated from the concrete block [10]

The boundary between these two cases, of prying or no prying, has to be determined and the length of the bolt is an indicator of this phenomenon. However, not all the bolt length is subjected to deformations. Therefore, an active length of the bolt needs to be calculated and compared with the minimum length required to exist prying forces.

To find this limit, the case of prying is studied and beam theory is used to describe deformed shape of the T-stub [10] (see Figure 2.11).

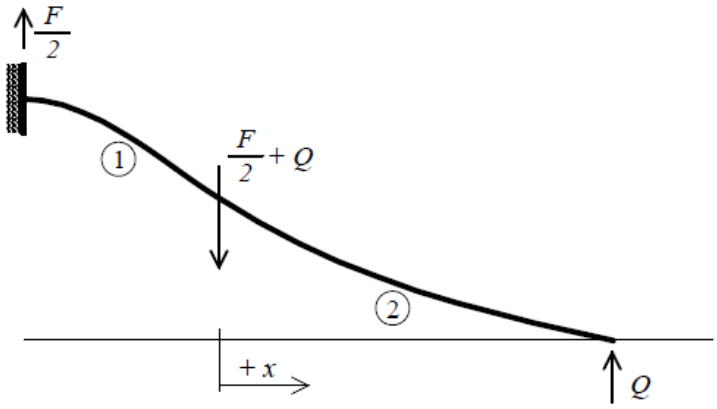


Figure 2.11 – Beam model of T-stub and prying force Q [7]

The deformed shape of the curve is derived from the following equation:

$$EI\delta'' = -M \tag{2.1}$$

After writing the above equation for both parts (1) and (2), by the application of suitable boundary conditions, the equations could be solved. The prying force, *Q*, is derived from these solved equations as [10]:

$$Q = \frac{F}{2}\frac{3(m^2\, n\, A_s - 2\, I)}{2\, n^2\, A_s\, (3m + n) + 3\, L_b\, I} \tag{2.2}$$

The boundary between prying and no prying is defined by the previous equation when *n=1.25m*. Therefore, the minimum length for no prying is*:*

$$L_b^* = \frac{8.8\, m^3\, A_s}{l_{eff,1}\, t^3} \tag{2.3}$$

Where:

- A_s - Tensile stress area of the bolt
- L_b - Equivalent length of the anchor bolt (see Figure 2.12)
- l_{eff} - Equivalent length of the T-stub determined by the help of Yield line method, presented in following part of the work

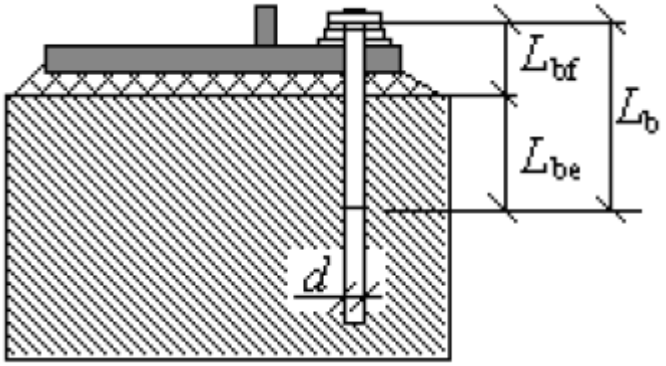


Figure 2.12 - Equivalent length of anchor bolt [2]

The equivalent length of the anchor bolt, L_b, is calculated according to Figure 2.12 as:

$$L_b = L_{be} + L_{bf} \tag{2.4}$$

Where:

$$L_{be} = 8\,d \tag{2.5}$$

2.3.1.1 Component resistance

In EN 1993-1-8 [1], three collapse mechanisms of the T-stub are described (shown in Figure 2.13). These modes can also be used for T-stubs in contact with the concrete foundation [7].

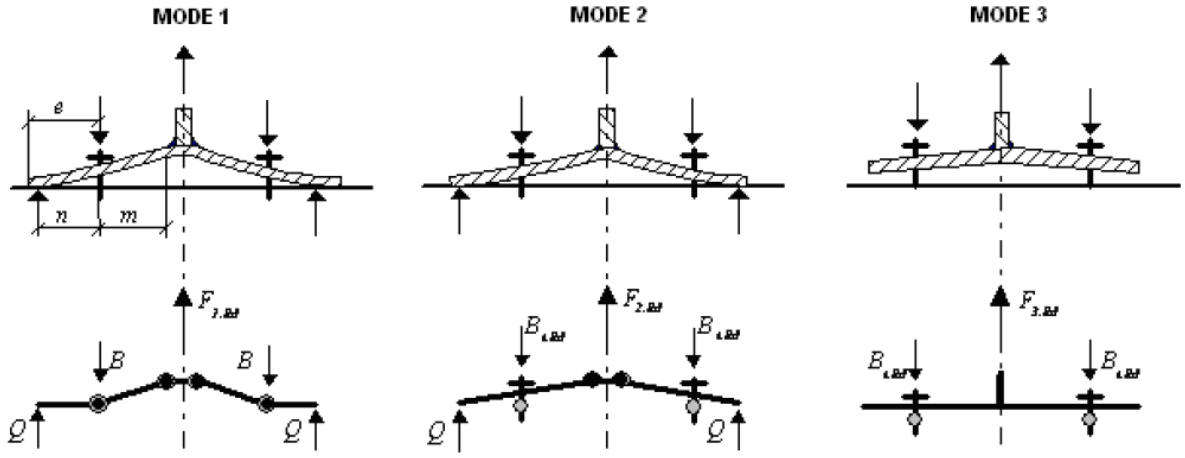


Figure 2.13 - Failure modes of the T-stub in contact with the concrete foundation [2]

These collapse modes are characterized as [2]:

- Mode 1 –occurs when the T-stub is composed by a thin base plate and high strength anchor bolts. The plastic mechanism takes place in the plate.
- Mode 2 –is a transition between Mode 1 and 3. The collapse is caused by mixed failure of anchor bolts and base plate.
- Mode 3 –happens for T-stubs with thick base plate and weak anchor bolts thus the failure is due to the bolts.

The design strength for the case of prying is then the smallest value of the previous modes resistances.

However, since the column bases have longer anchor bolts than beam-to-column connections, bigger deformations may arise [10]. This can lead to a different failure mode that is not likely to appear in the beam-to-column joints (Mode 1-2). This mode is similar to the mode 1 but the failure is due to yielding of the base plate without reaching the bolt strength. As shown in Figure 2.14, the plate is separated from the concrete and no prying occurs for this mode.

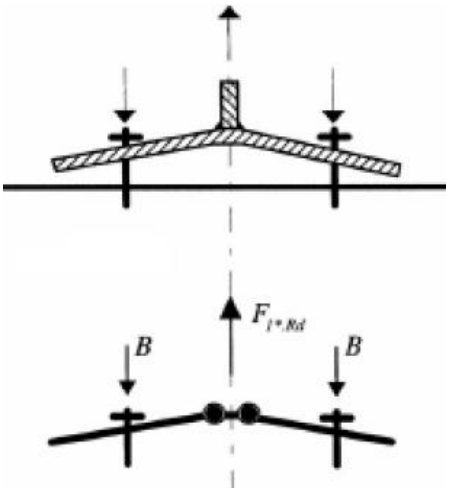


Figure 2.14 - T-stub without contact with the concrete foundation [2]

In Mode 1-2, after large deformations of the base plate, the contact between the edges of the plate and the concrete foundation can develop again [7]. Thus, the bolts are subjected to additional traction loads until failure is obtained by Mode 1 or 2. However, to reach the resistance necessary for collapse in these modes, very large deformations are observed which is not acceptable for design. The additional resistance between Mode 1 and Mode 1-2, which is represented in Figure 2.15, is disregarded.

Thereafter, in case of no contact of the T-stub and the concrete the failure results either from the anchor bolts in tension (Mode 3) or from yielding of the plate in bending (Mode 1-2).

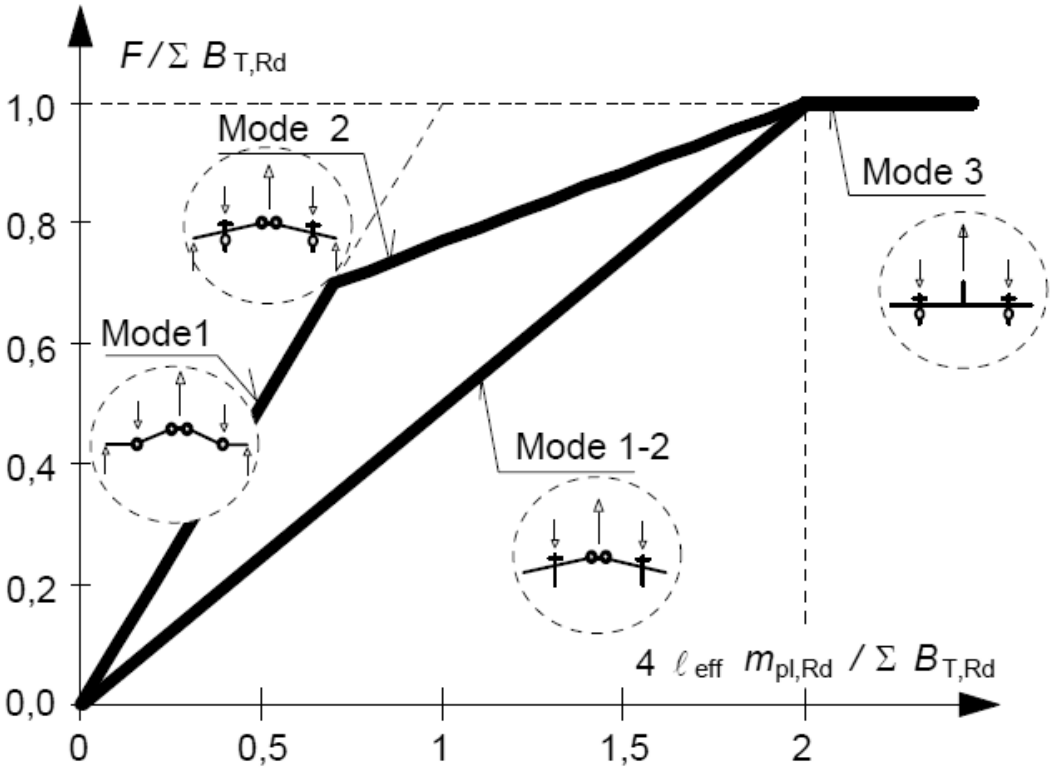


Figure 2.15 - The design resistance of the T-stub [10]

The following formulas associated to each resisting mechanism can be found in Table 6.2, cl. 6.2.6.5 of EN 1993-1-8 [1]. For modes 1 and 2, the European code provides two methods of calculation, but this work is only going to focus on method 1.

Mode 1:

$$F_{T,1,Rd} = \frac{4M_{pl,1,Rd}}{m} \tag{2.6}$$

Mode 2:

$$F_{T,2,Rd} = \frac{2\,M_{pl,2,Rd} + n\,\sum F_{t,Rd}}{m+n} \tag{2.7}$$

Mode 3:

$$F_{T,3,Rd} = \sum F_{t,Rd} \tag{2.8}$$

Mode 1-2:

$$F_{T,1-2,Rd} = \frac{2\,M_{pl,1-2,Rd}}{m} \tag{2.9}$$

Since $m_{pl,Rd}$ is the plastic bending moment capacity of the base plate per unit:

$$m_{pl,Rd} = \frac{1}{4}\frac{t^2 f_y}{\gamma_{M0}} \tag{2.10}$$

The plastic moment capacity for Mode i (i=1,2,1-2), $M_{pl,i,Rd}$, is this value multiplied for its according $l_{eff,i}$:

$$M_{pl,i,Rd} = \sum leff_i \, m_{pl,Rd} \Rightarrow M_{pl,i,Rd} = \sum leff_i \frac{1}{4} \frac{t^2 f_y}{\gamma_{M0}} \quad (2.11)$$

The $F_{t,Rd}$ is the design resistance of a single bolt and it is given by (EN 1993-1-8 Table 3.4):

$$F_{t,Rd} = \frac{0{,}9 \, f_{ub} A_s}{\gamma_{M2}} \quad (2.12)$$

In summary, the design resistance $F_{T,Rd}$ of the T-stub for the case of prying action is:

$$F_{T,Rd} = min\left(F_{T,1,Rd}, F_{T,2,Rd}, F_{T,3,Rd}\right) \quad (2.13)$$

And for the case of no prying action:

$$F_{T,Rd} = min\left(F_{T,1-2,Rd}, F_{T,3,Rd}\right) \quad (2.14)$$

2.3.1.2 Effective length of the T-stub

In the design procedure, the appropriate effective length should be chosen according the failure mode of the T-stub. The smallest value obtained for the possible yield mechanisms of each mode is used when characterizing the T-stub.

The yield line patterns are divided in two groups (watch Figure 2.16):

- Circular patterns – $l_{eff,cp}$;
- Non circular patterns – $l_{eff,nc}$.

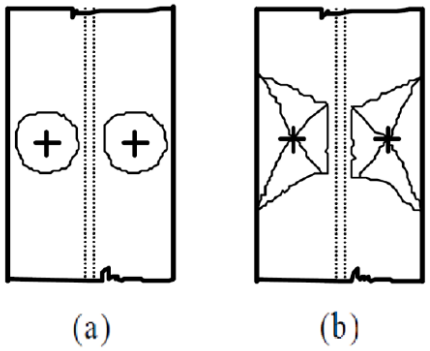


Figure 2.16 - The yield line patterns: a) circular patterns, b) non-circular patterns [7]

The main difference between them is related to the influence of prying forces. For example, if prying forces have influence in the calculation of the T-stub resistance, only the non-circular patters can be developed. Thus, the patterns are taken into account in the failure modes as follows [7]:

Mode 1: Prying forces do not have influence on the development of plastic hinges in the base plate. Thus, both circular and non-circular yield lines can occur in this mode.

Mode 2: First, the plastic mechanism develops in the base plate, closer to the web of the T-stub, which leads to contact between the plate's edges and the concrete block. As a result, prying forces are developed in the anchor bolts leading to the fracture of the bolts. Therefore, only non-circular patterns are possible in mode 2, since they are the ones that allow development of prying forces.

Mode 3: This mode does not include any yielding of the base plate, thus, no yield patterns are considered.

Mode 1-2: Since prying does not occur in this mode, both circular and non-circular patterns have to be taken into account.

Summarizing, the effective length is:

- Mode 1 (index p=prying)

$$l_{eff,1} = min\left(l_{eff,cp}; l_{eff,nc}\right) = min\left(l_{p,1}; l_{p,2}; l_{p,3}; l_{p,4}; l_{p,5}; l_{p,6}; l_{p,7}\right) \quad (2.15)$$

- Mode 2

$$l_{eff,2} = min\left(l_{eff,nc}\right) = min\left(l_{p,4}; l_{p,5}; l_{p,6}; l_{p,7}\right) \quad (2.16)$$

- Mode 1-2 (index np=no prying)

$$l_{eff,1-2} = min\left(l_{eff,cp}; l_{eff,nc}\right) = min\left(l_{np,1}; l_{np,2}; l_{np,3}; l_{np,4}; l_{np,5}; l_{np,6}; l_{np,7}\right) \quad (2.17)$$

Finally, Table 2.1 indicates the formulas of the effective lengths for typical base plates (i.e. two bolts at the tension zone) in cases of prying and no prying, organized by circular patterns and non-circular patterns. It includes only cases where the bolts are located on the flanges side, no yield lines are given for corner bolts.

The formulas of the prying case can be found in Table 6.6 of EN 1993-1-8 [1] and the ones of no prying case were taken from [7] where similar mechanisms for the case of no contact are introduced. All the illustrations of the mechanism were taken from [9] and the symbols used represent distances, see Figure 2.17. There are also formulas for the inside bolts, however this paper will only focus on exterior bolts.

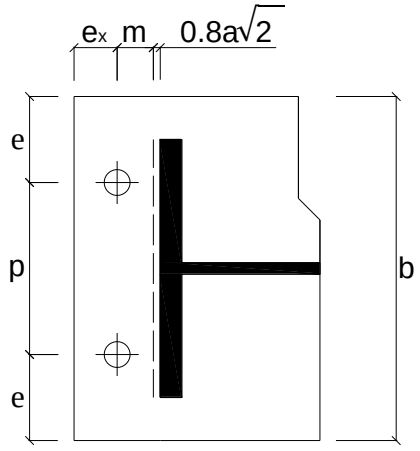
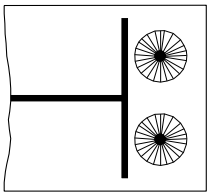
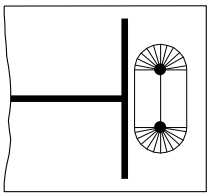
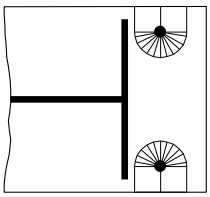
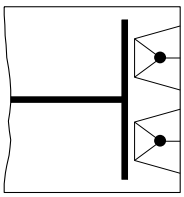
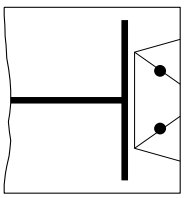
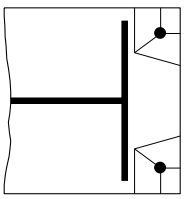
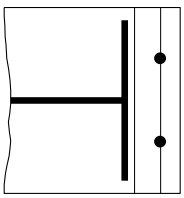


Figure 2.17 - Geometry and distances of the tension zone

Table 2.1 - Effective length of a T-stub in case of bending about the strong axis [7]

	Yield Mechanisms	Prying case	No prying case
Circular patterns		$l_{p,1} = 2\pi m$ (2.18)	$l_{np,1} = 2\pi$m (2.19)
		$l_{p,2} = \pi m + p$ (2.20)	$l_{np,2} = 2\pi m + 2p$ (2.21)
		$l_{p,3} = \pi m + 2e$ (2.22)	$l_{np,3} = \pi m + 4e$ (2.23)
Non circular patterns		$l_{p,4} = 4m + 1{,}25e_x$ (2.24)	$l_{np,4} = 4m + 1{,}25e_x$ (2.25)
		$l_{p,5} = 2m + 0{,}625e_x + 0{,}5p$ (2.26)	$l_{np,5} = 2m + 0{,}625e_x + 0{,}5p$ (2.27)
		$l_{p,6} = 2m + 0{,}625e_x + e$ (2.28)	$l_{np,6} = 2m + 0{,}625e_x + e$ (2.29)
		$l_{p,7} = 0{,}5b$ (2.30)	$l_{np,7} = 0{,}5b$ (2.31)

2.3.1.3 Component stiffness

The stiffness of the T-stub is determined through the deformation of the base plate in bending and the deformation of the bolts in tension. As for resistance, its calculation depends on whether there is contact or not between the edges of the base plate and the concrete foundation. The method for its calculation is described in [7].

When prying does not occur, the formula of the plate deformation is:

$$\delta_p = \frac{F}{2}\frac{m^3}{3\,E\,I} = \frac{F}{E\,k_p} \tag{2.32}$$

And the deformation of bolt in tension is:

$$\delta_b = \frac{F}{2}\frac{L_b}{A_s\,E} = \frac{F}{E\,k_b} \tag{2.33}$$

Where *I* is the inertia of the base plate's cross section:

$$I = \frac{l_{eff,ini}t^3}{12} \tag{2.34}$$

And the effective length of the T-stub for elastic behavior is assumed as [7]:

$$l_{eff,ini} = 0{,}85\,l_{eff} \tag{2.35}$$

Then, stiffness coefficients of the base plate and the bolts are obtained (they can be found in Table 6.11 from Eurocode 3 [1] as K_{15} and K_{16}, respectively):

$$k_p = k_{15} = \frac{0{,}425\,l_{eff}\,t^3}{m^3} \tag{2.36}$$

$$k_b = k_{16} = \frac{2\,A_s}{L_b} \tag{2.37}$$

For the case of prying, the stiffness coefficients were obtained through the deformed shape of the beam model from Figure 2.11. They are as follows (this also can be found in Table 6.11 of Eurocode 3 [1]):

$$k_p = k_{15} = \frac{0{,}85\,l_{eff}\,t^3}{m^3} \tag{2.38}$$

$$k_b = k_{16} = \frac{1{,}6\,A_s}{L_b} \tag{2.39}$$

Finally, the stiffness of the component base plate in bending and anchor bolts in tension is obtained:

$$k_T = \frac{1}{k_p} + \frac{1}{k_b} \tag{2.40}$$

2.3.2 BASE PLATE IN BENDING AND CONCRETE IN COMPRESSION

The component base plate in bending and concrete in compression represents the compressed part of the column base connection. Its resistance depends mostly on the bearing strength of the concrete under concentrated force and it is calculated by replacing the flexible plate by an equivalent rigid plate. This is done by considering the effective area that corresponds to the footprint of the column.

The grout layer is also considered in the resistance calculation of this component since it has influence on it. Other important factors which influence the compression resistance are: the concrete strength;

the compression areas; the relative location between the base plate and the concrete block; and the size of the concrete foundation.

The concrete in compression is mostly stiffer in comparison to the anchor bolts in tension. Thus, the stiffness behavior of column base connection subjected to a dominant bending moment is dependent mostly on elongation of anchor bolts. The deformation of concrete block and base plate in compression is only important in case of dominant axial compressive force [10].

2.3.2.1 Component resistance

The design model for resistance of the component base plate in bending and concrete in compression is described in [11] and is in accordance with cl. 6.2.5 of EN 1993-1-8 [1].

The resistance of this component, $F_{C,pl,Rd}$, expecting the constant distribution of the bearing stresses under the effective area, is given by (can also be found in cl. 6.2.5(3)):

$$F_{c,pl,Rd} = f_{jd}\, b_{eff}\, l_{eff} \tag{2.41}$$

Where b_{eff} and l_{eff} are the dimensions of the T-stub rigid plate, which is equivalent to the flexible base plate of the component, and f_{jd} is the design value of the bearing strength of the concrete (loaded by concentrated compression), which is determined as follows:

$$f_{jd} = \frac{\beta_j\, F_{Rd,u}}{b_{eff}\, l_{eff}} \tag{2.42}$$

There, β_j is the joint material coefficient and it represents the fact that the resistance under the plate might be lower due to the quality of the grout layer. The value 2/3 is used in cases where the characteristic resistance of the grout is at least 0.2 times the characteristic resistance of concrete and the thickness of the grout layer is 0.2 times bigger than the smallest dimension of the base plate. In case of a high quality grout, a less conservative procedure with a distribution of stresses under 45º may be adopted [11], see Figure 2.18. If the layer thickness is superior to 50mm, the characteristic value of its resistance should be at least the same as the concrete foundation [1].

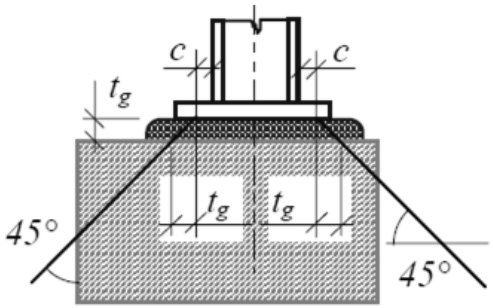


Figure 2.18 - Stress distribution in the grout [5]

And $F_{Rd,u}$ is the design resistance for a concentrated compression determined according to cl.6.7(2) of EN 1992-1-1 [12]:

$$F_{Rd,u} = A_{C0}\, f_{cd} \sqrt{\frac{A_{c1}}{A_{c0}}} \leq 3{,}0\, f_{cd}\, A_{c0} \tag{2.43}$$

Combining formulas (2.42) and (2.43), f_{jd} emerges as:

$$f_{jd} = \frac{\beta_j A_{C0}\, f_{cd} \sqrt{\frac{A_{c1}}{A_{c0}}}}{A_{c0}} = \beta_j\, f_{cd} \sqrt{\frac{A_{c1}}{A_{c0}}} \leq \frac{3{,}0\, f_{cd}\, A_{c0}}{A_{c0}} = 3{,}0\, f_{cd} \tag{2.44}$$

Where A_{c0} is the loaded area and, according to [1], it is equal to $b_{eff} \times l_{efff}$. Knowing that these effective lengths are dependent on the effective width *c*, which in turn is dependent on f_{jd} (it will be demonstrated later in this work), this would lead to an interactive procedure for the calculus of all these parameters. However, in [11] is proposed that as a first approach, when calculating f_{jd}, A_{c0} would be considered as the area of the plate:

$$A_{c0} = a\, b \tag{2.45}$$

And A_{c1} as the corresponding maximum spread area obtained by considering the geometry conditions imposed by cl.6.7(3) in EN 1992-1-1 [12] (see Figure 2.19):

$$A_{c1} = a_{\,2} b_2 \tag{2.46}$$

$$a_2 = min \begin{cases} a + h \\ 3a \\ a_1 \end{cases} \tag{2.47}$$

$$b_2 = min \begin{cases} b + h \\ 3b \\ b_1 \end{cases} \tag{2.48}$$

Where:

- a,b - Dimensions of the plate;
- a_1,b_1 - Dimensions of the concrete block;
- h - Height of the concrete block;
- a_2,b_2 - Dimensions of the maximum spread area.

Therefore, formula (2.44) becomes:

$$f_{jd} = \beta_j\, f_{cd} \sqrt{\frac{a_2\, b_2}{a\, b}} \leq 3\, f_{cd} \tag{2.49}$$

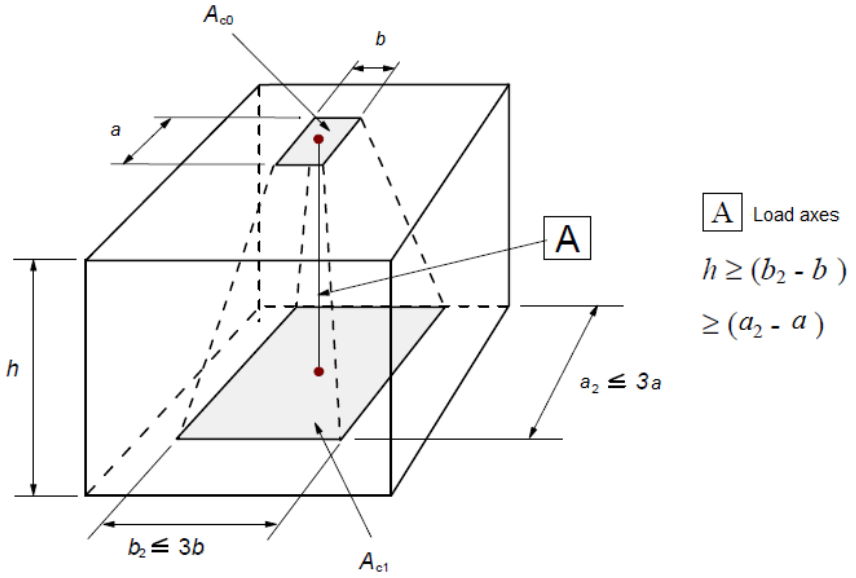


Figure 2.19 - Design distribution for concentrated forces, adapted from [12]

The equivalent width *c* of the T-stub is then determined assuming that no plastic deformations will occur in the flange of the T-stub [11]. The formula for its calculation is derived by equating the elastic bending moment capacity and the acting bending moment on the base plate. The distribution of forces in the compressed T-stub is represented in Figure 2.20.

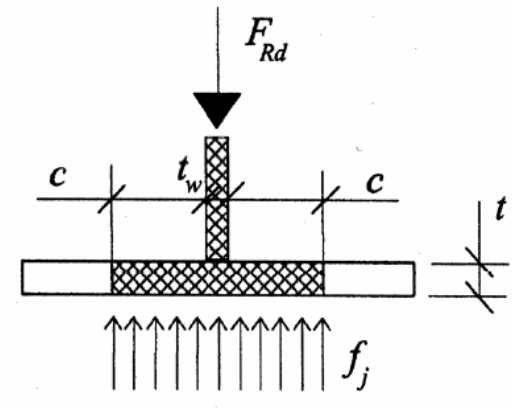


Figure 2.20 – Distribution of forces in the compressed T-stub [11]

Therefore, the elastic bending moment per unit length of the base plate is:

$$M' = \frac{1}{6} t^2 \frac{f_y}{\gamma_{M0}} \tag{2.50}$$

And the bending moment per unit length acting on the base plate is:

$$M' = \frac{1}{2} f_{jd} c^2 \tag{2.51}$$

When the moments are the same (formula (2.50) is equal to (2.51)), means that the plate reaches its bending resistance and, therefore, the equivalent width is obtained [11]:

$$c = t\sqrt{\frac{f_{yk}}{3\,f_{jd}\,\gamma_{M0}}} \tag{2.52}$$

The effective lengths (b_{eff} and l_{eff}) of the equivalent rigid plate are obtained so that the T-stub resistance to compression is the same as the component it represents. When the projection of the compressed component represented by the T-stub is less than the effective width, *c*, these lengths are obtained by adding *c* to the dimensions of the flange, as shown in Figure 2.21b). However, when the projection is short (Figure 2.21a)), the part of the additional projection beyond the width *c* should be ignored.

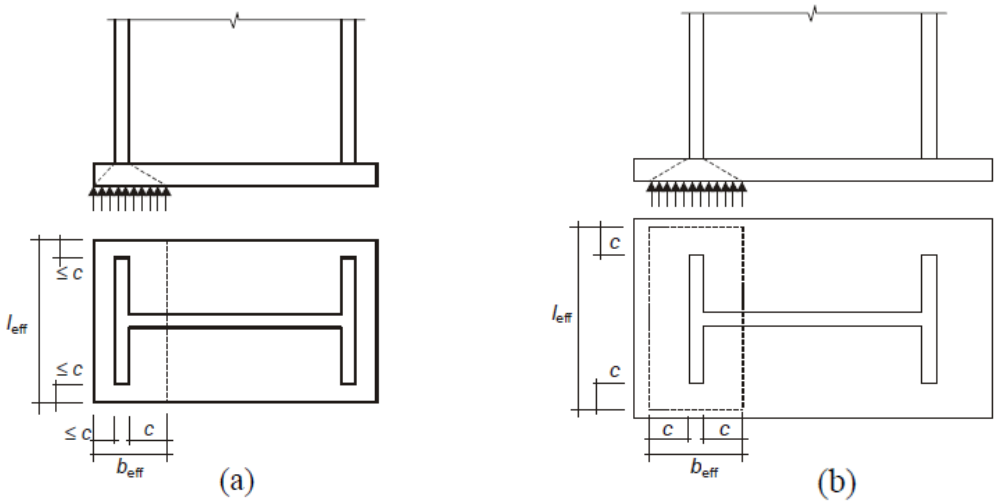


Figure 2.21 - Area of the equivalent T-stub in compression: a) short projection; b) Large projection [12]

Thus, these effective lengths are calculated according to:

$$b_{eff} = min\{c; (a - h_c)/2\} + t_f + c \tag{2.53}$$

$$l_{eff} = min\begin{cases} \mathrm{b} \\ \mathrm{b_c} + 2\mathrm{c} \end{cases} \tag{2.54}$$

2.3.2.2 Component stiffness

The method for predicting the stiffness behavior of the T-sub under compression is described in [11], which is based on assumptions similar to those made for the component resistance, i.e., the flexible plate is replaced by an equivalent rigid plate. First, the deformation of the rigid plate is expressed and then, the flexible plate is substituted, based on the same deformations of the rigid plate.

Regarding the elastic stiffness, it is influenced by the following factors [2]:

- flexibility of the plate;
- Young's modulus of the concrete;
- quality of the concrete surface the grout layer;
- size of the concrete block.

However, the influence of the block size can be neglected in practical cases [11].

About the rigid plate, when it is loaded with compression, the rectangular plate is pressed down into the concrete block. This leads to a deformation of the plate, which can be determined by theory of elastic semi-space:

$$\delta_r = \frac{F\ \alpha\ a_r}{E_c A_p} \tag{2.55}$$

Where:

F - Applied compressed force;

α - Shape factor of the plate dependent on the mechanical properties;

L_r, a_r - Length and width of equivalent rigid plate, respectively;

E_c - Elastic modulus of concrete;

A_r - Area of the rigid plate, $A_r = L_r\ a_r$.

Table 2.2 lists values for α dependent on the Poisson coefficient of the compressed material (ν ≈ 0,15 for concrete). The table also provides the approximation for α, which is given by $0{,}85\sqrt{L_r/a_r}$.

Table 2.2 -Factor α and its approximation for concrete [11]

L_r/a_r	α	Approximation as $\alpha \approx 0{,}85\sqrt{L_r/a_r}$
1	0,90	0,85
1,5	1,10	1,04
2	1,25	1,20
3	1,47	1,47
5	1,76	1,90
10	2,17	2,69

Considering this approximation, formula (2.55) can be rewritten as:

$$\delta_r = \frac{0{,}85\ F}{E_c\sqrt{L_r\ a_r}} \tag{2.56}$$

The following step is to express the flexible plate by means of the equivalent rigid plate based on the same deformations. For this purpose, half of a T-stub flange in compression is modeled as shown in Figure 2.22 [11].

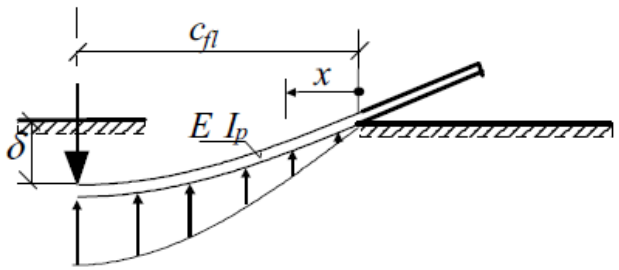


Figure 2.22 - Flange of a flexible T-stub [11]

Assuming that independent springs support the flange of a unit width, the deformation of the plate is expected to behave according to a sine function [11]:

$$\delta(x) = \delta \, sin\left(\frac{1}{2}\pi \, \frac{x}{c_{fl}}\right) \tag{2.57}$$

Where c_{fl} is the length of the flexible plate that is in contact with the concrete foundation, see Figure 2.22.

The uniform stress in the plate can then be replaced by the fourth differentiate of the deformation multiplied by EI_p [11] (data related to the flexible plate, see Figure 2.22, where $I_p = \frac{t^3}{12}$):

$$\sigma(x) = EI_p \left(\frac{1}{2}\frac{\pi}{c_{fl}}\right)^4 \delta \, sin\left(\frac{1}{2}\pi \, \frac{x}{c_{fl}}\right) = E\frac{t^3}{12}\left(\frac{1}{2}\frac{\pi}{c_{fl}}\right)^4 \delta \, sin\left(\frac{1}{2}\pi \, \frac{x}{c_{fl}}\right) \tag{2.58}$$

From the compatibility of the deformations, the stress in the concrete part should be:

$$\delta(x) = \frac{\sigma(x) h_{eq}}{E_c} \tag{2.59}$$

Where h_{eq} is the equivalent height of the concrete under the steel plate and it is assumed to be:

$$h_{eq} = \xi \, c_{fl} \tag{2.60}$$

Hence, combining equations (2.57)(2.81), (2.58), (2.59) and (2.60), the flexible length is obtained:

$$c_{fl} = t \sqrt[3]{\frac{(\pi/2)^4}{12} \, \xi \, \frac{E}{E_c}} \tag{2.61}$$

The equivalent rigid length, c_r, is expressed so that the uniform deformations under the rigid plate result in the same force as the non-uniform deformations under the flexible plate:

$$c_r = \, c_{fl} \, \frac{2}{\pi} \tag{2.62}$$

The factor ξ, which is the ratio between h_{eq} and c_{fl}, needs to be estimated. Thereunto, the equivalent height h_{eq} can be represented by $\alpha \, a_r$, where a_r is equal to t_f+2c_r. In addition, it is assumed in [11] that, for practical T-stubs, the factor α can be approximated to *1,4* and that t_f is equal to 0,5c_r. Hence, through expression (2.60) and (2.62):

$$\alpha \, a_r = \xi \, c_{fl} \Rightarrow 1{,}4(0{,}5 \, c_r + 2 \, c_r) = \xi \, c_{fl} \Rightarrow 1{,}4 \times 2{,}5 \times \frac{2 \, c_{fl}}{\pi} = \xi \, c_{fl} \Rightarrow \tag{2.63}$$

$$\Rightarrow \xi \approx 2{,}2 \tag{2.64}$$

Then, the equivalent rigid length for practical joints is obtained from formulas (2.61) and (2.62), ($E_c \approx 30000MPa$ and $E \approx 210000MPa$):

$$c_{fl} = t \sqrt[3]{\frac{(\pi/2)^4}{12} \, \xi \, \frac{E}{E_c}} = t \sqrt[3]{\frac{(\pi/2)^4}{12} \, 2{,}2 \, \frac{210000}{30000}} \Rightarrow c_{fl} \approx 1{,}98t \tag{2.65}$$

$$c_r = \, c_{fl} \, \frac{2}{\pi} = 1{,}98 \, t \, \frac{2}{\pi} \Rightarrow c_r = 1{,}25t \tag{2.66}$$

Thus, the dimensions of the T-stub are known:

$$b_{eff,s} = a_r = t_f + 2c_r \Rightarrow b_{eff,s} = t_f + 2{,}5t \tag{2.67}$$

$$l_{eff,s} = L_r = b_c + 2c_r \Rightarrow l_{eff,s} = b_c + 2{,}5t \tag{2.68}$$

Where:

t - Thickness of the base plate;

t_f - Thickness of the flange;

b_c - Width of the column.

It is important to notice that these effective lengths are only valid for means of stiffness.

Finally, the stiffness coefficient is derived from the deformation of the component, considering the influence of the quality of the concrete surface and the grout layer. This influence is taken into account by using a stiffness reduction factor equal to 1,5 [11]. Thus, the component stiffness is expressed by (see Table 6.11 from EN 1993-1-8 [1]):

$$k_c = k_{13} = \frac{E_c \sqrt{b_{eff,s}\, l_{eff,s}}}{1{,}275\, E} \tag{2.69}$$

2.3.3 COLUMN FLANGE AND WEB IN COMPRESSION

The compression resistance of the column flange and the adjacent compression zone of the column web is taken from cl. 6.2.6.7 of EN 1993-1-8 [1].

The design resistance is then:

$$F_{c,fc,Rd} = \frac{M_{c,Rd}}{(h_c - t_f)} \tag{2.70}$$

Where:

h_c - Depth of the connected column;

t_f - Flange thickness of the connected column;

$M_{c,Rd}$ - Design moment capacity of the column cross-section

According to cl. 6.2.5(2) of EN 1993-1-1 [13], the design moment capacity, $M_{c,Rd}$, is equal to design plastic moment capacity, $M_{pl,Rd}$:

$$M_{c,Rd} = M_{pl,Rd} = \frac{W_{y,pl}\, f_y}{\gamma_{M0}} \tag{2.71}$$

2.3.4 ANCHOR BOLTS IN SHEAR

The design model for shear resistance is given in cl. 6.2.2 of EN 1993-1-8 [1]. The model considers that for column bases that do not have any special element for resisting shear forces (e.g. shear lug), they are transferred by friction between the plate and the grout and by the anchor bolts.

By increasing horizontal displacement, the force will also increase until it reaches the friction capacity. After that, friction resistance stays constant with increasing displacements while the load continues to be transferred by the bolts.

Because the grout does not have sufficient strength to resist the bearing stresses between the bolts and the grout, considerable bending of the anchor bolts may occur. This leads to the development of tension in anchor bolts, see Figure 2.23. The horizontal component of the increasing tensile force gives an extra contribution to the shear resistance and stiffness. The increasing vertical component gives an extra contribution to the transfer of load by friction and increases resistance and stiffness as well [14].

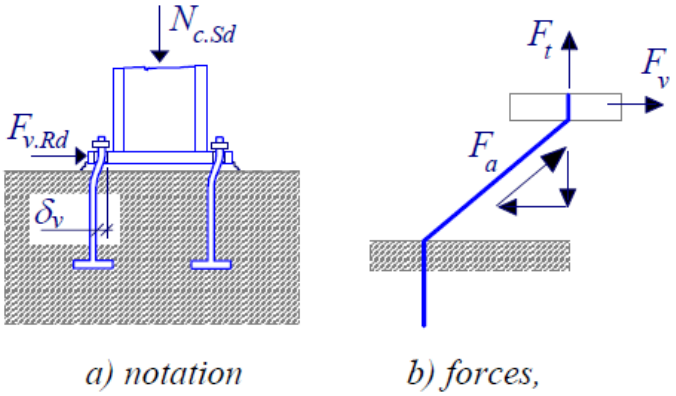


Figure 2.23 - Behavior of an anchor bolt loaded by shear [14]

The friction resistance may be determined as follows:

$$F_{f,Rd} = C_{f,d}\, N_{c,Ed} \tag{2.72}$$

Where $C_{f,d}$ is the friction coefficient between the base plate and the grout layer (for sand-cement mortar $C_{f,d}$ =0.20). The $N_{c,Ed}$ is the design value of the normal compressive force in the column. Only the anchor bolts in the compressed part of the base plate may be used to transfer shear force. Therefore, if the normal force applied in the column is a tension force, the friction resistance is zero ($F_{f,rd}$=0).

Regarding the design shear resistance of an anchor bolt, $F_{vb,rd}$ bolt, it should be taken as the smallest value of:

- $F_{1,vb,Rd}$, the design shear resistance of the anchor bolt (calculate according Table 3.4 of EN 1993-1-8 [1]);

$$F_{1,vb,Rd} = \frac{\alpha_v\, f_{ub}\, A_s}{\gamma_{M2}} \tag{2.73}$$

- $F_{2,vb,Rd}$, the bearing resistance for the anchor bolt-base plate (formula from cl. 6.2.2 (7) of EN 1993-1-8 [1])

$$F_{2,vb,Rd} = \frac{\alpha_b\, f_{ub}\, A_s}{\gamma_{M2}} \tag{2.74}$$

Where:

$$\alpha_b = 0{,}44 - 0{,}0003 f_{yb} \tag{2.75}$$

Finally, the design shear resistance of column bases is given by:

$$F_{v,Rd} = F_{f,Rd} + n\, F_{vb,Rd} \tag{2.76}$$

Where n is the number of anchor bolts.

2.3.5 COLUMN BASE ONLY SUBJECTED TO COMPRESSION

The resistance of column bases under simple compression is obtained according to cl. 6.2.8.2. of EN 1993-1-8 [1]. The model assumes that the resistance is given by three equivalent T-stubs which do not overlap each other: one T-stub for the column web and two for the column flanges, see Figure 2.24. The design resistance $N_{j,Rd}$ is obtained by adding the individual design resistance $F_{C,Rd}$ of each T-stub (calculated according to subchapter 2.3.2.1).

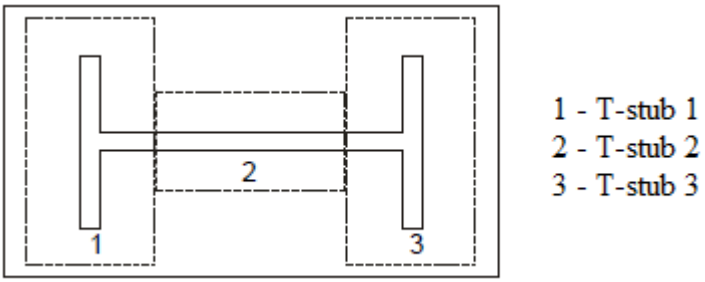


Figure 2.24 - T-stubs under compression [1]

2.3.6 ASSEMBLY

2.3.6.1 Bending resistance

When analyzing the joint's resistance, special attention should be given to the serviceability and the ultimate limit states. For the ultimate limit state, the failure load of the connection is important but, at this load large deformations of the joint and cracks in the concrete are expected. As a result, it is important that, under service loads, the concrete will not fail. This would lead to cracks first, then, with time, to a corrosion of the reinforcement of the concrete wall and, finally, to a failure of the construction [10].

Based on the combination of acting loads (axial force, N_{Ed}, and bending moment, M_{Ed}), see Figure 2.25, three patterns can be identified:

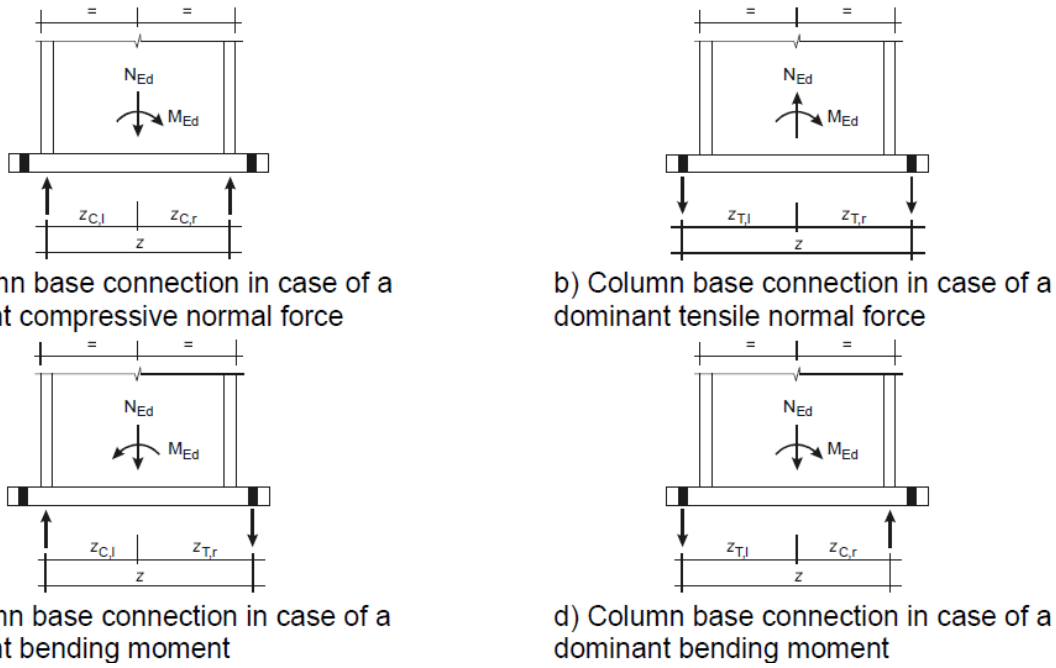


Figure 2.25 – Mechanical models of resistance for bending about the strong axis [1]

Pattern 1 – dominant compression axial force and no tension in the anchor bolts. The collapse of the connection is due to the concrete failure. (Figure 2.25a)

Pattern 2 – dominant bending moment leading to tension in one anchor bolts row and compression in the concrete. When collapsing, the concrete strength is not reached and the failure is due to yielding of the bolts or due to a plastic mechanism in the base plate. (Figure 2.25c and d)

Pattern 3 – dominant tension axial force which leads to tension in both rows of anchor bolts. The collapse is due to yielding of the bolts or because of a plastic mechanism in the base plate. (Figure 2.25b)

The calculation of the column base resistance $M_{j,Rd}$, based on the plastic force equilibrium on the base plate and applied in cl.6.2.8.3 of EN1993-1-8 [1], is described in [15]. The equilibrium is made by considering two reaction forces ($F_{C,Rd}$ and $F_{T,Rd}$) combined according Figure 2.25. The compression force is assumed to be located at the centre of the compressed part and the tensile force at the anchor bolts row or in the middle when there are more rows or bolts.

The tension resistance, $F_{T,Rd}$, is calculated as presented in subchapter 2.3.1.1 (for prying case or no prying case, respectively):

$$F_{T,Rd} = min\left(F_{T,1,Rd}, F_{T,2,Rd}, F_{T,3,Rd}\right) \tag{2.13}$$

$$F_{T,Rd} = min\left(F_{T,1-2,Rd}, F_{T,3,Rd}\right) \tag{2.14}$$

The compression resistance, $F_{C,Rd}$, is taken as the minimum value of the resistance of the component concrete in compression and base plate in bending, $F_{c,pl,Rd}$ (subchapter 2.3.2.1), and the resistance of the component column flange and web in compression, $F_{c,fc,Rd}$ (subchapter 2.3.3):

$$F_{C,Rd} = min\left(F_{c,pl,Rd}; F_{c,fc,Rd}\right) \tag{2.77}$$

For simplicity, only the contribution of the concrete under the flanges is taken into account for the compressive capacity, $F_{c,pl,Rd}$ (T-stub 2 from Figure 2.24, corresponding to the web, is omitted).

The method distinguishes between the resisting parts according to their location: right (index *r*) or left (index *l*); which makes it easier to apply to non-symmetric joints.

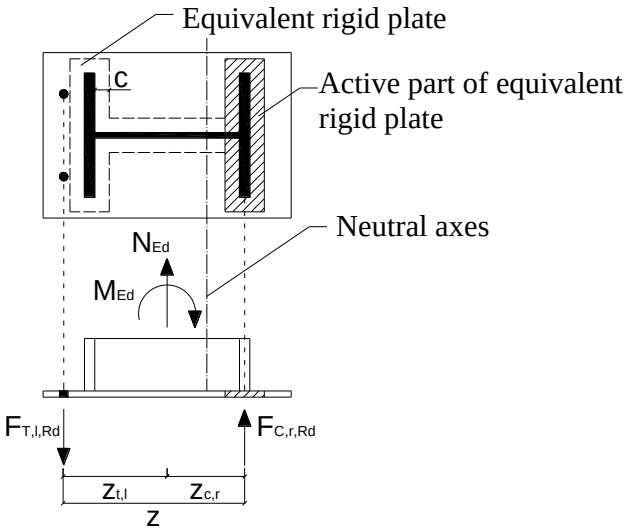


Figure 2.26 - Equilibrium of forces on the base plate in case of a dominant bending moment

The example of tension on the left and compression on the right (Figure 2.26) will be used to explain how the formulas of the Table 6.7 of EN 1993-1-8 [1] were obtained. It is important to note that, when the axial force is a tension force, the value of, N_{Ed}, is positive. When it is a compression force, N_{Ed} assumes a negative value.

From the equilibrium equations:

$$M_{Ed} \leq F_{T,l,Rd} z - N_{Ed} z_{C,r} \tag{2.78}$$

$$M_{Ed} \leq F_{C,r,Rd} z + N_{Ed} z_{T,l} \tag{2.79}$$

Thus, the moment capacity is given by:

$$M_{Rd} = min \begin{cases} F_{T,l,Rd}\, z - N_{Ed}\, z_{C,r} \\ F_{C,r,Rd}\, z + N_{Ed} z_{T,l} \end{cases} \tag{2.80}$$

However, according to Eurocode 3 [1], the moment capacity of the joint is calculated for a given eccentricity:

$$e = \frac{M_{Ed}}{N_{Ed}} = \frac{M_{Rd}}{N_{Rd}} \tag{2.81}$$

Then, equations (2.78) and (2.79) can be rewritten as:

$$M_{Ed} \leq \frac{F_{T,l,Rd} z}{z_{C,r}/e + 1} \tag{2.82}$$

$$M_{Ed} \leq \frac{-F_{C,r,Rd} z}{z_{T,l}/e + 1} \tag{2.83}$$

Hence, the moment of resistance of the joint, $M_{j,Rd}$, is:

$$M_{j,Rd} = min \begin{cases} \dfrac{F_{T,l,Rd} z}{z_{C,r}/e + 1} \\ \dfrac{-F_{C,r,Rd} z}{z_{T,l}/e - 1} \end{cases} \tag{2.84}$$

This case is valid for situations in which $N_{Ed}>0$ and $e>z_{T,l}$ or $N_{Ed}\leq 0$ and $e\leq -z_{C,r}$.

Table 2.3 has all the formulas required to calculate the bending resistance of column bases for each situation presented in Figure 2.25. The calculation of the lever arms is calculated in agreement with the same figure.

Table 2.3 - Design moment capacity $M_{j,Rd}$ of column bases [1]

Loading	Lever arm z	Design moment capacity $M_{j,Rd}$	
Left side in tension Right side in compression	$z = z_{T,l} + z_{C,r}$	$N_{Ed}>0$ and $e>z_{T,l}$	$N_{Ed}\leq 0$ and $e\leq -z_{C,r}$
		The smallest value of $\frac{F_{T,l,Rd}\, z}{z_{C,r}/e+1}$ and $\frac{-F_{C,r,Rd}\, z}{z_{T,l}/e-1}$	
Left side in tension Right side in tension	$z = z_{T,l} + z_{T,r}$	$N_{Ed}>0$ and $0<e<z_{T,l}$	$N_{Ed}>0$ and $-z_{T,r}<e\leq 0$
		The smallest value of $\frac{F_{T,l,Rd}\, z}{z_{T,r}/e+1}$ and $\frac{F_{T,r,Rd}\, z}{z_{T,l}/e-1}$	
Left side in compression Right side in tension	$z = z_{C,l} + z_{T,r}$	$N_{Ed}>0$ and $e<-z_{T,r}$	$N_{Ed}\leq 0$ and $e>z_{C,l}$
		The smallest value of $\frac{-F_{C,l,Rd} z}{z_{T,r}/e+1}$ and $\frac{F_{T,r,Rd} z}{z_{C,l}/e+1}$	
Left side in compression Right side in compression	$z = z_{C,l} + z_{C,r}$	$N_{Ed}\leq 0$ and $0<e<-z_{C,l}$	$N_{Ed}\leq 0$ and $z_{C,r}<e\leq 0$
		The smallest value of $\frac{-F_{C,l,Rd} z}{z_{C,r}/e+1}$ and $\frac{-F_{C,r,Rd} z}{z_{C,l}/e-1}$	
$M_{Ed}>0$ is clockwise, $N_{Ed}>0$ is tension $e = \frac{M_{Ed}}{N_{Ed}} = \frac{M_{Rd}}{N_{Rd}}$			

2.3.6.2 Stiffness

The process for calculating the bending stiffness of column bases can be found in cl. 6.3.4 of EN 1993-1-8 [1] and is described in [15]. The procedure is based on the deformation stiffness of the main components and it is compatible with beam-to-column model. The difference between these two methods is that, in column bases, the normal force has to be introduced.

Thus, the mechanical model used for the calculation of the stiffness will depend on the combination of the acting loads. Therefore, similarly to the resistance case, there are four possible basic collapse modes, as shown in Figure 2.27.

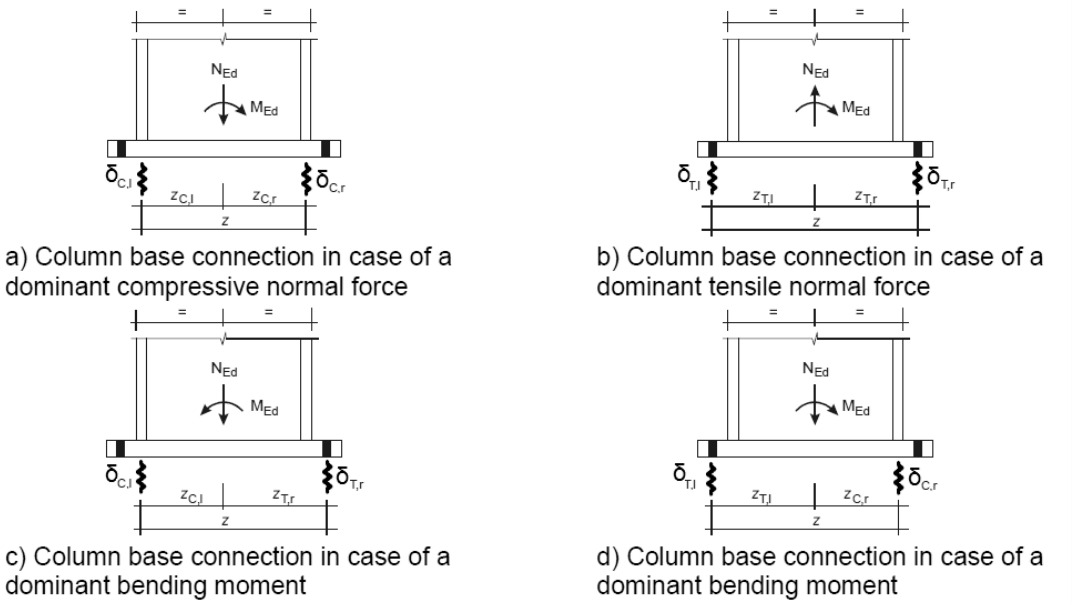


Figure 2.27 - Mechanical models of stiffness for bending about the strong axis, adapted from [1]

As it has been mentioned above, this calculation method accounts for the contribution of the axial force. Therefore, the initial stiffness is calculated for a given constant eccentricity, *e*. This means that the method assumes proportional loading (normal force and bending moment increase in the joint by the same ratio – *e*). In addition, the eccentricity, e_k, at which the rotation is zero, is also considered in the process.

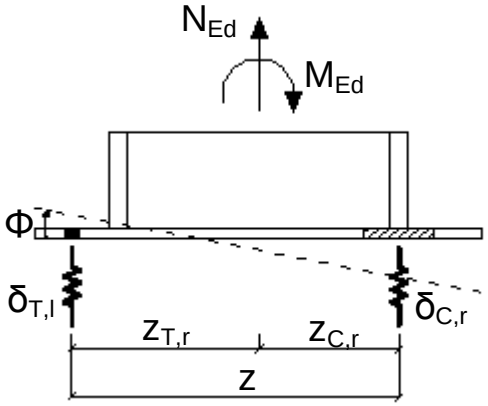


Figure 2.28 - Mechanical model in the case of a dominant bending moment

The stiffness estimation of the components needed for the procedure was described in previous sections of this work (stiffness of the tension component, k_T , is presented in subchapter 2.3.1.3 and stiffness of the compressed component, k_C, in subchapter 2.3.2.2).

The method is now described for the example shown in Figure 2.28. The elastic deformation of the base plate is expected and deformations of tension ($\delta_{T,l}$) and compression ($\delta_{C,r}$) parts are calculated:

$$\delta_{T,l} = \frac{F_{T,l}}{E\ k_{T,l}} \tag{2.85}$$

$$\delta_{C,r} = \frac{F_{C,r}}{E\ k_{C,r}} \tag{2.86}$$

Rewriting formulas (2.78) and (2.79) in function of the components resistance:

$$F_{T,l} \geq \frac{M_{Ed}}{z} + \frac{N_{Ed}\ z_{C,r}}{z} \tag{2.87}$$

$$F_{C,r} \geq \frac{M_{Ed}}{z} - \frac{N_{Ed}\ z_{T,l}}{z} \tag{2.88}$$

And replacing these parameters of resistance in equations (2.85) and (2.86):

$$\delta_{T,l} = \frac{\frac{M_{Ed}}{z} + \frac{N_{Ed}\ z_{C,r}}{z}}{E\ k_{T,l}} \Leftrightarrow \delta_{T,l} = \frac{M_{Ed} + N_{Ed}\ z_{C,r}}{E\ z\ k_{T,l}} \tag{2.89}$$

$$\delta_{C,r} = \frac{\frac{M_{Ed}}{z} - \frac{N_{Ed}\ z_{T,l}}{z}}{E\ k_{C,r}} \Leftrightarrow \delta_{C,r} = \frac{M_{Ed} - N_{Ed} z_{T,l}}{E\ z\ k_{C,r}} \tag{2.90}$$

The rotation of the column base can be calculated by:

$$\phi = \frac{\delta_{T,l} + \delta_{C,r}}{z} \Leftrightarrow \phi = \frac{1}{E\ z^2}\left(\frac{M_{Ed} + N_{Ed}\ z_{C,r}}{k_{T,l}} + \frac{M_{Ed} - N_{Ed} z_{T,l}}{k_{C,r}}\right) \tag{2.91}$$

Hence, the eccentricity, e_k, under zero rotation is obtained through expression (2.91):

$$\phi = \frac{1}{E\ z^2}\left(\frac{N_{Ed} e_k + N_{Ed}\ z_{C,r}}{k_{T,l}} + \frac{N_{Ed} e_k - N_{Ed} z_{T,l}}{k_{C,r}}\right) = 0 \tag{2.92}$$

$$\Rightarrow e_k = \frac{z_{C,r} k_{C,r} - z_{T,l} k_{T,l}}{k_{C,r} + k_{T,l}} \tag{2.93}$$

The bending stiffness of the base plate depends on the acting moment:

$$s_{j.ini} = \frac{M_{Ed}}{\phi} \tag{2.94}$$

By knowing that $e = \frac{M_{Ed}}{N_{Ed}} = \frac{M_{Rd}}{N_{Rd}}$, the initial stiffness of the column base is derived based on the above formula [15]:

$$s_{j.ini} = \frac{M_{Ed}}{M_{Ed} + N_{Ed}\ e_k} \frac{E\ z^2}{\left(1/k_{T,l} + 1/k_{C,r}\right)} = \frac{e}{e + e_k} \frac{E\ z^2}{\left(1/k_{T,l} + 1/k_{C,r}\right)} \tag{2.95}$$

The non-linear part of the moment-rotation curve (where $2/3M_{j,Rd} < M_{Ed} \leq M_{j,Rd}$) is represented by the stiffness ratio, μ:

$$\mu = \left(1.5 \frac{M_{Ed}}{M_{j,Rd}}\right)^{\Psi} \tag{2.96}$$

Here the coefficient Ψ is obtained from Table 6.8 of EN 1993-1-8 [1]. For base plate connections it assumes the value of 2,7.

Since $\mu=S_{j,ini}/S_{j,}$, the joint stiffness is obtained by:

$$S_j = \frac{E\,z^2}{\mu\left(1/k_T + 1/k_C\right)}\frac{e}{e+e_k} \tag{2.97}$$

This means that for the elastic part of the curve $\mu=1$ ($M_{Ed}\leq 2/3M_{j,Rd}$).

In conclusion, Table 2.4 presents the expressions for obtaining the rotational stiffness for the cases shown in Figure 2.27.

Table 2.4 - Rotational stiffness for column bases [1]

Loading	Lever arm z	Rotational stiffness S_j	
Left side in tension Right side in compression	$z = z_{T,l} + z_{C,r}$	$N_{Ed}>0$ and $e>z_{T,l}$	$N_{Ed}\leq 0$ and $e\leq -z_{C,l}$
		$\frac{E\,z^2}{\mu\left(1/k_{T,l}+1/k_{C,r}\right)}\frac{e}{e+e_k}$ where $e_k = \frac{z_{C,r}\,k_{C,r} - z_{T,l}\,k_{T,l}}{k_{T,l}+k_{C,r}}$	
Left side in tension Right side in tension	$z = z_{T,l} + z_{T,r}$	$N_{Ed}>0$ and $0<e<z_{T,l}$	$N_{Ed}>0$ and $-z_{T,r}<e\leq 0$
		$\frac{E\,z^2}{\mu\left(1/k_{T,l}+1/k_{T,r}\right)}\frac{e}{e+e_k}$ where $e_k = \frac{z_{T,r}\,k_{T,r} - z_{T,l}\,k_{T,l}}{k_{T,l}+k_{T,r}}$	
Left side in compression Right side in tension	$z = z_{C,l} + z_{T,r}$	$N_{Ed}>0$ and $e<-z_{T,r}$	$N_{Ed}\leq 0$ and $e>z_{C,l}$
		$\frac{E\,z^2}{\mu\left(1/k_{T,r}+1/k_{C,l}\right)}\frac{e}{e+e_k}$ where $e_k = \frac{z_{T,r}\,k_{T,r} - z_{C,l}\,k_{C,l}}{k_{T,r}+k_{C,l}}$	
Left side in compression Right side in compression	$z = z_{C,l} + z_{C,r}$	$N_{Ed}\leq 0$ and $0<e<z_{C,l}$	$N_{Ed}\leq 0$ and $z_{C,r}<e\leq 0$
		$\frac{E\,z^2}{\mu\left(1/k_{C,l}+1/k_{C,r}\right)}\frac{e}{e+e_k}$ where $e_k = \frac{z_{C,r}\,k_{C,r} - z_{C,l}\,k_{C,l}}{k_{C,l}+k_{C,r}}$	
$M_{Ed}>0$ is clockwise, $N_{Ed}>0$ is tension $e = \frac{M_{Ed}}{N_{Ed}} = \frac{M_{Rd}}{N_{Rd}}$			

It is worth noting that there is also the possibility to compute the stiffness for cases of non-proportional loading. Non-proportional loading means that the axial force is applied to the column base first, and then the bending moment is applied (i.e. constant normal force and variable eccentricity). However, this is not expected to happen in the reality of steel structures. Nevertheless, most of the experiments done for this kind of joints are made with this type of loading.

Figure 2.30 shows the difference between the moment-rotation curves for proportional loading and non-proportional loading. As it is easy to understand, the stiffness in the case of non-proportional loading is higher than in the case of proportional loading. This is due to the presence of the axial force in the column, which keeps the base plate in contact with the concrete in case of low bending moments. Only when the axial force and the moment have the same value ($M_{Ed=}e_k N_{Ed}$), the rotations in the joint are identical for both loading cases (rotation is zero) [16].

For this type of loading, where the axial force is applied first, the initial stiffness is derived according to:

$$s_{j.ini} = \frac{M_{Ed} - e_k\, N_{Ed}}{\phi} \tag{2.98}$$

Resulting expression is [9]:

$$s_{j.ini} = \frac{E\, z^2}{\left({}^{1}/_{k_{T,l}} + {}^{1}/_{k_{C,r}}\right)} \tag{2.99}$$

This means that for these cases, the initial stiffness is calculated the same way as regular joints, like it is described in EN 1993-1-8 [1] cl. 6.3.1(4).

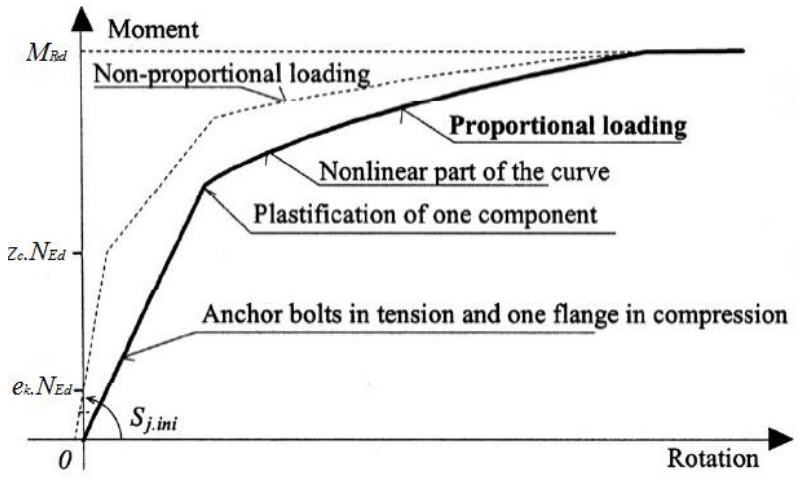


Figure 2.29 - Moment-rotation curves for non-proportional loadings and proportional loadings [15]

2.4 CLASSIFICATION OF COLUMN BASE JOINTS

2.4.1 ACCORDING TO RESISTANCE

The classification according to resistance can be found in EN 1993-1-8 [1] cl 5.2.3. The joint is classified as pinned, full-strength or partial-strength. When the design moment capacity of the joint is lower than 25% of the design plastic moment capacity of the column, the joint is nominally-strength (pinned). Whereas the full-strength joint has the design moment capacity superior to the design plastic moment capacity of the column connected to it. This means that the column has the full capacity to absorb all the acting loads, thus the plastic mechanism will happen in the column and not in the joint. In addition, there is an intermediate state where the joint is named as partial-strength joint. In this case, the plastic mechanism can develop in the joint resulting in a more ductile behavior and consequently a redistribution of the internal forces.

In summary, the joint is classified as:

- Pinned if $M_{j,Rd} < 0{,}25 M_{pl,rd}$
- Partial-strength if $0{,}25 M_{pl,rd} \leq M_{j,Rd} \leq M_{pl,rd}$
- Full-strength: if $M_{j,Rd} > M_{pl,rd}$

2.4.2 ACCORDING TO STIFFNESS

Depending on the structural system (sway or non-sway frames), different rigid stiffness boundaries for the classification of column bases may be derived. Derivation of the boundaries is based on a sensitivity study of the structural system to the variation of the rotational stiffness properties of column bases [16].

The limits that allow the classification of a joint as rigid are described EN 1993-1-8 [1] cl. 5.2.2.5(2). In case the joint is part of a non-sway frame (where the bracing system reduces the horizontal displacement by at least 80% and where the effects of deformation may be neglected), the joint is classified as rigid if:

- $\lambda_0 \leq 0.5$
- $0.5 < \lambda_0 < 3{,}93$ and $S_{j,ini} \geq 7(2\lambda_0 - 1)EI_c/L_c$
- $\lambda_0 \geq 3{,}93$ and $S_{j,ini} \geq 48EI_c/L_c$

Where λ_0 is the slenderness of a column in which both ends are assumed to be pinned; I_c and L_c are the inertia of the cross section of the column and the height of the column, respectively.

For all the other cases (sway frames), the joint is rigid if:

- $S_{j,ini} \geq 48EI_c/L_c$

A schematic representation of the boundaries between rigid and semi-rigid joints for both cases, sway frames and non-sway frames, is shown in Figure 2.30. For the sway frames, a particular value of the slenderness was chosen for the illustration ($\lambda_0 = 1{,}36$).

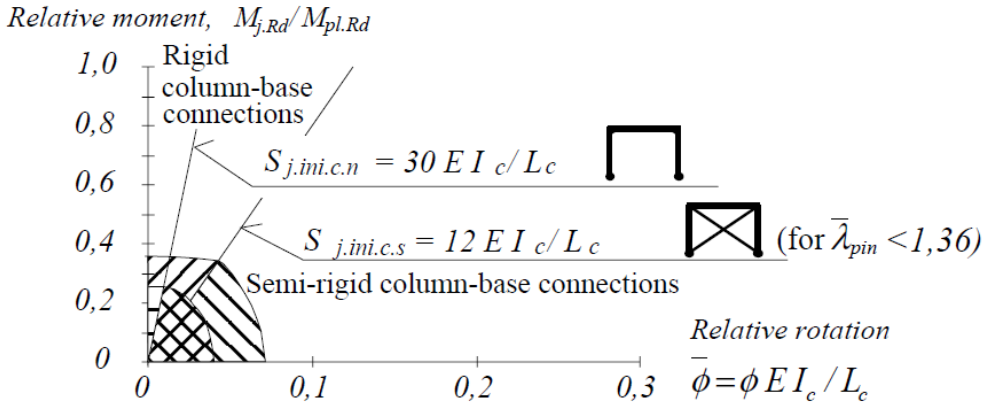


Figure 2.30 - Proposed classification system according to the initial stiffness [16]

3
NUMERICAL MODEL

3.1 INTRODUCTION

In this chapter the behavior of column bases subjected to strong axis bending is studied through the Finite Element Method (FEM). The main goal is to compare the results provided by the FE model with the results provided by the component method for a proportional type of loading (i.e., axial force and bending moment increase by the same factor, representing a constant load eccentricity).

The ABAQUS software was selected for this purpose and the geometry and boundary conditions of the numerical model were chosen to best simulate a column base used in experiments carried out at Brno University Technology [17]. This would make possible validating the model by subjecting it to the same types of loading used in the experiments (strong axis bending and biaxial bending with non-proportional loading) and comparing the moment-rotation diagrams obtained by the model with the corresponding experimental diagrams.

Thus, after validating the model, the column is subjected to strong axis bending, with a proportional loading, to obtain the moment capacity and initial stiffness of the joint and then compare them with the results provided by the component method.

3.2 MODEL DESCRIPTION

The components of the connection were modeled using the graphical interface CAE of ABAQUS. The model is expected to reproduce the column base tested in experiments carried out at Brno University of Technology [17]. Thus, for a simplified model, only the main components of the connection were modeled: base plate, column, bolts and concrete block. The shear lug was not represented. Moreover, since the most important function of the grout layer is the transmission of the friction forces, this model does not include this component but it is represented by considering a proper contact interaction, so that these forces are transmitted from the base plate to the concrete block.

The column, which cross section is HEB 240 and steel grade is S235, was modeled with the height of 1,83m which corresponds to the height where the horizontal force was applied in the experiment. The base plate, with size 440x330x20mm and steel grade also S235, is welded to the bottom of the column. To avoid convergence problems caused by the contacts and boundary conditions, only one part was created for these two components (see Figure 3.1a). The welds are introduced in the model because their presence causes a bigger resistance of the joint by reducing the distance between the bolts and the side of the column (especially for the case of bending about the strong axis).

The concrete block is made of grade C16/20 and its size is 1500x1000x400mm. The holes for introducing the bolts were represented (see Figure 3.1b).

To prevent unnecessary geometry complexities, the anchor bolts of steel grade 8.8 were modeled with a cylinder shape which diameter was chosen so that it corresponds to a tensile area of 220mm^2. This area is considered because in the experiment the bolts were milled off so that the strain gauge could be glued to its surface. The bolts are fully connected to steel plates of grade S235 and size 60x60x20mm (see Figure 3.1c), which means that only one part was created for bolts and these plates.

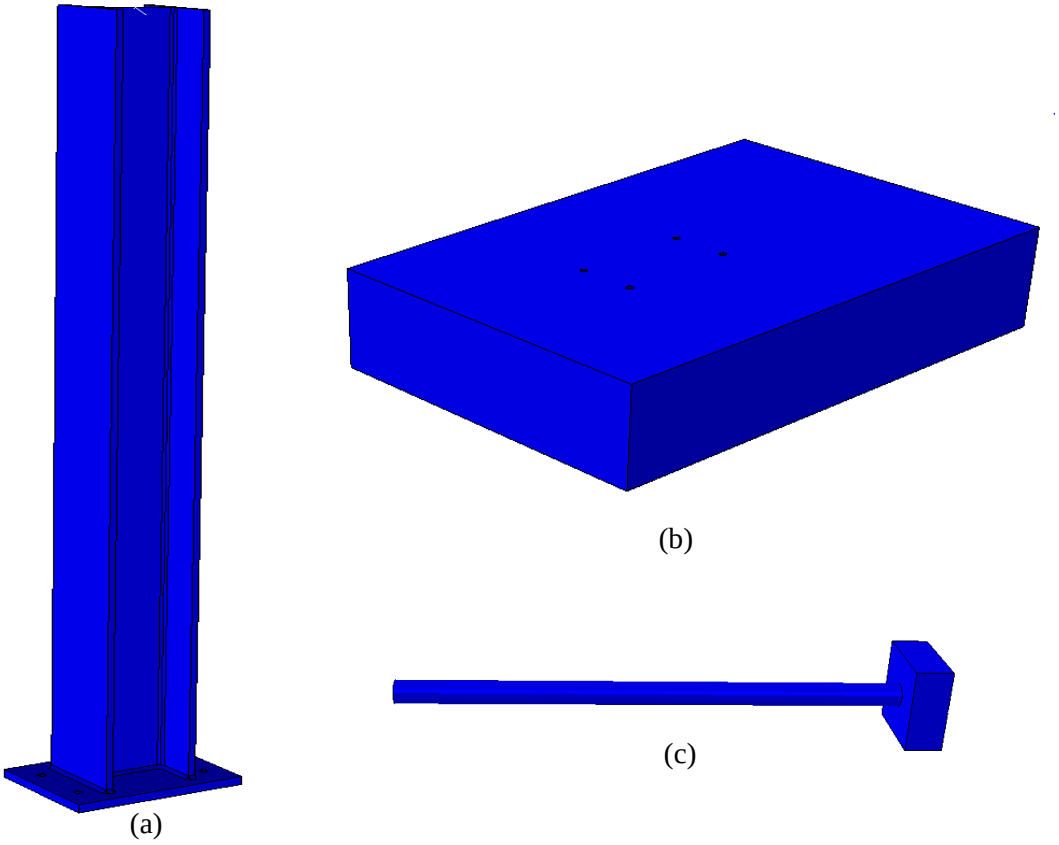


Figure 3.1 - Components of the model: a) column welded to the base plate; b) concrete block; c) bolt and head of the bolt

3.2.1 MATERIAL PROPERTIES

The non-linearity was considered in the material properties of the numerical model. The stress-strain relationships for the structural steel components (column, base plate and bolts) were considered to be quadri-linear [18], as it is shown in Figure 3.2. The modulus of elasticity for steel, *E*, is considered to be 210GPa and the Poisson's ratio, *v*, 0,3. For steel grade S235, the yield stress is 235MPa and the ultimate stress is 360MPa. For the bolts, the yield stress is 660MPa and the ultimate stress is 830MPa. The tangential stiffness after the yield point is taken as 2% of the initial modulus of elasticity until the strain $11\varepsilon_y$ is reached (ε_p). The ultimate strain, ε_u, is equal to $120\varepsilon_y$.

The nominal values were chosen for the definition of the steel material because steel components were not tested in the experiment to find their real values.

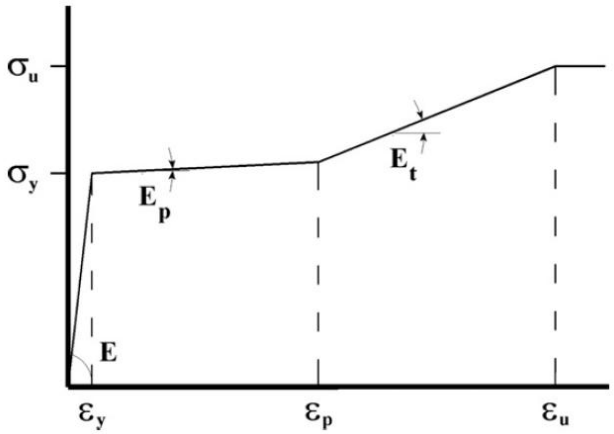


Figure 3.2 - Material behavior used in FEM analysis for column, base plate and anchor bolts [18]

Since the failure of the column base connection tested in [17] was never due to the concrete, but always due the steel components, a simple stress-strain curve was chosen for the concrete material in order to overcome convergence problems. Thus, a bi-linear relationship is considered with corresponding young's modulus, ultimate stress and Poisson's ratio of 20,9MPa, 22,6MPa and 0,2, respectively.

3.2.2 ASSEMBLY

The components of the joint were modeled as solid 3D deformable elements. Therefore, each part instance presented its own coordinate system. The assembly was made by arranging the parts in a single unit through the relevant position constrains and translations. Figure 3.3 shows the assembly of the connection parts.

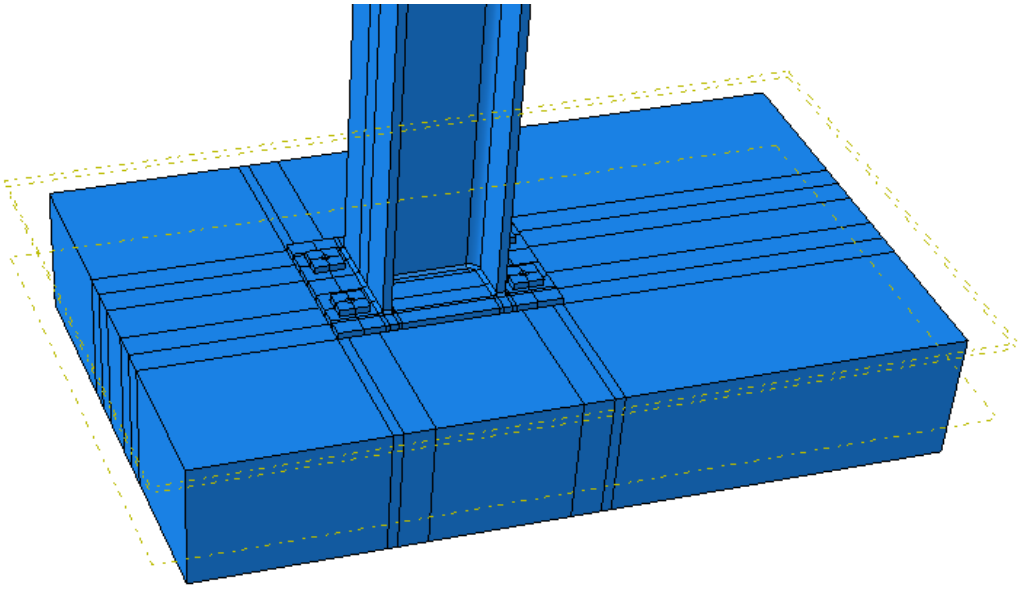


Figure 3.3 - Assembly of the column base connection

3.2.3 CONTACT INTERACTIONS

The assembly module puts everything together but does not establish contact between the elements, even if their surfaces are together. Thereby, the contact must be defined by creating surfaces for the regions that will be together and assigning them the correct contact properties, so that the stresses are transferred through the elements.

One of the most difficult aspects of modeling column bases joints with FEM is to find the appropriate parameters to define the properties of the major contact interfaces: the head of the bolt with the base plate upper surface; the base plate lower surface with the concrete upper surface; and the anchor bolts lateral surfaces with the surfaces inside the holes of the foundation.

The interface between the base plate and bolt head was considered as a surface-to-surface contact of finite sliding with Coulomb coefficient of 0,3, defined for sliding resistance [18]. For the normal behavior, the "hard" contact was chosen and the separation after contact was permitted. This allows that the pressure is transmitted through the surfaces, as long as there is contact between them. The same method was applied to the interaction between the base plate and the concrete block [18]. In order to model the interaction between the bolts and the concrete, the lateral surfaces of the bolts were tied to the surfaces inside the concrete holes, which will prevent the bolts to have relative displacements with respect to the concrete. This assumption is only possible to take when concrete failure around the bolts is not expected, which is the case of the experiment.

3.2.4 BOUNDARY CONDITIONS

The boundary conditions describe the behavior of the assembled parts in terms of displacement and rotation during the analysis steps. Thus, the only element which has been assigned boundary conditions was the concrete block which is assumed to be fixed to the ground at the bottom only. Thus, all degrees of freedom of the bottom surface of the foundation are constrained, whereas all the degrees of freedom on lateral sides are released.

3.2.5 LOADING AND ANALYSIS STEPS

The loading on the model was introduced by two types of loads: one vertical and one horizontal. The vertical load, *N*, was carried out by pressure which was applied at the upper surface of the column. This load will cause an axial force on the connection. The horizontal load, *F*, was applied by surface traction on the top of the column, which will cause a bending moment at the column base. The angle of the resulting horizontal force with the z axis of the column is 0º for the case of strong axis bending, and 25,56º for the case of out-of-plane bending.

Regarding the analysis steps, for the validation of the model by the comparison with the experimental results three steps were created: the initial step where the boundary conditions and the contact interactions are established; step-1 where the vertical load, *N*, with resulting value of 400KN is applied in its entirety; and step-2 where the horizontal load, *F*, increases until failure of the connection.

The model was used for analyzing the results provided by the component method described in Eurocode 3 [1]. Thus, since the method is only suitable for column bases subjected to proportional loading, which is not the case of the experiment, different steps were created for this matter: an initial step which is the same as the one for validating the model and step-1 which included both loads, vertical and horizontal. These loads assumed values so that they would increase until failure by a

particular ratio (which corresponds to the load eccentricity $e = \frac{M}{N} = \frac{F \times 1,83}{N}$, where M is the bending moment).

3.2.6 ELEMENT TYPE AND MESHING

Meshing is one of the most important features of FEM in order to achieve good accuracy of the stress distribution with a reasonable analysis time. To avoid unnecessarily increase the degrees of freedom of the various part instances, the structured mesh had varying densities according the interest of the regions, being denser around the places where there are stress concentrations (see Figure 3.4).

In the model, an 8 node brick with 3 degrees of freedom (C3D8R) solid and continuum element type was chosen to model all the components of the joint. If these elements are fine enough, they provide better results for high nonlinearities and plate warping that might develop due to the creation of prying forces during the analysis, than the 20 node brick elements [18].

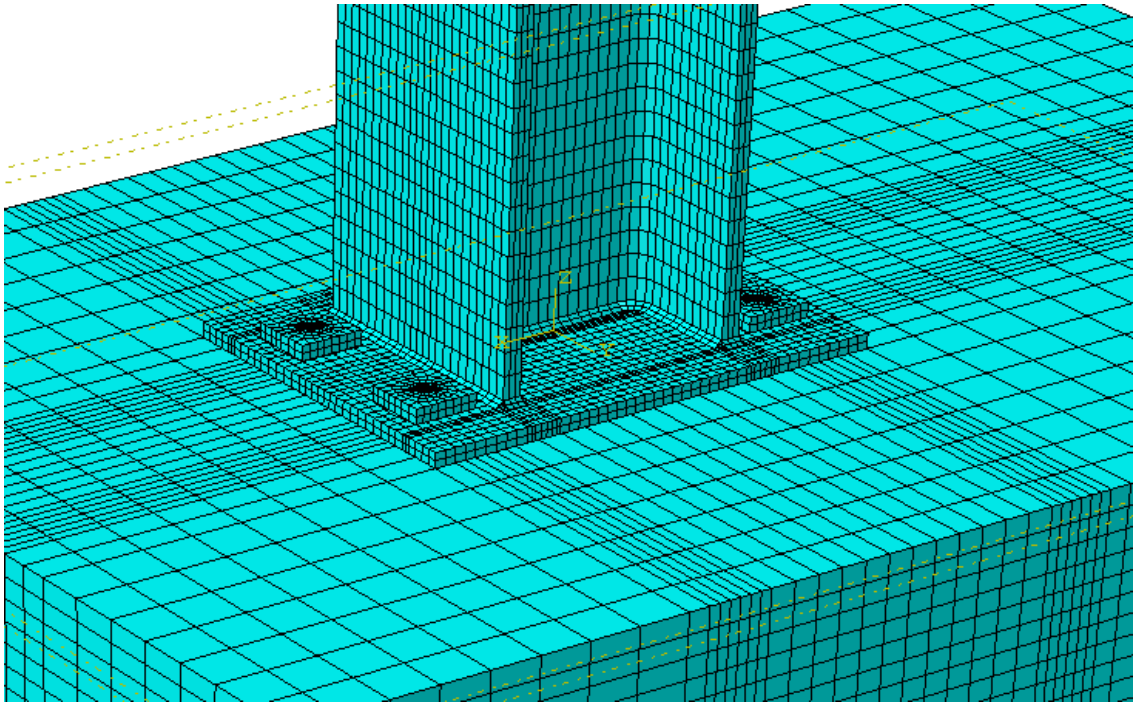


Figure 3.4 - Mesh of the column base assembly

3.3 VALIDATION OF THE NUMERICAL MODEL

For the correct validation of the model, there was an effort to find experiments made to a column base subjected to bending. This tested column base had to have valid geometry for comparing the component method described in Eurocode 3 [1], since that is the main goal of this chapter. In addition, the numerical model would also be used for the validation of the analytical model (which provides the moment capacity of column bases under weak axis bending or biaxial bending). Thus, it would be appropriate that the tests included weak axis bending or biaxial bending.

However, the number of tests on column bases is very limited, while there are more than a thousand tests published about beam-to-column connections. Furthermore, amongst the small number of

existing experiments, almost all of them focused on in-plane bending (bending about the strong axis of the column). There are some about weak axis bending but almost none focusing on biaxial bending.

Therefore, it is very difficult to find suitable experiments in column bases under weak axis bending or biaxial bending with valid geometry for comparing the component method described in Eurocode 3 [1].

Recently, Brno University of Technology performed tests on a basic type of column base [17], simple enough to be analyzed by the component method. The tests included strong axis bending as well as out-of-plane bending and the main purpose was to analyze the real behavior of statically loaded anchor joints.

Thereby, at present part of the work, this experiment will be explained and the test results are studied. Then, the numerical results are presented for the same types of loading of the experiment and compared with the experimental results.

3.3.1 EXPERIMENTAL TESTS ON A COLUMN BASE

This experiment is part of a research program which focus is the development of a simplified engineering model of steel or steel-to-concrete joints of a structure that should require only the most necessary parameters, geometry and short duration of solution. Therefore, the aim of the study is to find the parameters that mostly influence the precision of the results and the ones that can be neglected, to simplify the model as much as possible but with similar accuracy. These parameters have to be based on experimental research and that is why these tests were performed.

The article where the experiments are presented includes the description of specimen, where the join components are described as well as the loading of the joint, and the test results for weak axis bending and biaxial bending. In the case of strong axis bending, the article also includes a brief comparison between the experimental results and results provided by the component method.

3.3.1.1 Description of specimen

Four specimens consisting of reinforced concrete pad, cast-in anchors and steel column were subjected to a constant compressive force and an increasing bending moment. The geometry and materials used were the same for all the specimens.

The cast-in anchors were made of threaded rods M20, of steel grade 8.8; corresponding nuts and steel plates with dimension 60x60x20mm and a hole in the middle, which served as a head of the bolt; and big washers to cover the holes in base plate. Strain gauges and force washer were introduced in the bolts. Therefore, parts of the thread on the anchor bolts in tension were milled off so the strain gauge could be glued to the bolts surface [17]. Thus, the tensile area was reduced (A_s=220mm^2).

The concrete used was C16/20 and the dimension of the concrete block was 1500mm of length, 1000mm of width and 400mm of height. 136 days after the set-up of the experiment, nine testing specimens (which were prepared with the same concrete at the same time as the blocks used in the test) were tested. The average of the compressive cube strength and the modulus of elasticity were 22,6MPa and 20,9GPa, respectively.

The base plate with 20 mm of thickness was welded to bottom and of column HEB 240. Its dimensions were 330x440 mm. The joint was improved by adding a shear lug which was welded to

the bottom of the base plate. This component was IPE 100 with length 100mm. All these elements were from steel grade S235.

Figure 3.5 shows a schematic detail of the test set-up.

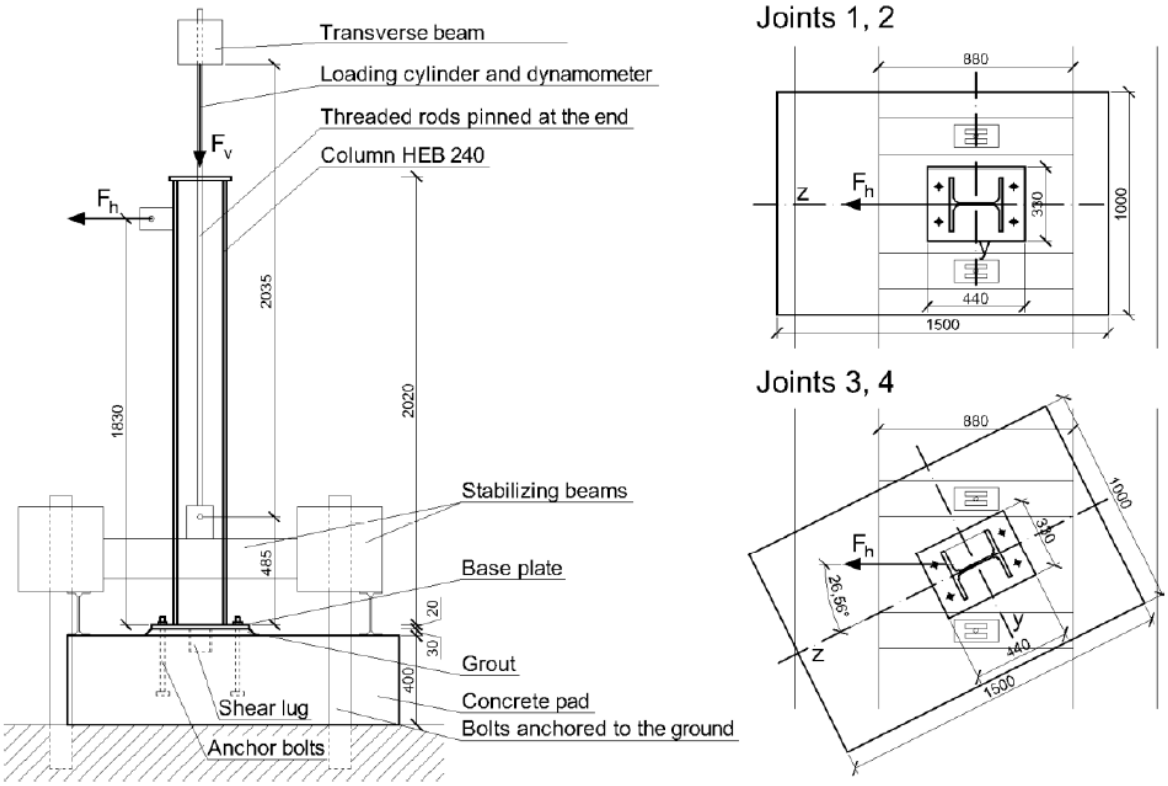


Figure 3.5 - Test set-up [17]

Two types of forces were applied separately to the joint by loading actuators. The axial force was applied first and kept constant at 400KN and then an increasing horizontal force was applied. The horizontal load was applied in the height of 1.83m above the base plate which caused bending moment and shear forces in the column base.

Specimens 1 and 2 were subjected to in-plane bending and specimens 3 and 4 to out-of-plane bending. The biaxial bending of the last specimens was provided by a rotation of 26.56º along the vertical axis (see Figure 3.5).

3.3.1.2 Test results

The moment-rotation curve obtained for the case of bending about the strong axis (specimens 1 and 2) is shown in Figure 3.6. The moment capacity of joint 1 was approximately 195KN.m and 183KN.m for joint 2. The initial stiffness was calculated from the difference between M_y=100KN.m and M_y=20KN.m, and the results were: for joint 1 $s_{j,ini}$=9,32MN.m/rad and for joint 2 $s_{j,ini}$=10,77MN.m/rad.

In the same figure the moment-rotation curve is calculated through the component method described in Eurocode 3 [1]. According to that essay [17], the design moment capacity is M_y=128KN.m for an axial force N_{Ed}=400KN and the initial stiffness is $s_{j,ini}$=22,17KN.m/rad. Thus, by the analysis of these results, it is proved that the component method is very conservative in terms of resistance since there

is an error of more than 30%. Regarding the stiffness, both experimental exhibited approximately half the stiffness estimated with the component method.

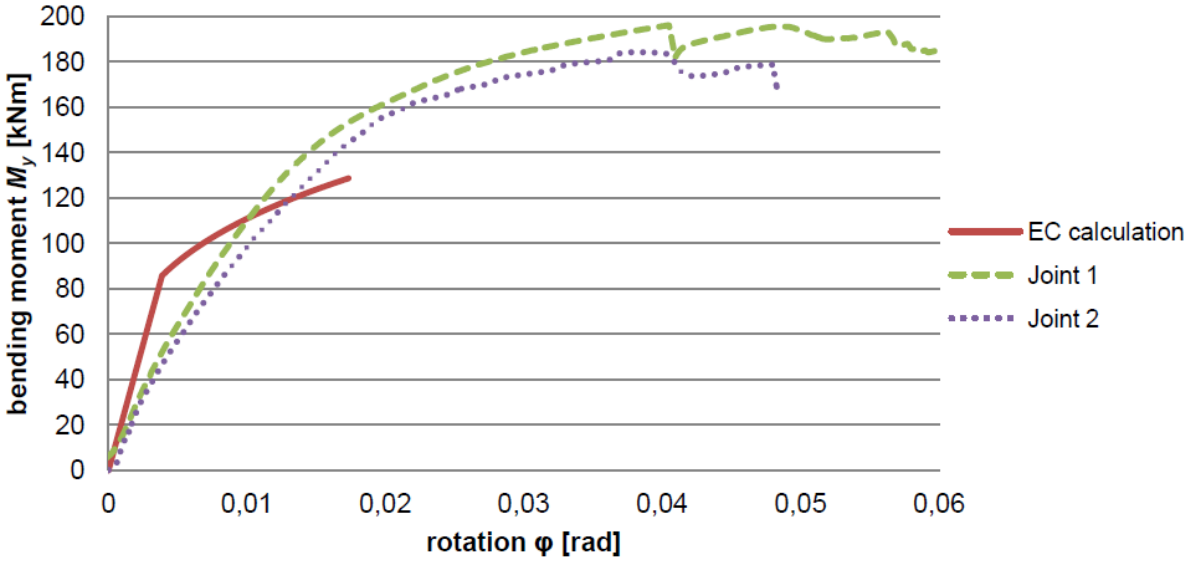


Figure 3.6 - Bending moment-rotation diagram of specimens 1 and 2 subjected to axial force and in-plane bending moment and calculation according to EC3 [17]

For the case of joints 3 and 4, Figure 3.7 shows the moment-rotation diagrams measured in: the plane of bending (curve φ); in the strong axis plane (curve φ_y) and in the weak axis plane (curve φ_z). The moment capacity, for each joint and curve, is approximately: M_3=165KN.m, M_{3y}=148KN.m, M_{3z}=74KN.m, M_4=175KN.m, M_{4y}=157KN.m and M_{4z}=78KN.m. In addition, the measured initial stiffness is: $s_{j,ini,3}$=5,5MN.m/rad, $s_{j,ini,3y}$=5,3MN.m/rad, $s_{j,ini,3z}$=6,7MN.m/rad, $s_{j,ini,34}$=6,9MN.m/rad, $s_{j,ini,4y}$=6,7MN.m/rad and $s_{j,ini,4z}$=9,5MN.m/rad.

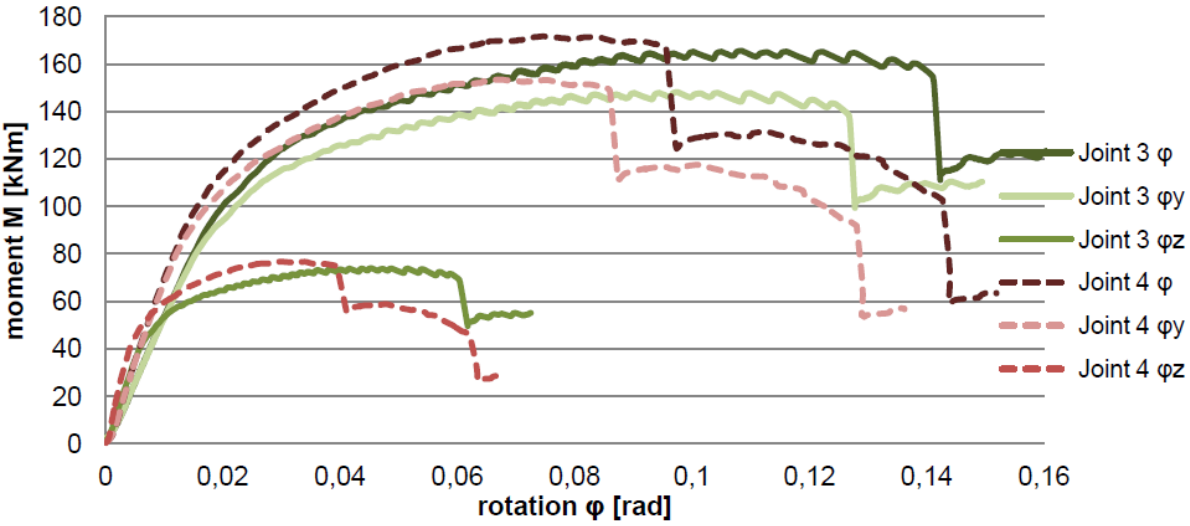


Figure 3.7 - Bending moment-rotation diagram of specimens 3 and 4 subjected to axial force and out-of-plane bending moment [17]

It is important to refer that in all the cases the steel failure (combined failure of the base plate and the anchor bolts) was governing the ultimate resistance of the joint despite that the concrete pad exhibited many cracks [17].

The behavior of the bolts was also studied in the tests. Thus, it is represented in Figure 3.8 the results of the forces on the bolts from joints 1 and 2, measured by force washers and strain gauges. The forces from the strain gauges were obtained by multiplying the measured strain by the modulus of elasticity (E=210GPa) and the reduced cross section of the bolts (A_s=220mm^2). The moment that the bolts start to yield can be noticed when the results of the strain gauges start to differ from the results of the force washers.

For joints 3 and 4, the results of the forces on the bolts were not published because the measurements were not accurate.

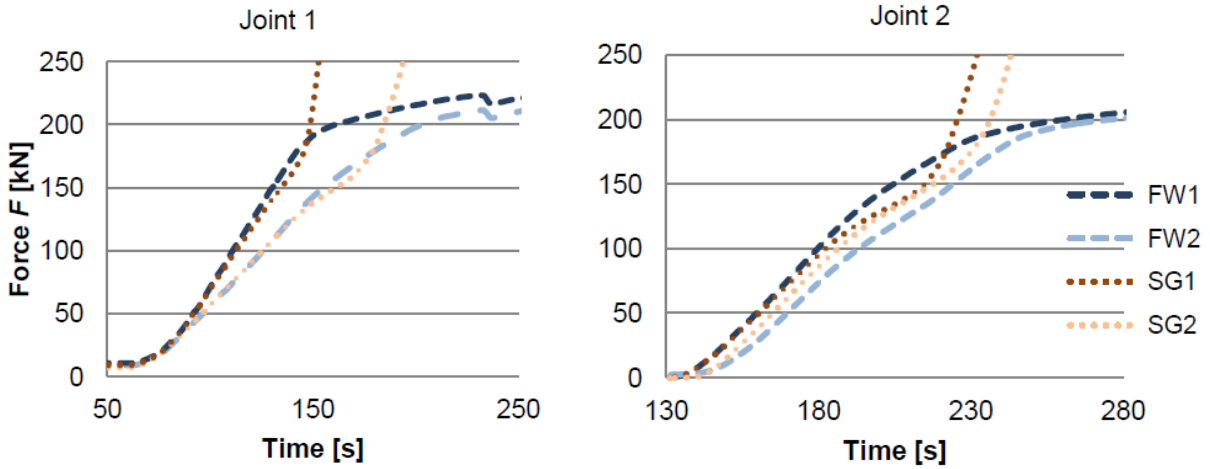


Figure 3.8 - Force on anchor bolts measured with force washers (FW) and straing gauges (SG) [17]

3.3.2 NUMERICAL RESULTS

The experimental results presented were used to validate the numerical model by the comparison of the moment-rotation diagrams, which are represented in Figure 3.9 and Figure 3.10 for strong axis bending and out-of-plane bending (26,56º), respectively. As previously explained the model was loaded in two different stages: first the axial force is applied and only then the bending moment increases until failure of the joint.

As it clear, there are slight differences between the model and the reality which are related to the assumptions made for the material properties and for the connections between the elements. The most significant difference is related to the shape of the curves end, where the experimental curves shows a sharp decrease due to failure of one of the bolts which does not happen in the numerical curves. This is associated to the diagram chosen for representing the material properties of steel where this decrease is not taken into account. Furthermore, there is a disagreement on the ultimate strain in which the model shows a larger strain for the case of strong axis bending and a minor strain for the case of out-of-plane bending. This is also due to the material properties of the model. Nevertheless, this is considered not to be a problem for obtaining proper results of the model.

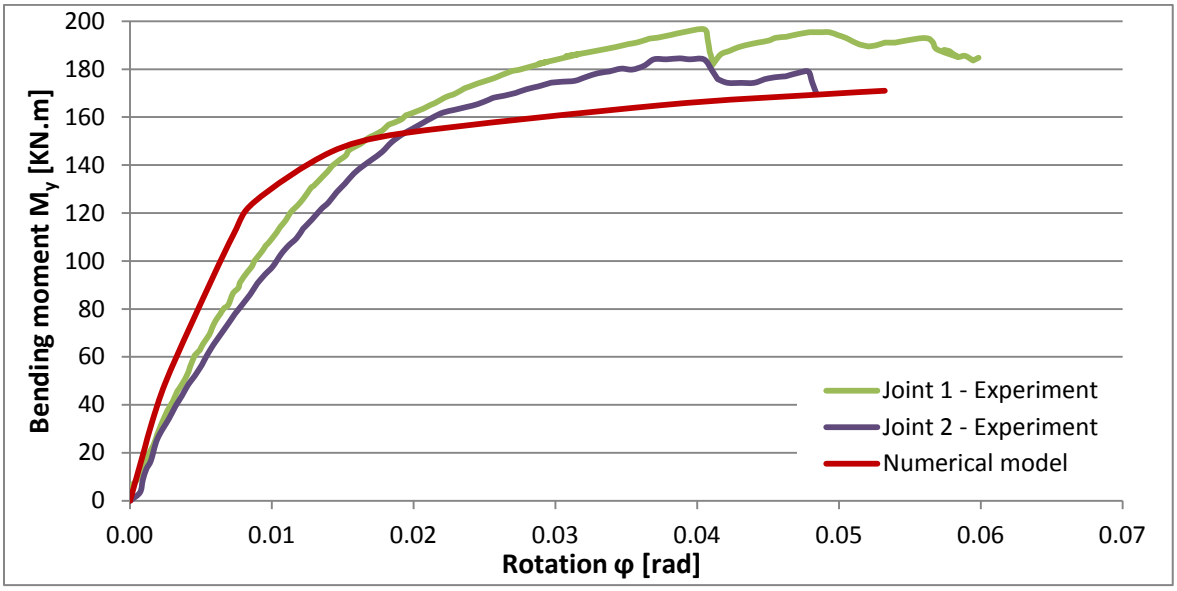


Figure 3.9 - Comparison of moment-rotation diagrams for strong axis bending

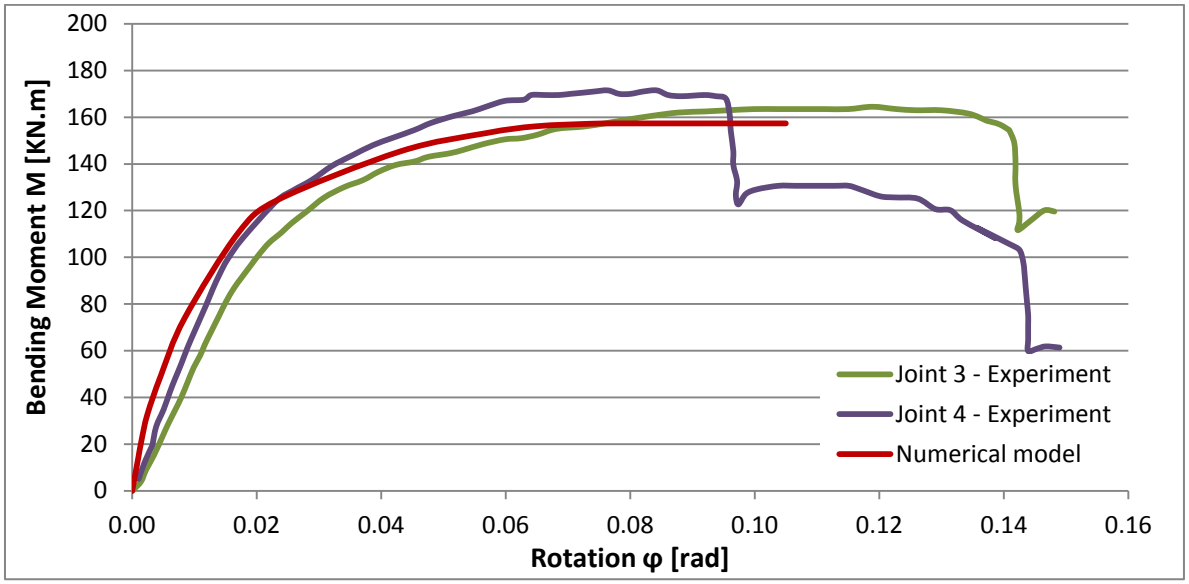


Figure 3.10 - Comparison of moment-rotation diagrams for out-of-plane bending (26,56º)

Concerning the failure of the model, it was always the same as the experiments, in other words, the collapse of the joint was always due to a combined failure of the base plate and the anchor bolts. The point when the steel components start to yield can be found in Figure 3.9 and Figure 3.10 where the slope of the curves changes, right after the initial length which corresponds to the initial stiffness.

Regarding the moment capacity and initial stiffness obtained by the model, Table 3.1 and Table 3.2 show the comparison between the numerical results and the experimental results for the cases of strong axis bending and out-of-plane bending, respectively.

Table 3.1 - Comparison of numerical results with experimental results for strong axis bending

		Moment Capacity [KN.m]	Initial Stiffness [MN.m/rad]
Experiment	Joint 1	195	9,32
	Joint 2	183	10,77
	Average	189	10.05
Numerical results		**173**	**14,25**
Ratio Num./Exp.average		0,92	1,42

Table 3.2 - Comparison of numerical results with experimental results for out-of-plane bending (26,56º)

		Moment Capacity [KN.m]	Initial Stiffness [MN.m/rad]
Experiment	Joint 3	165	5,70
	Joint 4	172	6,96
	Average	169	6,33
Numerical results		**157**	**8,02**
Ratio Num./Exp.average		0,93	1,27

Regarding the joint resistance, the model provides accurate results since the error is less than 10% (ratio for strong axis bending is 0,92 and 0,93 for out-of-plane bending). Concerning the stiffness, numerical results are a bit higher that what was expected (1,42 and 1,27 times higher than the experimental results). However, this difference could be explained by the modulus of elasticity chosen for the steel components. While the concrete used in the experiment was tested to find its real value, the same was not done for the steel components and the design value was selected to characterize the same (210GPa). Nonetheless, the real value can be lower than that (between 190GPa and 210GPa) which would significantly decrease the joint stiffness value. Another explanation would be related to the connections between the elements. In the numerical model, components base plate, welds and column are fully tied which is not what happens in reality.

In conclusion, despite the differences between the model and the experiment, the model gives adequate results for resistance which is the main focus of this work. Thereby, the model is considered to be accurate.

3.4 COMPARISON WITH THE COMPONENT METHOD DESCRIBED IN EUROCODE 3

Even though in the article were the experiment is presented [17] there is already a brief comparison between experimental results and the component method, the type of loading of the experiment was non-proportional (axial force is applied first and only then bending is applied). Since that type of loading is not the focus of the component method described in Eurocode 3[1], it is considered to be appropriate to make a new comparison for a proportional type of loading.

Thus, for the comparison with the component method described in Eurocode 3, a particular eccentricity was chosen, e= -0,25m (which corresponds to a case of a dominant bending moment combined with a compression force), and the column base from the numerical model was subjected to corresponding loads. In Figure 3.11 is the moment-rotation diagram obtained by ABAQUS for the current type of loading and in Table 3.3 is the comparison between the analytical results and the

numerical results, as well as their ratio. The calculation of the analytical results can be found in Annex 1 of this work.

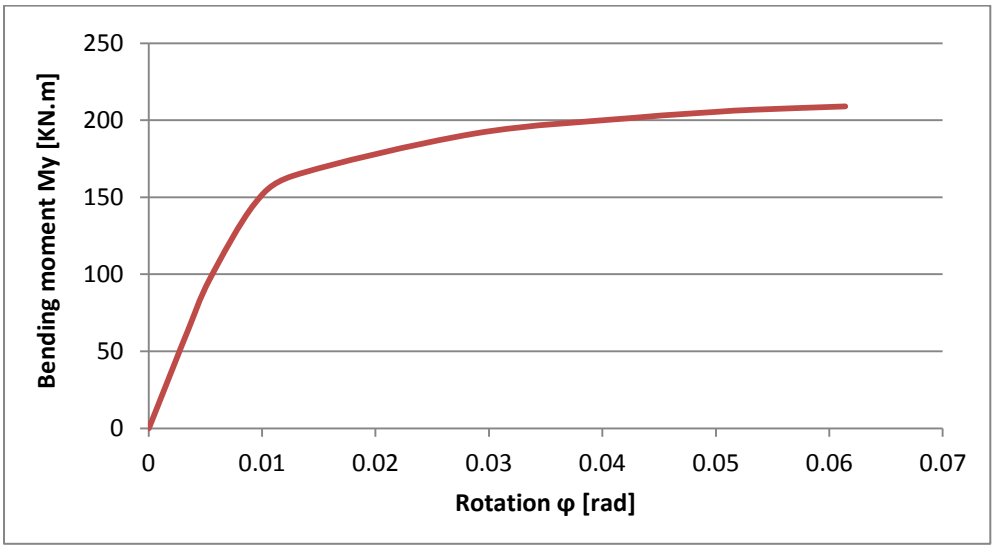


Figure 3.11 - Moment-rotation diagram for strong axis bending with proportional loading (e=-0,250m)

Table 3.3 - Comparison between numerical results and analytical results for strong axis bending with proportional loading (e=-0,25m)

	Moment Capacity [KN.m]	Initial Stiffness [MN.m/rad]
Analytical results	96	33,33
Numerical results	209	18,02
Ratio Analyt./Numer.	0,46	1,85

As it is clear, the component method is very conservative in terms of resistance. Therefore, the solution provided by this method is safe but not economic which should be a concern in further studies. Regarding the stiffness, the method provides results almost twice bigger than the numerical model, similarly to what happened with the comparison with the experimental results. Thus, the calculation of this parameter should also be improved.

4
ANALYTICAL MODEL

4.1 INTRODUCTION

The aim of this chapter is to develop a method that provides the moment capacity of column bases under combined biaxial bending and axial force. Therefore, a M_z-M_y interaction curve should be generated for a constant load eccentricity, $e= M_{Ed}/ N_{Ed}$, based on the moment capacities $M_{y,Rd}$ (resistance for strong axis bending) and $M_{z,Rd}$ (resistance for weak axis bending).

The procedure to determinate the moment capacity for bending about the strong axis was presented in the Chapter 2, which is in line with the component method described in EN 1991-1-8[1]. This method depends on the geometry of the joint and on the eccentricity of the acting loads.

Since the European code does not provide guidance for characterizing the behavior of the joint when it is subjected to bending about its weak axis, a method to compute the moment capacity and initial stiffness for bending about its weak axis is introduced. This procedure is also in accordance with the component method and is based on similar assumptions as the ones made for the strong axis bending. Furthermore, this method also depends on the acting loads since the load eccentricity is required for the calculation.

Although both procedures referred above are independent, it is considered that the eccentricity, e, necessary for their calculation, is obtained for the acting deviated moment, $M_{\alpha,Ed}$ (see Figure 4.1): $e= M_{\alpha,Ed}/N_{Ed}$. The acting deviated moment is calculated by the square root of the some of the squares of the acting moments $M_{y,Ed}$ and $M_{z,Ed}$: $M_{\alpha,Ed} = \sqrt{{M_{y,Ed}}^2 + {M_{z,Ed}}^2}$.

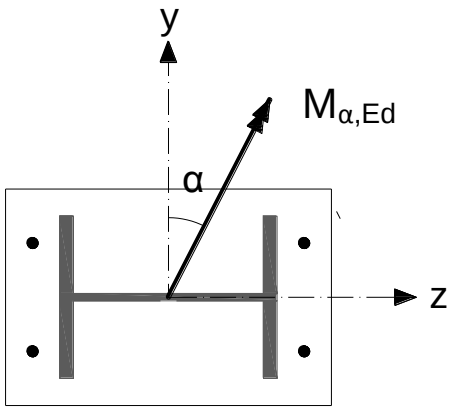


Figure 4.1 - Applied moment in the column base

Thereby, knowing the values of these resistance parameters ($M_{y,Rd}$ and $M_{z,Rd}$), the interaction curve is determined, and the moment capacity of biaxial bending is obtained.

A worked example is presented at the end of this chapter.

4.2 COMPONENT METHOD FOR WEAK AXIS BENDING

The behavior of column bases under bending about the weak axis will be approached through the component method. The final objective is to obtain the moment capacity and the initial stiffness of the joint when subjected to this type of loading.

As it was previously mentioned, the method considers the joints as a set of individual basic components. Thus, the components are analyzed separately by means of resistance and stiffness and their characteristics are assembled together to obtain the structural behavior of the joint.

Regarding the identification of the components, they are the same as for the strong axis bending (see Figure 4.2):

- Base plate in bending and anchor bolts in tension;
- Base plate in bending and concrete in compression;
- The anchor bolts in shear;
- Column web and flange in compression.

However, the tension and compression components behave differently from the case of strong axis bending. Therefore, they have to be properly characterized. On the other hand, the component anchor bolts in shear is expected to work the same way. Thus, this component will not be studied in this part of the work.

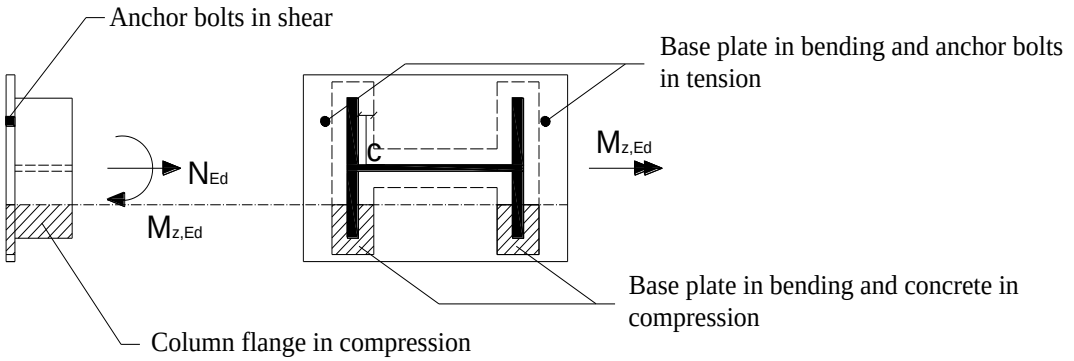


Figure 4.2 - Components of column bases under bending about weak axis

After studying the main components, their properties are assembled together to obtain the resistance and stiffness of the joint, similarly to what was explained for the case of bending about the strong axis.

4.2.1 BASE PLATE IN BENDING AND ANCHOR BOLTS IN TENSION

When the column is subjected to bending along the z axis (weak axis), if the magnitude of the moment is enough, the bolts in the tension zone will be activated and the base plate will deform. Therefore, the tension part is simulated by a T-stub with corresponding resistance, which is provided by giving the T-stub an equivalent length, see Figure 4.3.

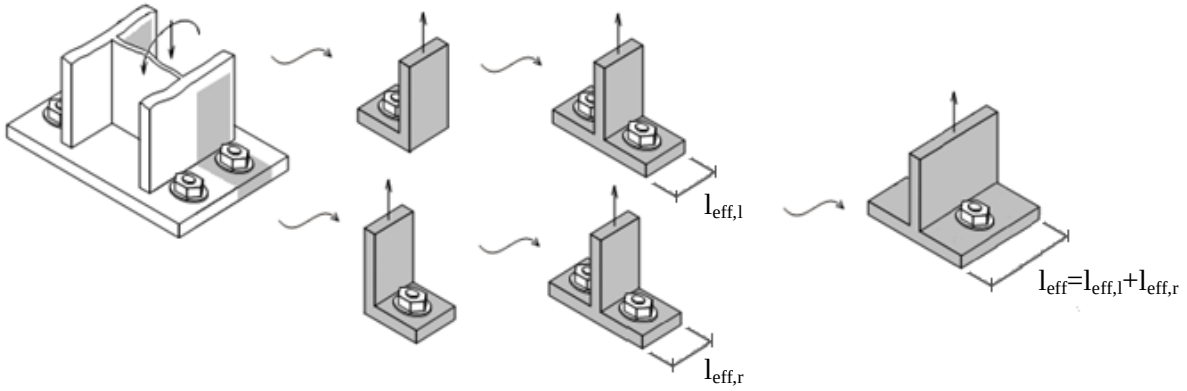


Figure 4.3- Tension zones and equivalent T-stub for bending moment in turn of the weak axis, adapted from [9]

The collapse modes of the T-stub are described in Chapter 2 of this essay. The T-stub is expected to behave similarly, the only difference is in how to properly calculate the effective length so that the T-stub has the same tensile resistance as the component it represents.

Regarding the stiffness calculation, the process is the same as for the case of bending about the strong axis.

4.2.1.1 Component resistance

The T-stub resistance is calculated according to the presence, or not, of prying action. Therefore, the boundary of prying has to be defined (see subchapter 2.3.1):

$$L_b^* = \frac{8.8\, m^3\, A_s}{l_{eff,1}\, t^3} \tag{2.3}$$

If L_b (also defined in subchapter 2.3.1) is bigger than L_b*, prying does not occur on the T-stub. If not, prying forces exist.

With this information, the design resistance, $F_{T,Rd}$, is obtained according to the possible failure mechanisms, which are described in Section 2.3.1.1, as well as the formulas to obtain their resistance.

The T-stub resistance for the case of prying is given by:

$$F_{T,Rd} = min\left(F_{T,1,Rd}, F_{T,2,Rd}, F_{T,3,Rd}\right) \tag{2.13}$$

And, if no prying action occurs, the resistance is:

$$F_{T,Rd} = min\left(F_{T,1-2,Rd}, F_{T,3,Rd}\right) \tag{2.14}$$

Where, $F_{T,i,Rd}$(i=1,2,3,1-2) is the design resistance of the failure mode i, and it is calculated according to equations (2.6), (2.7), (2.8) and (2.9), respectively.

With the exception for mode 3, the resistance of the failure mode depends on the effective length of the corresponding mode. Thus, the procedure for its calculation is explained in the next section.

This method assumes that the tension force acts at the line of the bolts. Hence, the lever arm of the tension component is:

$$z_t = {}^{p}/_{2} \tag{4.1}$$

Where p is the distance between the bolts on the side of the flange, measured according to the y-axis, see Figure 2.17.

4.2.1.2 Effective length of the T-stub

The effective length is the required length of the T-stub so that its resistance is the same as the component it represents. The method for obtaining this length involves the study of the possible yield lines of the component. It considers that at impending collapse, yield lines are developed at the location of the maximum moments [2]. Only the smallest effective length of the possible collapse mechanism is taken into account, which corresponds to the lowest failure load.

The effective lengths will be calculated based on the ones proposed for the strong axis bending. The main difference is that, in case of weak axis bending, only one of the two bolts located on the side of the flanges will be in tension. Therefore, it is not possible to develop group yield lines, i.e. yield lines connected between bolts. These cases correspond to mechanisms 2 and 5 from Table 2.1 (see Figure 4.4).

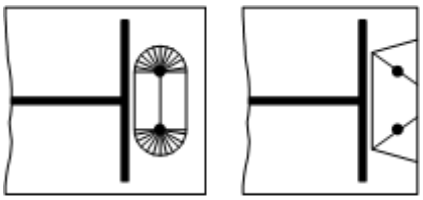


Figure 4.4 - Group yield lines [9]

Furthermore, it is important to note that the yield lines only develop in the tension zone. Therefore, the collapse mechanism where a straight line appears on the side of the flange (mechanism 7 from Table 2.1, see Figure 4.5) is not possible to occur because one part will be in compression.

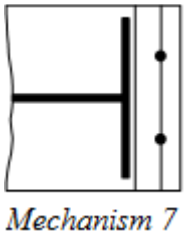
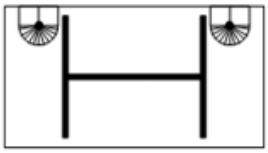
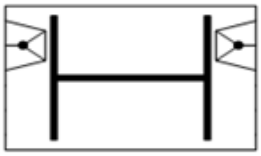
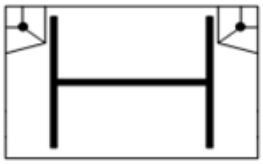


Figure 4.5 - Straight yield line [9]

Hence, there remain only four possible mechanisms for this type of loading, two with circular patterns and two with non-circular patterns. Since for these mechanisms the yield lines are individual, in other words, there is one yield line for each bolt in tension, the effective lengths are equal for both types of loading, even though the bolts in tension are not in the same side of the column base.

Table 4.1 shows illustrations for each mechanism (adapted from [9]) and the corresponding effective lengths, for the case of prying and no prying. The parameters needed for the calculation correspond to distances related with the bolts position, which are represented in Figure 2.17.

Table 4.1 - Effective length of a T-stub in case of bending is weak axis

	Yield Mechanisms	Prying case	No prying case
Circular Patterns		$l_{p,1} = 2\pi m$ (4.2)	$l_{np,1} = 2\pi$m(4.3)
		$l_{p,3} = \pi$m $+ 2$e (4.4)	$l_{np,3} = \pi$m $+ 4$e (4.5)
Non circular patterns		$l_{p,4} = 4$m $+ 1{,}25$e$_x$ (4.6)	$l_{np,4} = 4$m $+ 1{,}25$e$_x$ (4.7)
		$l_{p,6} = 2$m $+ 0{,}625$e$_x$ + e (4.8)	$l_{np,6} = 2$m $+ 0{,}625$e$_x$ + e (4.9)

The effective length is then chosen as the smallest value of the possible mechanisms for each failure mode. For Mode 1, where prying exist, both circular and non-circular patterns can occur. Therefore, its effective length is calculated as follows:

$$l_{eff,1} = \min\left(l_{p,1}; l_{p,3}; l_{p,4}; l_{p,6}\right) \quad (4.10)$$

In Mode 2, where the plastic mechanism develops due to a combined failure of the base plate and bolts, only non-circular patterns are expected:

$$l_{eff,2} = \min\left(l_{p,4}; l_{p,6}\right) \quad (4.11)$$

In case of no prying action, both circular and non-circular patterns are considered (Mode 1-2):

$$l_{eff,1-2} = \min\left(l_{np,1}; l_{np,3}; l_{np,4}; l_{np,6}\right) \quad (4.12)$$

4.2.1.3 Component stiffness

Even though the moment is applied at a perpendicular direction, the base plate is expected to deform in a similar way as in the case of bending about the strong axis. Therefore, the stiffness coefficients of the base plate and the bolts are obtained from the same expressions.

Thus, in case of no prying action, the expressions are as follows:

$$k_p = k_{15} = \frac{0.425\, l_{eff}\, t^3}{m^3} \tag{2.36}$$

$$k_b = k_{16} = \frac{2\, A_s}{L_b} \tag{2.37}$$

And for the case of prying action:

$$k_p = k_{15} = \frac{0.85\, l_{eff}\, t^3}{m^3} \tag{2.38}$$

$$k_b = k_{16} = \frac{1.6\, A_s}{L_b} \tag{2.39}$$

Finally, the stiffness of the component is obtained from:

$$k_T = \frac{1}{\frac{1}{k_p} + \frac{1}{k_b}} \tag{2.40}$$

4.2.2 BASE PLATE IN BENDING AND CONCRETE IN COMPRESSION

The behavior of the component is studied across a T-stub that simulates the flexibility of the base plate with an equivalent rigid plate. The method considers that compression stresses are transmitted by the footprint of the column which corresponds to an effective area. In the case of bending about the strong axis, the area is considered to be the one around the flange. However, for the type of loading that is under investigation, at least a part of each flange is under compression. Therefore, a different approach needs to be taken when studying the column base bending in turn of its weaker axis.

To fully describe the resistance of the component, the bearing strength of the concrete block under the base plate needs to be estimated. The procedure for its calculation was previously described in this essay. Finally, the resistance is defined by the compressed area and the concrete strength.

As for the tensile component, the procedure for the stiffness calculation is the same as for the case of bending about the strong axis, the only difference is in the calculation of the effective area.

4.2.2.1 Component resistance

The resistance of the component is given by the effective area and the bearing strength of the concrete:

$$F_{c,pl,Rd} = f_{jd}\, A_{eff} \tag{4.13}$$

Where f_{jd} is the bearing strength and its calculation is described in Section 2.3.2.1

The model presented in Chapter 2 considers that the effective area is always the same and equal to the footprint of the flange in compression. However, such a simple assumption cannot be taken in this case since only a fraction of the flanges is in compression. Therefore, the effective area will be calculated based on the location of the neutral axis for the case of full resistance of the tension part. This means that this method is only suitable for cases where the resistance is governed by the tension component.

The assumptions of the method are:

- The bolts are working under full resistance.
- Only the effective area under the flanges influences the resistance of the component (the web resistance is neglected);
- The compression force acts at the center of the area under compression;
- The area under compression cannot cross the z axis of the joint.

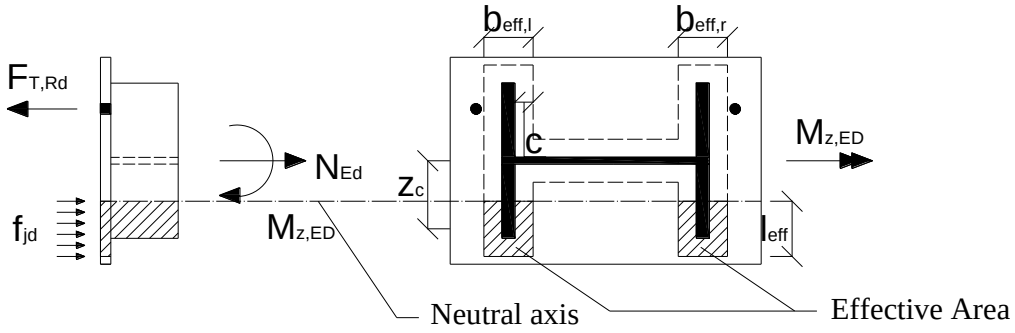


Figure 4.6 – Effective area of the compressed T-stub

Thus, the compressed effective area, A_{eff} , required to match the tensile strength, is obtained by the equilibrium equation in the vertical direction (see Figure 4.6):

$$N_{Ed} = F_{T,Rd} - A_{eff}\, f_{jd} \Leftrightarrow \tag{4.14}$$

$$\Leftrightarrow A_{eff} = \frac{F_{T,Rd} - N_{Ed}}{f_{jd}} \tag{4.15}$$

To fully define the effective area, its dimensions are determined. For that, the width, *c*, is necessary (the procedure for its calculation is defined in subchapter 2.3.2.1).

The effective width of the T-stub, b_{eff}, is determined according to the limitations presented in Figure 2.21:

$$b_{eff} = b_{eff,l} + b_{eff,r} = 2 \times \left(t_f + c + min\left\{c; \frac{a - h_c}{2}\right\}\right) \tag{4.16}$$

The effective length is calculated as a function of the effective area, taking into account that it cannot cross the z axis of the joint:

$$l_{eff} = min \begin{cases} A_{eff} / b_{eff} \\ b_c / 2 + c \\ b / 2 \end{cases} \tag{4.17}$$

And the location of the compression force is given by:

$$z_c = \; min\left(\frac{b_c}{2} + c; \frac{b}{2}\right) - \frac{l_{eff}}{2} \tag{4.18}$$

Where b_c, h_c and t_f are the width, length and thickness of the flange of the column's cross section, respectively; and b is the length of the base plate.

4.2.2.2 Component stiffness

The stiffness coefficient is calculated using the same expression derived in Section 2.3.2.2:

$$k_c = k_{13} = \frac{E_c \sqrt{b_{eff,s}\, l_{eff,s}}}{1{,}275\, E} \tag{2.69}$$

However, the geometry of the component, $b_{eff,s}$ and $l_{eff,s}$, is different. The effective width b_{eff} is simple to obtain, by adding the equivalent rigid length to the thickness of the flange. On the other hand, the effective length $l_{eff,s}$ will depend on the position of the neutral axis . Therefore, the length of the flange that is in compression needs to be calculated and then the equivalent rigid length is added to that.

Thus, the effective width $b_{eff,s}$ is given by:

$$b_{eff,s} = t_f + 2c_r \Rightarrow b_{eff,s} = t_f + 2{,}5t \tag{4.19}$$

The compressed length of the flange (l_c) is obtained through the effective length of the resistance calculation (l_{eff}):

$$l_c = l_{eff} - min\left(c; \frac{b - b_c}{2}\right) \tag{4.20}$$

Then, the effective length in terms of stiffness is:

$$l_{eff,s} = l_c + c_r \Rightarrow l_{eff,s} = l_c + 1{,}25t \tag{4.21}$$

4.2.3 COLUMN FLANGE IN COMPRESSION

When the column is subjected to bending about its weak axis, only one part of the flanges is in compression. Therefore, the compression resistance of the column, when exposed to this type of loading, will be calculated considering that the neutral axis coincides with the symmetrical axis of the cross section, see Figure 4.7.

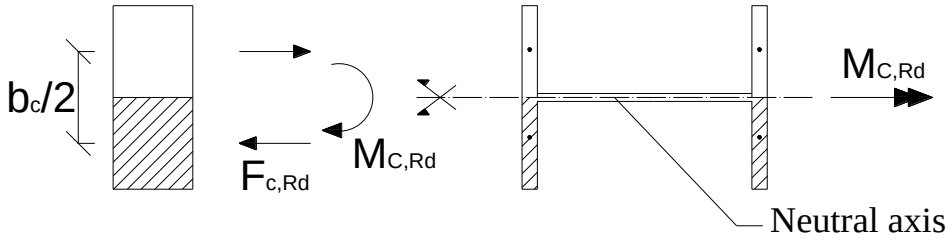


Figure 4.7 - Column flange in compression

The design resistance is then:

$$F_{c,fc,Rd} = \frac{M_{c,Rd}}{\left(b_c/_2\right)} \tag{4.22}$$

Where b_c is the length of the connected column and $M_{c,Rd}$ the design moment capacity of the column cross section.

According to EN 1993-1-1[13] cl. 6.2.5(2), the design moment capacity, $M_{c,Rd}$, is equal to design plastic moment capacity, $M_{pl,Rd}$:

$$M_{c,Rd} = M_{pl,Rd} = \frac{W_{z,pl}\, f_y}{\gamma_{M0}} \tag{4.23}$$

4.2.4 ASSEMBLY OF THE COMPONENTS

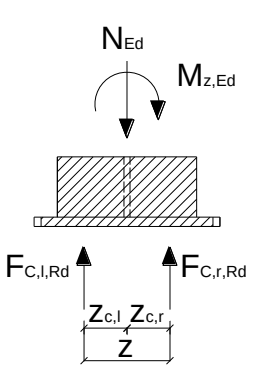
4.2.4.1 Bending resistance

Four possible loading cases are proposed for the calculation of the moment capacity of the column base when subjected to weak axis bending. One case is when a dominant tensile force occurs and all the bolts are in tension (Figure 4.8a). Another one is the opposite, where there is no tension in the anchor bolts because a dominant compression force is acting on the column (Figure 4.8b). The two other cases are the ones where a dominant bending moment is acting on the column base (Figure 4.8c and d).

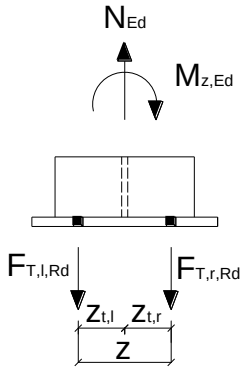
The parameters required for the calculation of the moment capacity, $M_{j,Rd}$, are:

- The load eccentricity, $e=M_{Ed}/N_{Ed}$;
- The resistance of the tension part, $F_{T,Rd}$ (described in Section 4.2.1.1);
- The resistance of the compression part, $F_{C,Rd}$, taken as the minimum of $F_{c,pl,Rd}$ (see Section 4.2.2.1) and $F_{c,fc,Rd}$ (see Section 4.2.3);
- The lever arms z, z_c and z_t, calculated according to Figure 4.8.

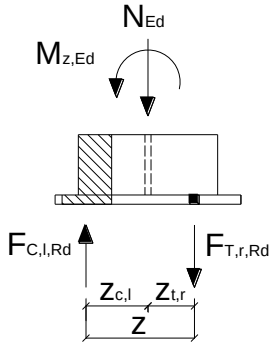
The method for its calculation is in Table 2.2 of this work.



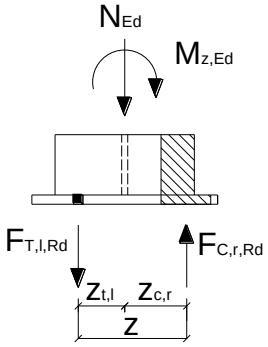
a) Column base connection in case of a dominant compressive normal force



b) Column base connection in case of a dominant tensile normal force



c) Column base connection in case of a dominant bending moment



d) Column base connection in case of a dominant bending moment

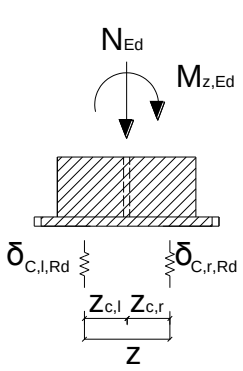
Figure 4.8 – Loading cases for calculation of the moment capacity about the weak axis

4.2.4.2 Stiffness

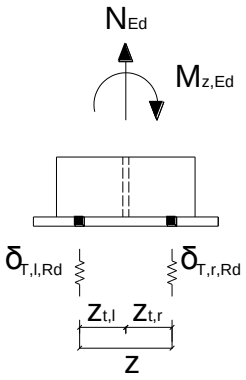
The initial stiffness of the joint is calculated according to the four possible loading cases shown in Figure 4.9. To fully describe it, the stiffness of the main components is required: the tension component stiffness, k_T (calculation procedure in Section 4.2.1.3), and the compression component stiffness, k_C (method of estimation in Section 0).

In addition, the lever arms have also to be considered. They are calculated according to Figure 4.9, assuming that the tensile force is applied at the bolts row and that the compression force acts at the center of the compression zone.

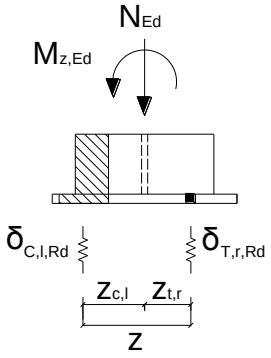
Table 2.4 from this work presents the formulas to estimate the rotational stiffness of column bases under bending about the strong axis. However, it also works for bending about the weak axis if the correct parameters are chosen (k_T, k_C, z, z_c and z_t). Therefore, the procedure for obtaining the rotational stiffness, for the current study case, can be done according to that table.



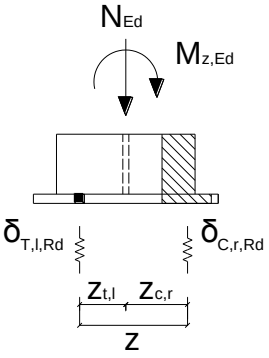
a) Column base connection in case of a dominant compressive normal force



b) Column base connection in case of a dominant tensile normal force



c) Column base connection in case of a dominant bending moment



d) Column base connection in case of a dominant bending moment

Figure 4.9 - Mechanical models of stiffness for bending about the weak axis

4.3 M_z-M_y INTERACTION CURVE

The objective of the interaction curve is to provide the moment capacity of column bases under combined biaxial loading with axial force. This is done by choosing a curve that would describe best the relation between the moment capacity for bending about the strong axis, $M_{y,Rd}$, and the moment capacity for bending about the weak axis, $M_{z,Rd}$, for a constant load eccentricity, $e=M_{\alpha,Ed}/N_{Ed}$.

A conservative procedure would be to consider that this relation is linear, i.e, to assume that the interaction curve is defined by a straight line connecting $M_{y,Rd}$ and $M_{z,Rd}$ (see Figure 4.10):

$$\frac{M_z}{M_{z,Rd}} + \frac{M_y}{M_{y,Rd}} = 1 \tag{4.24}$$

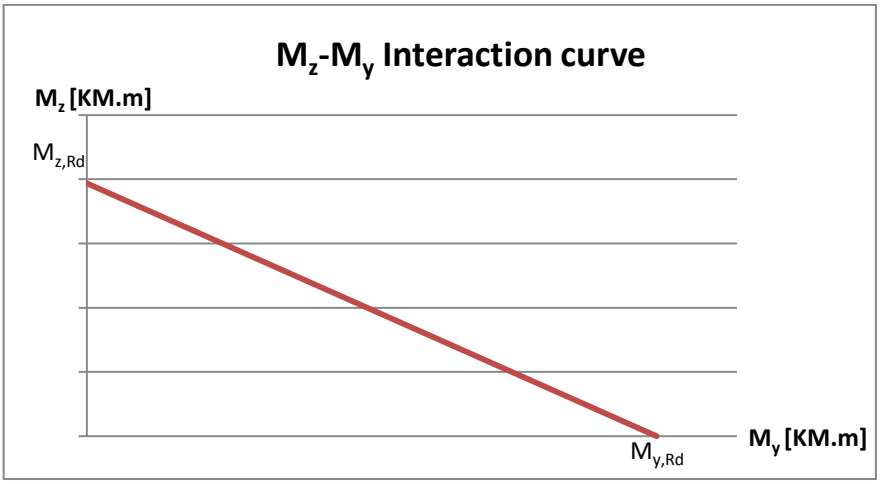


Figure 4.10 - Linear M_z-M_y Interaction curve

However, this approach is far from reality. Hence, there is the need for investigation on order to reach for a more realistic interaction curve that will also contribute for a more economical design of column base connections.

Therefore, it is known that a good approximation would be an interaction defined by a curved line. In addition, due to the double symmetry of the joint, the tangent of the curve at the points where it intersects the main axes must be perpendicular to those. Thus, a shape that verifies these criteria is an ellipse and its function is given by:

$$\left(\frac{x}{a}\right)^2 + \left(\frac{y}{b}\right)^2 = 1 \tag{4.25}$$

Knowing that a is the ordinate of the point where the curve intersects the x-axis and that b is the coordinate of the point where the curve interests the y-axis, the equation of the study case can be obtained by:

$$\left(\frac{M_z}{M_{z,Rd}}\right)^2 + \left(\frac{M_y}{M_{y,Rd}}\right)^2 = 1 \tag{4.26}$$

Figure 4.11 shows the difference between the linear curve (red line) and the elliptical curve (blue line). It is easy to understand that a whole range of joints would be neglected for the case of the linear curve, as it is shown by the stripped area.

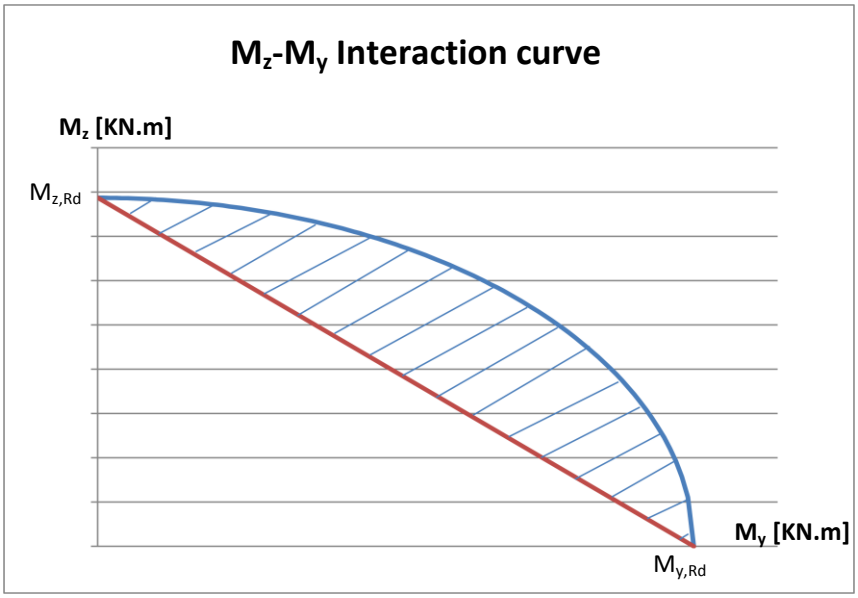


Figure 4.11 – Elliptical M_z-M_y interaction curve

Proceeding, with the shape of the interaction curve defined, it remains to explain how to obtain the final moment capacity from the curve. This is done by intersecting the curve with a line which is described by the following function:

$$M_z = \tan(\alpha) \cdot M_y \tag{4.27}$$

Where α is the angle between the applied moment and the strong axis, see Figure 4.1 and Figure 4.12.

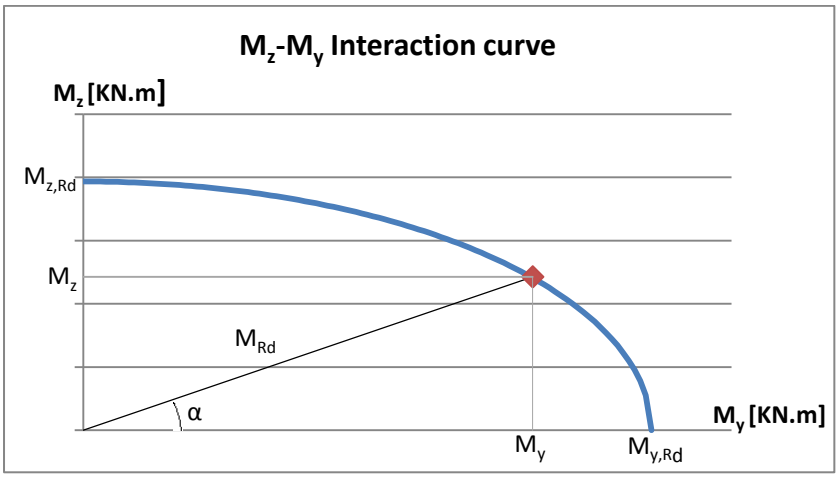


Figure 4.12 - Determination of the moment capacity

Finally, the distance from the origin of the diagram to the point obtained by equating formulas (4.26) and (4.27), gives the moment capacity value for bending in any direction (α):

$$M_{\alpha,Rd} = \sqrt{{M_y}^2 + {M_z}^2} \tag{4.28}$$

4.4 VALIDATION OF THE ANALYTICAL MODEL

The analytical model was compared with the numerical model for the purpose of validation.

Thus, to verify the procedure for studying the behavior of the joint under weak axis bending, the column base modeled in ABAQUS was subjected to bending about the weak axis (z) with a proportional loading, corresponding to a load eccentricity of *e= -0,25m*.

Then, to validate the proposed interaction curve, three different curves, corresponding to three different eccentricities, were obtained using ABAQUS. The first curve was obtained for an eccentricity of *e= -0,25m*, which corresponds to a case of dominant bending moment combined with a compression force. The second one corresponds to a dominant bending moment case combined with a tensile force: *e= +0,25m*. The third curve is about bending with no axial force, thus, corresponding eccentricity is infinite: $e=M/N=M/0=\infty$.

These curves were reached by subjecting the column of the numerical model to bending about various planes with a proportional loading, obtaining the moment capacity for each case. Then, these moment capacities were plotted in a M_z-M_y diagram, for each eccentricity. The planes differ with each other by the angle between them and the plane that contains the y axis of the column. The chosen angles were: 0º (which corresponds to bending about the strong axis, y); 13,28º; 26,56º; 38,84º; 45º; 50,15º; 63,43º; 76,72º; and 90º (which corresponds to bending about the weak axis, z).

4.4.1 WEAK AXIS BENDING

For the validation of the procedure for studying the behavior of column bases under weak axis bending, the moment-rotation diagram was drawn for a particular eccentricity (*e= -0,25m*), see Figure 4.13. The moment capacity and the initial stiffness of the numerical model were obtained by this diagram and are presented in Table 4.2, as well as the analytical results. The analytical calculation can be found in Annex 1 of this work.

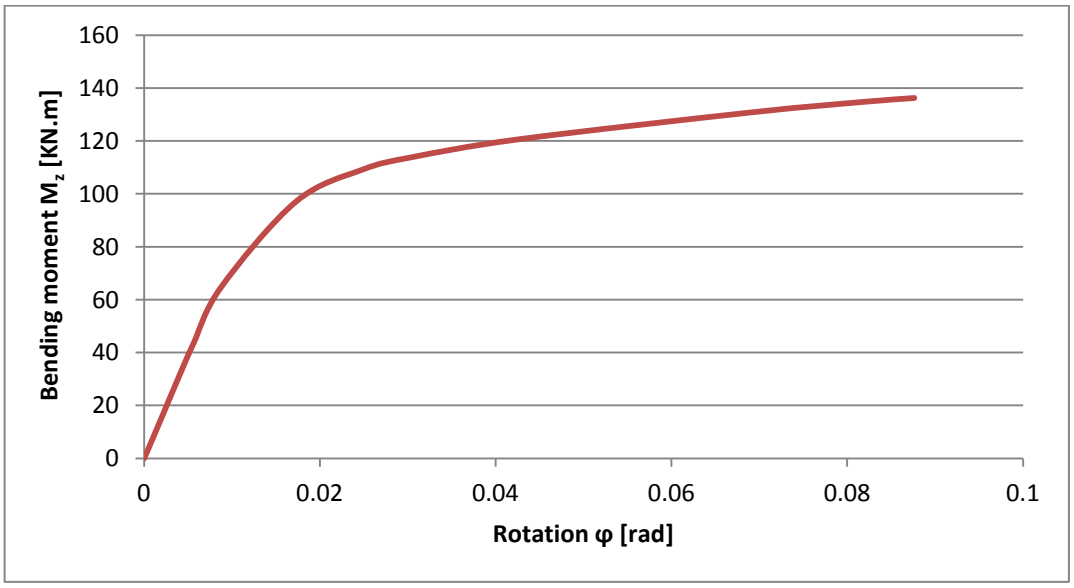


Figure 4.13 - Moment-rotation diagram for weak axis bending with proportional loading (e= -0,250m)

Table 4.2 - Comparison between numerical results and analytical results for weak axis bending with proportional loading (e=-0,25m)

	Moment Capacity [KN.m]	Initial Stiffness [MN.m/rad]
Analytical results	60	10,39
Numerical results	136	7,39
Ratio Analyt./Numer.	0,44	1,40

The ratio of the moment capacity is very similar to the one obtained by the comparison between the component method described in Eurocode 3 (strong axis bending) and the numerical model, which was 0,46 (see Table 3.3). Thus, the proposed model seems to be acceptable. However, like for the case of strong axis bending, the model is very conservative.

Regarding the initial stiffness, the analytical result is closer to the numerical result than what was observed for the strong axis bending. In this case the ratio was 1,40, and for the strong axis bending case the ratio was 1,85 (see Table 3.3).

4.4.2 INTERACTION CURVE

Like previously explained, three different curves were obtained using the numerical model, for three different eccentricities: *e= -0,25m*; *e= +0,25m*; and *e= M/0=∞*. For each case, another curve was represented with the same shape as the one proposed in the analytical model (elliptical shape), using the moment capacities for bending about the strong and weak axis bending obtained by ABAQUS. Furthermore, for the same three eccentricities, three curves were determined by the analytical model (calculation in Annex 1, 2, and 3).

Figure 4.14, Figure 4.15 and Figure 4.16 show the comparison between the curves for the eccentricities *e= -0,25m*; *e= +0,25m*; and *e= M/0=∞*, respectively.

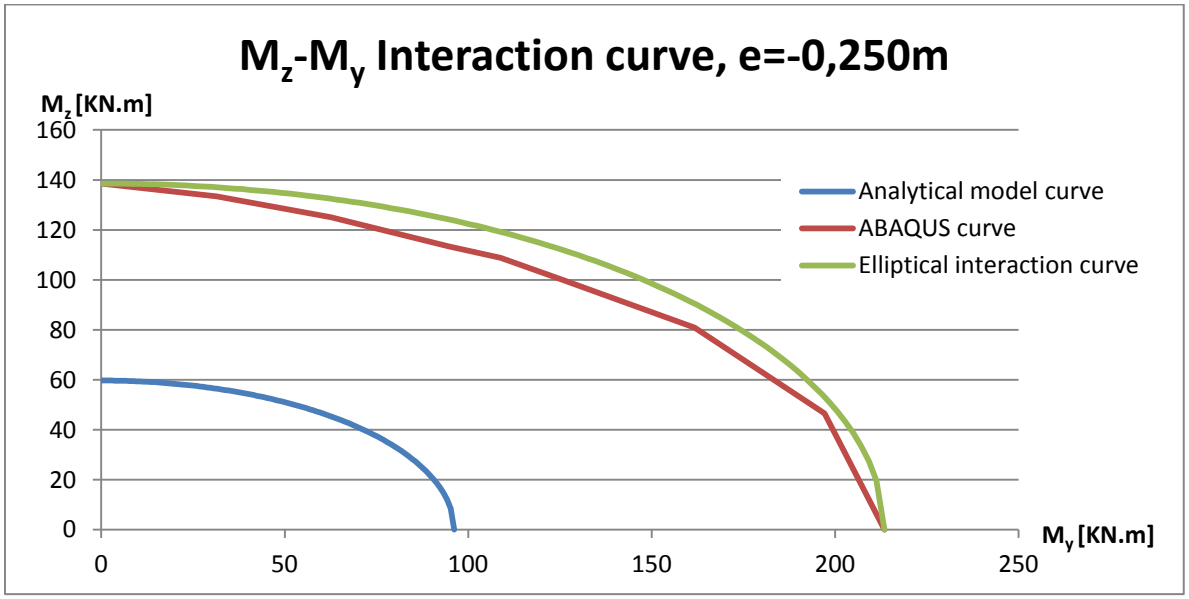


Figure 4.14 - M_z-M_y interaction curves for e=-0,250m

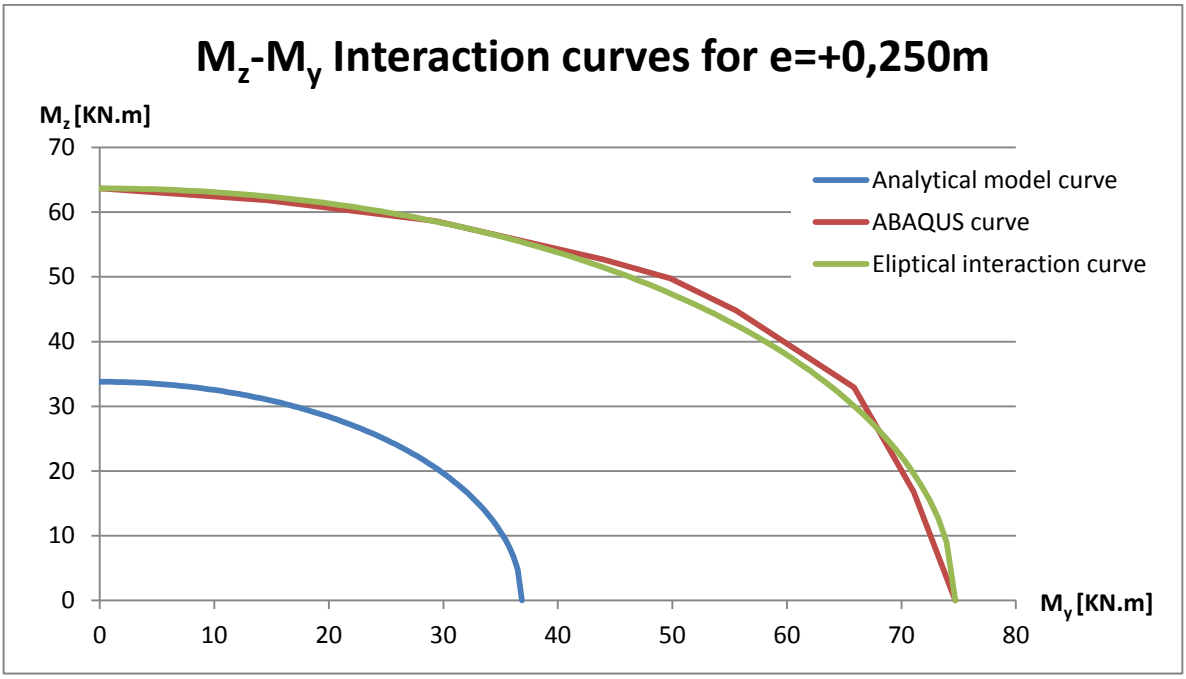


Figure 4.15 - M_z-M_y interaction curves for e=+0,250m

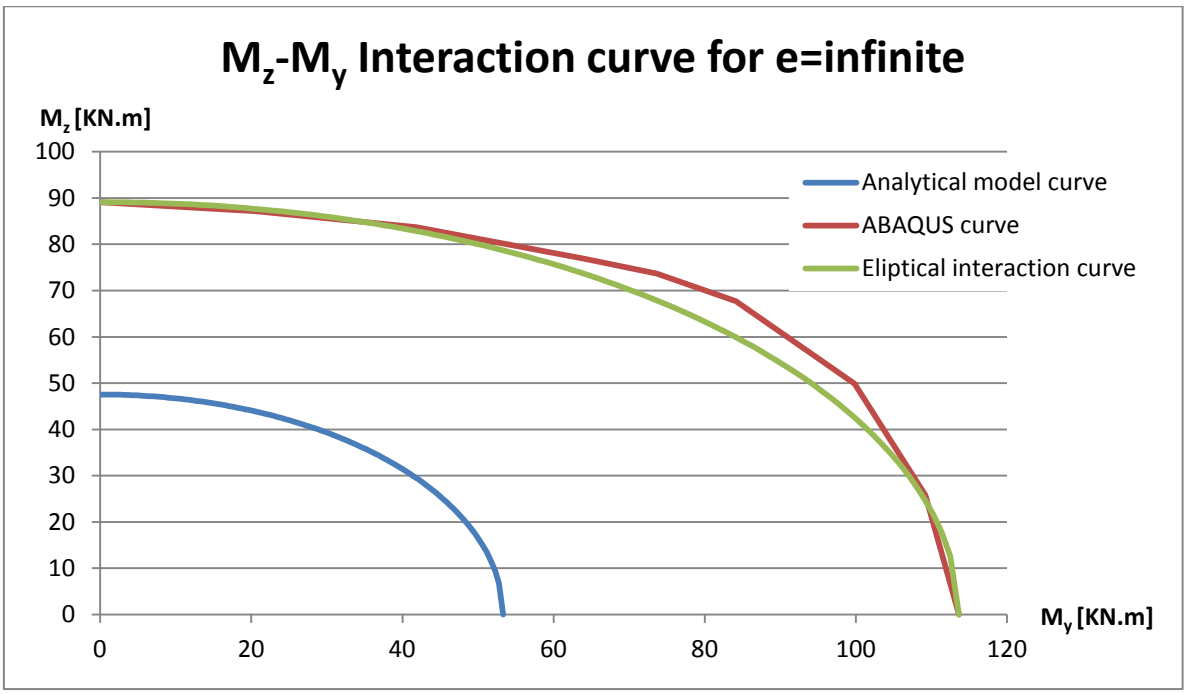


Figure 4.16 - M_z-M_y interaction curves for e=infinite

Observing the three diagrams, it is concluded that the selected shape for the interaction curve of the analytical model is appropriate. The green lines, which are the proposed elliptical curves drawn from the moment capacities of the main axis obtained with ABAQUS, are almost coincidental with the red lines, which are the curves obtained by the moment capacities of different loading planes, also reached by the numerical model.

The blue lines, which are the analytical curves, are a lot smaller than the numerical curves. This is due the conservative values that the component method provides. Thus, the analytical curve is also conservative.

4.5 WORKED EXAMPLE

An example of a column base loaded with normal force and biaxial bending is now introduced. The purpose of the example is to show how to properly calculate every parameter in a design situation where the moment capacity of the joint is needed.

Resistance of all main components is calculated separately for the two axes (y and z), as well as the stiffness. Assembly of the properties is then carried out to obtain the maximum capacity and initial stiffness for each axis.

Finally, a M_z-M_y interaction curve is generated and the maximum bending moment of the column base is obtained for the desired loading direction.

4.5.1 DATA OF THE JOINT

The data of the joint was chosen based on the experiment that was presented in this work. The geometry of the column base is the same as well as the material properties. However, the loading is considered to be proportional, i.e., the axial force and bending moment increase by the same factor (constant eccentricity). To obtain the design values, safety factors are considered as: γ_{M0}=1,0; γ_{M2}=1,25 and γ_c=1,5, in line with what is proposed by Eurocode 3.

The column HEB240 of steel grade S235 is loaded by a normal force N_{Ed}= -200KN and by a bending moment $M_{26,56,Ed}$ =50KN that is deviated from the strong axis by an angle α=26.56º. Thus, the corresponding eccentricity is $e = \frac{M_{26,56,Ed}}{N_{Ed}} = -250\ mm$. The steel grade of the base plate is also S235 and its thickness is 20mm. The concrete block size is 1500x1000x400mm and its grade is C16/20. The connection between the base plate and the concrete is carried out through four threaded rods of steel grade 8.8 with 20mm of diameter and an embedment depth of 250mm. The head of the bolt is made by steel plates with 20mm thickness.

The remaining dimensions can be found in Figure 4.17 and Table 4.3 shows a resume of the data needed for calculation.

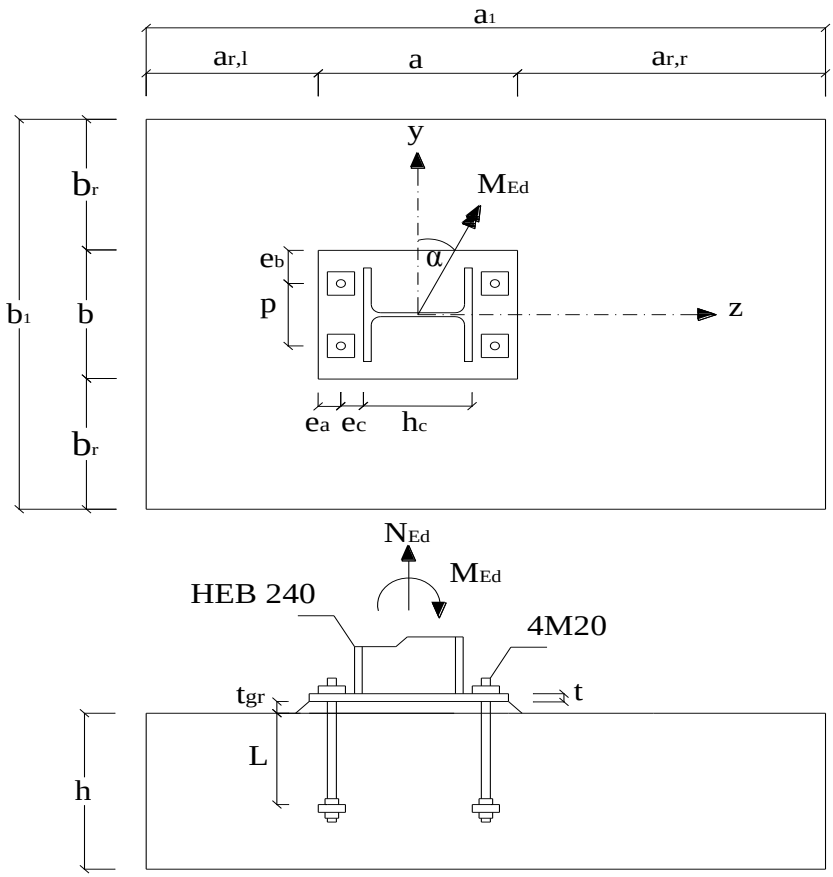


Figure 4.17 - Design of the column base

Table 4.3 - Data of the joint

	Column		Base plate		Concrete		Bolts	
Material Properties		Steel S235		Steel S235		C16/20		Grade 8.8
	f_y	235 MPa	f_y	235 MPa	f_{ck}	22,6 MPa	f_{ub}	830 MPa
	E	210 GPa	E	210 GPa	E_c	20,9 GPa	E	210 GPa
Dimensions		HEB 240	a	440 mm	a_1	1500 mm		M20
	h_c	240 mm	b	330 mm	b_1	1000 mm	d	20 mm
	b_c	240 mm	t	20 mm	h	400 mm	A_s	220 mm^2
	t_w	10 mm	e_a	50 mm	$a_{r,l}$	380 mm	L	250 mm
	t_f	17 mm	e_b	85 mm	$a_{r,r}$	680 mm	h_{bh}	20 mm
	A	1,06x10^6 mm^2	e_c	50 mm	b_r	335 mm		
	$I_{c,y}$	1,126x10^8 mm^4	p	160 mm	t_{gr}	30 mm		
	$w_{y,pl}$	1,053x10^6 mm^3	a_{wf}	8mm				
	$I_{c,z}$	3,923x10^7 mm^4						
	$w_{z,pl}$	4,984x10^5 mm^3						

4.5.2 COLUMN BASE UNDER STRONG AXIS BENDING

4.5.2.1 Bending resistance

The resistance of the main components will be calculated separately and then assembled to obtain the bending resistance of the joint.

Resistance of the component base plate in bending and anchor bolts in tension

Starting with the tension component, the anchor bolt lever arm needs to be defined (considering that fillet weld is a_{wf}=8mm):

$$m = e_c - 0.8\, a_{wf}\sqrt{2} = 409mm$$

The T-stub length calculation depends on the fact if there are prying forcers or not, therefore the effective length needs to be checked:

$$L_{bf} = t + t_{gr} + h_{bh} = 60mm$$

$$L_{be} = 8d = 160\ mm$$

$$L_b = L_{bf} + L_{be} = 220\ mm$$

$$L_{b,min} = \frac{8.82\ m^3\ A_s}{l_{eff,1}\ t^3} = 100{,}9\ mm$$

$$L_b > L_{b,min} \Rightarrow No\ prying\ forces$$

As it is shown above there are no prying forces, so the effective length for each mechanism is given by:

$$l_{np,1} = 2\pi \mathrm{m} = 257.3\ mm$$

$$l_{np,2} = 2\pi \mathrm{m} + 2p = 577{,}3\ mm$$

$$l_{np,3} = \pi \mathrm{m} + 4e = 468{,}6\ mm$$

$$l_{np,4} = 4\mathrm{m} + 1{,}25\mathrm{e_x} = 226{,}3\ \mathrm{mm}$$

$$l_{np,5} = 2\mathrm{m} + 0{,}625e_x + 0{,}5p = 193{,}1\ mm$$

$$l_{np,6} = 2\mathrm{m} + 0{,}625e_x + e = 198{,}1\ mm$$

$$l_{np,7} = 0{,}5b = 165\ mm$$

Then, the effective length of the T-stub is:

$$l_{eff,1-2} = min\left(l_{np,1}; l_{np,2}; l_{np,3}; l_{np,4}; l_{np,5}; l_{np,6}; l_{np,7}\right) = 165mm$$

The resistance of the T-stub in tension is verified for the two possible failure modes for the case of no prying. First step is to calculate the plastic bending moment capacity of the base plate:

$$m_{pl,Rd} = \frac{1}{4}t^2 f_{yd} = 23{,}5KN.m/m$$

The resistance of failure Mode 1-2 is:

$$F_{T,1-2,Rd} = \frac{2\ l_{eff,1-2}\ m_{pl,Rd}}{m} = 189{,}4\ KN$$

In Mode 3, the tension resistance of the bolts needs to be checked. According to [1] that resistance is:

$$F_{t,Rd} = \frac{0{,}9\, f_{ub}\, A_s}{\gamma_{M2}} = 131{,}5\ KN$$

Since there are two anchor bolts in tension, the resistance of this mode is:

$$F_{T,3,Rd} = \sum B_{t,Rd} = 2BF_{t,Rd} = 262{,}9\ KN$$

Finally, the T-stub in tension resistance is:

$$F_{T,Rd} = min\left(F_{T,1-2,Rd}, F_{T,3,Rd}\right) = 189{,}4\ KN$$

And the lever arm of the tension part is the distance from the bolts row to the column axes of symmetry:

$$z_t = \frac{h_c}{2} + e_c = 170\ mm$$

Resistance of the component base plate in bending and concrete in compression

To evaluate the compressed part resistance, the bearing strength needs to be calculated. For that, the loaded area, $A_{C0,}$ as well as the spread area, $A_{C1,}$ are essential:

$$A_{c0} = a\ b = 1{,}452 \times 10^5\ mm^2$$

$$a_2 = min\begin{cases} a + h = 840\ mm \\ 3a = \ 1320\ mm \\ a_1 = 1500\ mm \end{cases} = 840\ mm$$

$$b_2 = min\begin{cases} b + h = 730\ mm \\ 3b = 990\ mm \\ b_1 = 1000\ mm \end{cases} = 730\ mm$$

$$A_{c1} = a_2\ b_2 = 6{,}132 \times 10^5\ mm^2$$

The next step is to calculate the bearing strength, but first the influence of the grout needs to be checked:

$$0{,}2 \min(a; b) = 66mm > t = 20\ mm \Rightarrow no\ influence$$

Since the grout as no influence, the joint material coefficient, β_j, is 2/3. Thus, the bearing strength is calculated on that basis:

$$f_{jd} = \beta_j\, f_{cd} \sqrt{\frac{A_{c1}}{A_{c0}}} = 20{,}642\ MPa \leq 3\, f_{cd} = 45{,}2MPa$$

The width of the strip, *c*, that replaces the flexible plate into a rigid plate of equivalent area, is calculated from:

$$c = t \sqrt{\frac{f_{yk}}{3\, f_{jd}\, \gamma_{M0}}} = 39{,}0\ mm$$

Thereby, the effective length, l_{eff}, is:

$$l_{eff} = min\begin{cases} b_c + 2\, c = 332{,}6\ mm \\ b = 330\ mm \end{cases} = 330\ mm$$

And the effective with, b_{eff}, is:

$$b_{eff} = min\{c; (a - h_c)/2\} + t_f + c = 94{,}9mm$$

Then, the effective area becomes:

$$A_{eff} = b_{eff}\, l_{eff} = 3{,}018 \times 10^4\ mm^2$$

Finally, the compressed part resistance is calculated:

$$F_{c,pl,Rd} = A_{eff}\, f_{jd} = 622{,}9\ KN$$

And the lever arm of the compression force is obtained:

$$z_c = \frac{h_c}{2} - \frac{t_f}{2} = 111{,}5\ mm$$

Resistance of the component column flange and web in compression

The component resistance depends on the plastic bending moment capacity of the column:

$$M_{c,Rd} = M_{pl,y,Rd} = \frac{W_{y,pl}\, f_{yk}}{\gamma_{M0}} = 247{,}5\ KN.m$$

Thus, the design compression resistance of the flange is:

$$F_{c,fc,Rd} = \frac{M_{c,Rd}}{\left(h_c - t_f\right)} = 1109{,}7\ KN$$

Assembly of the components

For the calculation of the bending resistance, the load eccentricity is needed:

$$e = \frac{M_{26{,}56,Ed}}{N_{Ed}} = \frac{50}{-200} = -250\ mm$$

This corresponds to the case of a dominant bending moment with tension on the left side and compression acting on the right side ($N_{Ed} \leq 0$ and $e \leq -z_{C,l}$).

The resistance of the tension part is:

$$F_{T,l,Rd} = 189{,}4\ KN$$

And its lever arm is:

$$z_{T,l} = 170\ mm$$

The compression part resistance is taken as the minimum resistance of the components column flange and web in compression or concrete in compression and base plate in bending:

$$F_{C,r,Rd} = min\left(F_{c,pl,Rd}; F_{c,fc,Rd}\right) = 622{,}9\ KN$$

And the lever arm is:

$$z_{C,r} = 111{,}5\ mm$$

Thus, knowing that $z = z_T + z_C$, the joint resistance is given by:

$$M_{y,Rd} = min\begin{cases} \dfrac{F_{T,l,Rd}z}{z_{C,r}/e + 1} = 96{,}2\ KN.m \\ \dfrac{-F_{C,r,Rd}z}{z_{T,l}/e - 1} = 104{,}4\ KN.m \end{cases} = 96{,}2\ KN.m$$

Regarding the classification according to resistance, the joint is classified as partial-strength:

$$M_{y,Rd} = 96{,}2\ KN.m \begin{cases} \geq 0{,}25M_{pl,y,Rd} = 61{,}9\ KN.m \\ \leq M_{pl,y,Rd} = 247{,}5\ KN.m \end{cases}$$

4.5.2.2 Initial Stiffness

As for the resistance, the initial stiffness of the joint is calculated based on the stiffness of the main components.

Stiffness of the component base plate in bending and anchor bolts in tension

The stiffness coefficients of the component are calculated on the basis of whether there are prying forces or not. As demonstrated in the resistance calculation of the same component, there are no prying forces, so the bolt stiffness coefficient is calculated as follows:

$$k_b = 2{,}0\ \frac{A_s}{L_b} = 2{,}000\ mm$$

And stiffness coefficient of the T-stub is given by:

$$k_p = \frac{0{,}425\ l_{eff,1-2}t^3}{m^3} = 8{,}170\ mm$$

Finally, the component stiffness is evaluated:

$$k_T = \frac{1}{\dfrac{1}{k_b} + \dfrac{1}{k_p}} = 1{,}607\ mm$$

Stiffness of the component base plate in bending and concrete in compression

In order to calculate the component stiffness, it is necessary to express the flexible plate in terms of an equivalent rigid plate. Therefore, the equivalent lengths of the T-stub are (see Figure 4.18):

$$b_{eff,s} = t_f + 2{,}5t = 67mm$$

$$l_{eff,s} = b_c + 2{,}5t = 290mm$$

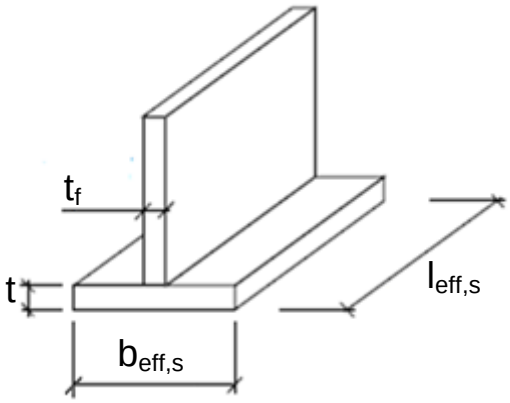


Figure 4.18 – Compressed T-stub

At last, component stiffness is obtained:

$$k_C = k_{13} = \frac{E_c \sqrt{b_{eff,s}\, l_{eff,s}}}{1{,}275\, E} = 10{,}881\ mm$$

Assembly of the components

The lever arms, required for the calculation, are:

$$z_{C,r} = 111{,}5\ mm$$

$$z_{T,l} = 170\ mm$$

$$z = z_{C,r} + z_{T,l} = 281{,}5\ mm$$

The stiffness is calculated for a specific eccentricity, consequently the eccentricity, e_k, at which the rotation is zero, is needed:

$$e_{k,z} = \frac{k_c\, z_{C,l} - k_t\, z_{T,l}}{k_c + k_t} = 75{,}3\ mm$$

At last, the bending initial stiffness is obtained for the previously calculated eccentricity (e= -250mm):

$$s_{y,j,ini} = \frac{e}{e + e_{k,z}} \frac{E_s\, z^2}{\frac{1}{k_c} + \frac{1}{k_t}} = 33{,}334\ MN.m/rad$$

About the classification according to stiffness, the joint is evaluated in comparison to the column bending stiffness. For column length L_c=2m and cross section HEB 240, the relative bending stiffness is:

$$\bar{s}_{y,j,ini} = s_{y,j,ini} \frac{L_c}{E_s I_{c,y}} = 2{,}81$$

Then, the designed column base can be classified as semi-rigid whether it is used in a sway or non-sway frame because (for a particular value λ_0 = 1,36):

$$\bar{s}_{y,j,ini} = 2{,}81 \geq 0{,}5$$

$$\bar{s}_{y,j,ini} = 2{,}81 \leq 12 = \bar{s}_{j,ini,nsf}$$

$$\bar{s}_{y,j,ini} = 2{,}81 \leq 30 = \bar{s}_{j,ini,sf}$$

4.5.3 COLUMN BASE UNDER WEAK AXIS BENDING

4.5.3.1 Bending resistance

At first the resistance of the main components will be introduced and then assembled to get the bending capacity of the joint.

Resistance of the component base plate in bending and anchor bolts in tension

As it was previously checked, there are no prying forces for a bolt active length L_b=220mm. Therefore, the effective lengths for each possible mechanism are given by (with m_x=40,9mm):

$$l_{np,1} = 2\pi m = 257.3\ mm$$

$$l_{np,3} = \pi m + 4e = 468{,}6\ mm$$

$$l_{np,4} = 4m + 1{,}25e_x = 226{,}3\ mm$$

$$l_{np,6} = 2m + 0{,}625e_x + e = 198{,}1\ mm$$

And the effective length of the T-stub is:

$$l_{eff,1-2} = \min\left(l_{np,1}; l_{np,3}; l_{np,4}; l_{np,6}\right) = 198{,}1\ mm$$

Then, the resistance of the T-stub in tension is verified for the two possible failure modes for the case of no prying ($m_{pl,Rd}$=23,5KN.m as previously demonstrated):

Mode 1-2

$$F_{T,1-2,Rd} = \frac{2\ l_{eff,1-2}\ m_{pl,Rd}}{m} = 227{,}4\ KN$$

And Mode 3 ($F_{t,Rd}$= 131,5KN)

$$F_{T,3,Rd} = \sum F_{t,Rd} = 2F_{t,Rd} = 262{,}9\ KN$$

Finally, the T-stub in tension resistance is:

$$F_{T,Rd} = min\left(F_{T,1-2,Rd}, F_{T,3,Rd}\right) = 227{,}4\ KN$$

And its lever arm:

$$z_t = \frac{p}{2} = 80\ mm$$

Resistance of the component base plate in bending and concrete in compression

The bearing strength calculation is presented above (f_{jd}=20,642MPa), as well as the width of the strip (c=39,0 mm).

Therefore, the only remaining parameter essential to calculate the component resistance is the effective area:

$$A_{eff} = \frac{N_{Ed} + F_{T,Rd}}{f_{jd}} = 3{,}040 \times 10^5 mm^2$$

The effective width is:

$$b_{eff} = 2 \times \left(t_f + c + min\left\{c; \frac{a - h_c}{2}\right\}\right) = 189{,}8\ mm$$

And the effective length is calculated in function of the effective area:

$$l_{eff} = \begin{cases} \dfrac{A_{eff}}{b_{eff}} = 160{,}1mm \\ {}^{b_c}/_{2} + c = 159{,}0\ mm = 159{,}0mm \\ {}^{b}/_{2} = 165\ mm \end{cases}$$

The component's resistance is then obtained:

$$F_{C,Rd} = b_{eff}\ l_{eff}\ f_{jd} = 627{,}4\ KN$$

And the lever arm of the compression force is:

$$z_c = \ min\left(\frac{b_c}{2} + c; \frac{b}{2}\right) - \frac{l_{eff}}{2} = 78{,}9\ mm$$

Resistance of the component column flange in compression

The component resistance depends on the plastic bending moment capacity of the column:

$$M_{c,Rd} = M_{pl,z,Rd} = \frac{W_{z,pl}\ f_{yk}}{\gamma_{M0}} = 117{,}1\ KN.m$$

Thus, the design compression resistance of the compression part of the flange is:

$$F_{c,fc,Rd} = \frac{M_{c,Rd}}{(b_c/2)} = 976{,}0\ KN$$

Assembly of the components

The tension part resistance is:

$$F_{T,l,Rd} = 227{,}4\ KN$$

And its lever arm:

$$z_{T,l} = 80\ mm$$

The compression part resistance is taken as the minimum resistance of the components column flange and web in compression or concrete in compression and base plate in bending:

$$F_{C,r,Rd} = min\left(F_{c,pl,Rd}; F_{c,fc,Rd}\right) = 627{,}4\ KN$$

And the lever arm is:

$$z_{C,r} = 78{,}9\ mm$$

Since the eccentricity is $e = \frac{M_{26,56,Ed}}{N_{Ed}} = -250\,mm$, which corresponds to the case of a dominant bending moment with tension on the left side and compression in the right side ($N_{Ed} \leq 0$ and $e \leq -z_{C,l}$), the joint's resistance is calculated by:

$$M_{z,Rd} = min \begin{cases} \frac{F_{T,l,Rd} z}{z_{C,r}/e + 1} = 52{,}8 KN.m \\ \frac{-F_{C,r,Rd} z}{z_{T,l}/e - 1} = 75{,}5\ KN.m \end{cases} = 52{,}8\ KN.m$$

About the classification according to resistance, the joint is categorized as partial-strength because:

$$M_{z,Rd} = 52{,}8\ KN.m \begin{cases} \geq 0{,}25 M_{pl,z,Rd} = 29{,}3\ KN.m \\ \leq M_{pl,z,Rd} = 117{,}1\ KN.m \end{cases}$$

4.5.3.2 Initial Stiffness

Stiffness of the component base plate in bending and anchor bolts in tension

As it is known, there are no prying forces, so the bolt stiffness coefficient is calculated as following:

$$k_b = 2{,}0\ \frac{A_s}{L_b} = 2{,}000\ mm$$

And the stiffness coefficient of the T-stub as:

$$k_p = \frac{0{,}425\ l_{eff,1-2} t^3}{m^3} = 8{,}170\ mm$$

Finally, the component stiffness is:

$$k_T = \frac{1}{\frac{1}{k_b} + \frac{1}{k_p}} = 1{,}661\ mm$$

Stiffness of the component base plate in bending and concrete in compression

The equivalent width of a rigid plate is the same as previous:

$$b_{eff,s} = t_f + 2{,}5t = 67mm$$

But the effective length is different. Thus, the compressed length of the flange (l_c) is needed:

$$l_c = l_{eff} - min\left(c; \frac{b - b_c}{2}\right) = 121{,}2\ mm$$

Then, the effective length in terms of stiffness is:

$$l_{eff,s} = l_c + 1{,}25t = 146{,}2\ mm$$

Finally, the stiffness of the component is:

$$k_c = k_{13} = \frac{E_c \sqrt{b_{eff,s}\ l_{eff,s}}}{1{,}275\ E} = 7{,}724\ mm$$

Assembly of the components

The lever arms are:

$$z_c = 78{,}9\ mm$$

$$z_t = 80\ mm$$

$$z = z_c + z_t = 158{,}9\ mm$$

Stiffness is calculated for particular eccentricity, consequently the eccentricity e_k, at which the rotation is zero, is required:

$$e_{k,y} = \frac{k_c\, z_c + k_t\, z_t}{k_c + k_t} = 50{,}8\ mm$$

Ultimately, the bending initial stiffness is obtained for the previously calculated eccentricity (e_y= -250mm):

$$s_{y,j,ini} = \frac{e_y}{e_y + e_{k,y}} \frac{E_s\, z^2}{\frac{1}{k_c} + \frac{1}{k_t}} = 9{,}098\ MN.m/rad$$

For the classification according to stiffness, the relative bending stiffness of the column needs to be calculated. For a column length L_c=2m and cross section HEB 240:

$$\bar{s}_{z,j,ini} = s_{z,j,ini}\ \frac{L_c}{E_s I_{c,z}} = 2{,}21$$

The designed column base is semi-rigid in sway frames as well as non-sway frames (λ_0 = 1,36) because:

$$\bar{s}_{z,j,ini} = 2{,}21 \geq 0{,}5$$

$$\bar{s}_{z,j,ini} = 2{,}21 \leq 12 = \bar{s}_{j,ini,nsf}$$

$$\bar{s}_{z,j,ini} = 2{,}21 \leq 30 = \bar{s}_{j,ini,sf}$$

4.5.4 M_z-M_Y INTERACTION CURVE

The interaction curve is defined by the following function:

$$\left(\frac{M_z}{M_{z,Rd}}\right)^2+\left(\frac{M_y}{M_{y,Rd}}\right)^2=1 \Leftrightarrow M_z=\sqrt{\left(1-\left(\frac{M_y}{M_{y,Rd}}\right)^2\right){M_{z,Rd}}^2}$$

The moment capacity for each axis is:

$$M_{z,Rd}=52{,}8\ KN.m$$

$$M_{y,Rd}=96{,}2\ KN.m$$

The moment capacity for the deviated direction is obtained by equating the function of the curve to the function of the line which is deviated from the strong axis by an angle α=26,56º:

$$\begin{cases} M_z=\sqrt{\left(1-\left(\frac{M_y}{M_{y,Rd}}\right)^2\right){M_{z,Rd}}^2} \\ M_z=\tan(\alpha)\cdot M_y \end{cases} \Rightarrow \begin{cases} \sqrt{\left(1-\left(\frac{M_y}{96{,}2}\right)^2\right)52{,}8^2}=\tan(26{,}56)\cdot M_y \\ M_z=\tan(\alpha)\cdot M_y \end{cases}$$

$$\begin{cases} M_y=71{,}1KN.m \\ M_z=35{,}6KN.m \end{cases}$$

Finally, the moment capacity is:

$$M_{26,56,Rd}=\sqrt{{M_y}^2+{M_z}^2}=79{,}5KN.m$$

This verifies the safety condition:

$$M_{26,56,Ed}=50\ KN.m \le M_{26,56,Rd}=79{,}5KN.m$$

Figure 4.19 shows the interaction curve and the representation of the moment capacity.

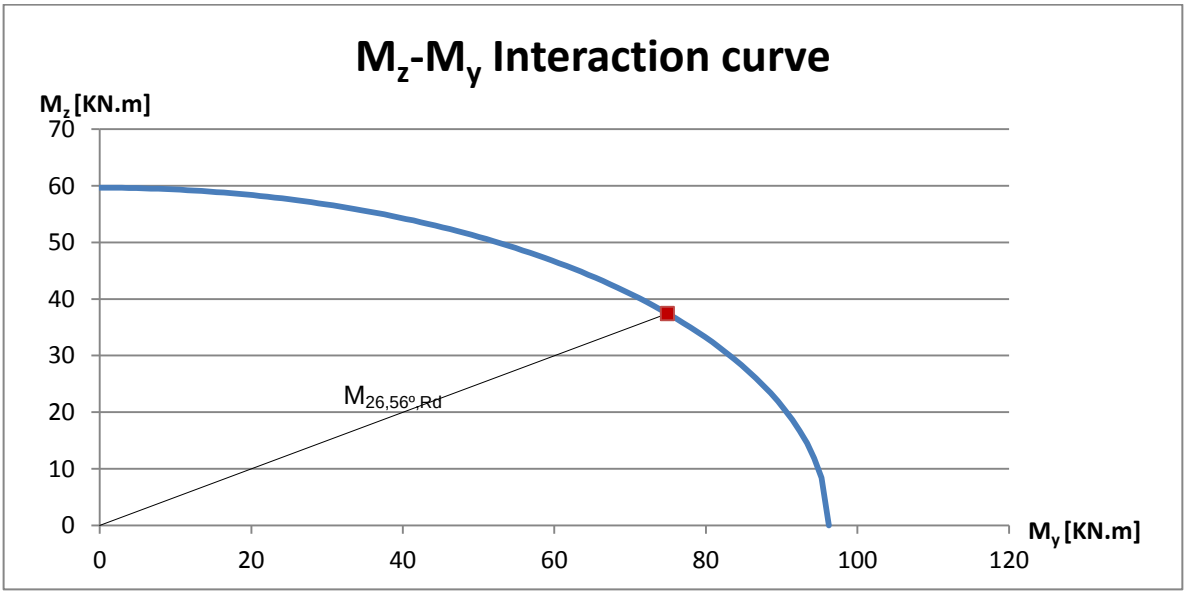


Figure 4.19- Mz-My Interaction curve (worked example)

5
CONCLUSION

This dissertation focused on the analysis and design of column base connections. Special attention was given to the most common method used for studying steel joints and composite joints, which is the component method. The procedure was analyzed in detail to fully understand its foundations. Moreover, experiments suitable for comparing with this method (i.e., experiments on a simple column base) were searched. Thus, tests performed by Brno University of Technology were found and described in this essay.

The component method, which is described in EN 1993-1-8, considers that joints can be characterized as a set of individual components. Thus, the main components of column bases were identified and a closer look was made to their individual behavior. The tension component is modeled as a T-stub and its effective length is the main characteristic of the component. This is a very difficult parameter to obtain as it demands an extensive knowledge of the subject. With regard to the compression part of the joint, the most important parameter is the bearing strength of the concrete when subjected to a concentrated force.

A numerical model is created using a Finite Element software (ABAQUS), and validated with experimental results. The model was then subjected to bending about the strong axis and the results were compared with the component method. The comparison revealed that the component method is very conservative in terms of estimating the resistance of the joint. However, the initial stiffness was proved to be almost twice smaller than that obtained from the numerical analysis. The numerical model was also used in the validation of the proposed analytical model.

A model for predicting the column base behavior under weak axis bending was proposed. The model is in accordance with the component method for strong axis bending. The differences between the model for weak and strong axis bending were identified. The component which differs most is the tension component since not all the yield mechanisms are possible in this case. Regarding the component in the compression, the effective area is calculated according to the position of the neutral axis instead of considering that this area is always the same, independently of the acting loads (like what happens in the strong axis bending).

The analytical model allows to estimate the moment capacity of the joint for bending in any direction. This was made possible by the help of an interaction curve between the moment capacities of the joint for bending about the main axes assuming an elliptical shape.

Finally, the analytical model was validated by the comparison with the numerical model. At first, the column base model in ABAQUS was subjected to weak axis bending with a load eccentricity of $e= -0,25m$ and the results were compared. Then, the column was subjected to various loading planes

with three different eccentricities ($e= -0,25m$; $e= +0,25m$ and $e=\infty$) and an interaction curve was drawn for the three cases.

The comparison for the weak axis bending proved that the model is accurate but also conservative in terms of resistance, like for the case of strong axis bending. Regarding the initial stiffness, the values of the analytical method showed a smaller ratio than for the case of strong axis bending. However, they were still much higher than the numerical results. Therefore, further studies should be performed aiming at dealing with this issue for both strong axis bending and weak axis bending.

It has been found that the proposed shape for the interaction curve is appropriate since it provides consistent results with those obtained with the numerical model. Once the analytical curve is obtained by moment capacities that are very conservative, the analytical curves are also very conservative.

In conclusion, the proposed analytical model may be considered for practical design. However, further validation should be carried out in the future. It is suggested that the model is applied to a large number of column base cases and that the estimates obtained with the analytical model are compared with the results from FE analyses. It is also suggested that the FE model presented in this dissertation is further improved in order to account for a more realistic behavior of the concrete side of the joint under tension.

REFERENCES

[1] *EN 1993-1-8: Eurocode 3: Design of steel structures, Part 1-8: - Design of joints,* European Comitee for Standardization, 2003.

[2] Horová, K., *Base plates of hollow sections,* Czech Technical University in Prague, 2010.

[3] Grauvilardell, J., Lee, D., Hajjar, J., Dexter, R., *Synthesis of Design, Testing, and Analysis Research on Steel Column Base Plate Connections in High-seismic Zones,* 2005. [Online]. Available: http://www.aisc.org/uploadedFiles/Research/Research_Reports/Hajjar%20-%20Synthesis%20of%20Base%20Plate%20Connections.pdf. [Accessed on 28 03 2014].

[4] Abejide, O., *Effectiveness of Base Plate Thickness Design Criteria in Steel Columns*, Medwell Journals, n.º 2, pp. 1207-1217, 2007.

[5] Sokol, Z, *Column Bases*, 18 10 2005. [Online]. Available: http://people.fsv.cvut.cz/www/wald/CESTRUCO/Texts_of_lessons/07-GB_Column_Bases.pdf. [Accessed on 28 03 2014].

[6] Correia, R., *Dimensionamento de Bases de pilares metálicos - Versão para discussão*, Faculdade de Engenharia da Universidade do Porto, 2013.

[7] Wald, F., Sokol, Z., Jaspart, J., *Base Plate in Bending and Anchor Bolts in Tension*, Heron, vol. 53, n.º 1/2, pp. 21-50, 2008.

[8] European Comission, Directorate-General for Research and Innovation, *New Market Chances for Steel Structures by Innovative Fastening Solutions between Steel and Concrete*, Research Programme of the Research Fund for Coal and Steel; Stuttgart, Prague, Coimbra, Bielefeld and Dreieich, 2010.

[9] Sokol, Z. , Wald, F., *Modelování tuhosti a únosnosti tažené části patek sloupů*, Czech Technical University in Prague, 2000.

[10] Wald, F., Hofmann, J., Kuhlmann, U., *Design of steel-to-concrete joints, Design manual I - version for revision*, Czech Technical University in Prague, February 2014.

[11] Steenhuis, M., Wald, F., Sokol, Z., Stark, J, *Concrete in compression and base plate in bending,* Heron, vol. 53, n.º 1/2, pp. 51-68, 2008.

[12] *EN 1992-1-1: Eurocode 2: Design of concrete structures, Part 1-1: - General rules and rules for buildings,* European Comitee for Standardization, 2004.

[13] *EN 1993-1-1: Eurocode 3: Design of steel structures, Part 1-1: - General rules and rules for buildings,* Instituto Português de Qualidade, 2005.

[14] Gresnigt, N., Romeijn, A., Wald, F., Steenhuis, M., *Column bases in shear and normal force*, Heron, vol. 53, n.º 1/2, 2008.

[15] Wald, F., Sokol, Z., Jaspart, J., *Component Method for Steel Column Bases*, Heron, vol. 53, n.º 1/2, pp. 3-20, 2008.

[16] Jaspart, J., Wald, F., Weynand, K., Gresnight, N., *Steel column base classification*, Heron, vol. 53, n.º 1/2, 2008.

[17] Bajer, M., Vild, M., Barnat, J., Homolek, J., *Influence of selected parameters on desing optimization of anchor joint*, 12th International Conference on Steel, Space and composite structures, 28-30 May 2014, Prague.

[18] Khodaie, S., Mohamadi-shooreh, M., Mofid, M. *Parametric analyses on the initial stiffness of the SHS column base plate connections using FEM*, Engineering Structures, vol. 34, pp. 363-370, 2012.

ANNEX 1

CALCULATION FOR THE COMPARISON WITH THE NUMERICAL MODEL – e= -0,25m

The following table shows the data of the joint.

Table 1 - Data of the joint

	Column		Base plate		Concrete		Bolts	
Material Properties		Steel S235		Steel S235		C16/20		Grade 8.8
	f_y	235 MPa	f_y	235 MPa	f_{ck}	16 MPa	f_{ub}	830 MPa
	E	210 GPa	E	210 GPa	E_c	29 GPa		
Dimensions		HEB 240	a	440 mm	a_1	1500 mm		M20
	h_c	240 mm	b	330 mm	b_1	1000 mm	d	20 mm
	b_c	240 mm	t	20 mm	h	400 mm	A_s	220 mm^2
	t_w	10 mm	e_a	50 mm	$a_{r,l}$	380 mm	L	250 mm
	t_f	17 mm	e_b	85 mm	$a_{r,r}$	680 mm	h_{bh}	20 mm
	A	$1,06x10^6$ mm^2	e_c	50 mm	b_r	335 mm		
	$I_{c,y}$	$1,126x10^8$ mm^4	p	160 mm	t_{gr}	30 mm		
	$w_{y,pl}$	$1,053x10^6$ mm^3	a_{wf}	8mm				
	$I_{c,z}$	$3,923x10^7$ mm^4						
	$w_{z,pl}$	$4,984x10^5$ mm^3						

COLUMN BASE UNDER STRONG AXIS BENDING

RESISTANCE OF COMPONENT BASE PLATE IN BENDING AND ANCHOR BOLTS IN TENSION

Anchor bolt lever arm:

$$m = e_c - 0.8\, a_{wf}\sqrt{2} = 40.9mm$$

Verification of the prying effects:

$$L_{bf} = t + t_{gr} + h_{bh} = 60mm$$

$$L_{be} = 8d = 160\ mm$$

$$L_b = L_{bf} + L_{be} = 220\ mm$$

$$L_{b,min} = \frac{8.82\, m^3\, A_s}{l_{eff,1}\, t^3} = 100.9\ mm$$

$$L_b > L_{b,min} \Rightarrow No\ prying\ forces$$

Effective lengths for each mechanism:

$$l_{np,1} = 2\pi m = 257.3\ mm$$

$$l_{np,2} = 2\pi m + 2p = 577{,}3\ mm$$

$$l_{np,3} = \pi m + 4e = 468{,}6\ mm$$

$$l_{np,4} = 4m + 1{,}25e_x = 226{,}3\ mm$$

$$l_{np,5} = 2m + 0{,}625e_x + 0{,}5p = 193{,}1\ mm$$

$$l_{np,6} = 2m + 0{,}625e_x + e = 198{,}1\ mm$$

$$l_{np,7} = 0{,}5b = 165\ mm$$

Effective length of the T-stub:

$$l_{eff,1-2} = min\left(l_{np,1}; l_{np,2}; l_{np,3}; l_{np,4}; l_{np,5}; l_{np,6}; l_{np,7}\right) = 165mm$$

Plastic bending moment capacity of the base plate:

$$m_{pl,Rd} = \frac{1}{4} t^2 f_{yd} = 23{,}5\ KN.m/m$$

Resistance of failure Mode 1-2:

$$F_{T,1-2,Rd} = \frac{2\, l_{eff,1-2}\, m_{pl,Rd}}{m} = 189{,}4\ KN$$

Tension resistance of the bolts:

$$F_{t,Rd} = \frac{0{,}9\, f_{ub}\, A_s}{\gamma_{M2}} = 164{,}3\ KN$$

Resistance of failure Mode 3:

$$F_{T,3,Rd} = \sum B_{t,Rd} = 2BF_{t,Rd} = 328{,}7\ KN$$

Resistance of the tension T-stub:

$$F_{T,Rd} = min\left(F_{T,1-2,Rd}; F_{T,3,Rd}\right) = 189{,}4\ KN$$

Lever arm of the tension part:

$$z_t = \frac{h_c}{2} + e_c = 170\ mm$$

RESISTANCE OF COMPONENT BASE PLATE IN BENDING AND CONCRETE IN COMPRESSION

Loaded area, A_{C0}, and spread area, A_{C1}:

$$A_{c0} = a\ b = 1{,}452 \times 10^5\ mm^2$$

$$a_2 = min\begin{cases} a + h = 840\ mm \\ 3a = \ 1320\ mm \\ a_1 = 1500\ mm \end{cases} = 840\ mm$$

$$b_2 = min\begin{cases} b + h = 730\ mm \\ 3b = 990\ mm \\ b_1 = 1000\ mm \end{cases} = 730\ mm$$

$$A_{c1} = a_2\ b_2 = 6{,}132 \times 10^5\ mm^2$$

Checking the influence of the grout:

$$0{,}2\ \min(\ a; b) = 66mm > t = 20\ mm$$

Thus, the joint material coefficient β_j is 2/3 and the bearing strength is:

$$f_{jd} = \beta_j\ f_{cd}\ \sqrt{\frac{A_{c1}}{A_{c0}}} = 30{,}962\ MPa \leq 3\ f_{cd} = 67{,}8MPa$$

Width of the strip:

$$c = t\ \sqrt{\frac{f_{yk}}{3\ f_{jd}\ \gamma_{M0}}} = 31{,}8\ mm$$

Effective length:

$$l_{eff} = min\begin{cases} b_c + 2\ c = 332{,}6\ mm \\ b = 330\ mm \end{cases} = 303{,}6\ mm$$

Effective width:

$$b_{eff} = min\{c; (a - h_c)/2\} + t_f + c = 80{,}6mm$$

Effective area:

$$A_{eff} = b_{eff}\ l_{eff} = 2{,}447 \times 10^4\ mm^2$$

Lever arm of the compression force:

$$z_c = \frac{h_c}{2} - \frac{t_f}{2} = 111{,}5\ mm$$

Compressed part resistance:

$$F_{c,pl,Rd} = A_{eff}\ f_{jd} = 757{,}9\ KN$$

RESISTANCE OF THE COMPONENT COLUMN FLANGE AND WEB IN COMPRESSION

The component resistance depends on the plastic bending moment capacity of the column:

$$M_{c,Rd} = M_{pl,y,Rd} = \frac{W_{y,pl}\, f_{yk}}{\gamma_{M0}} = 247{,}5\ KN.m$$

Thus, the design compression resistance of the flange is:

$$F_{c,fc,Rd} = \frac{M_{c,Rd}}{\left(h_c - t_f\right)} = 1109{,}7\ KN$$

ASSEMBLY

For the calculation of the bending resistance, the load eccentricity needed:

$$e = -250\ mm$$

This corresponds to the case of a dominant bending moment with tension on the left side and compression in the right side (N_{Ed}≤0 and e≤-$z_{C,l}$).

The tension part resistance is:

$$F_{T,Rd} = 189{,}4\ KN$$

And its lever arm:

$$z_t = 170\ mm$$

The compression part resistance:

$$F_{C,Rd} = min\left(F_{c,pl,Rd}; F_{c,fc,Rd}\right) = 666{,}1\ KN$$

And the lever arm is:

$$z_c = 111{,}5\ mm$$

Thus, knowing that $z = z_t + z_c$, the joint resistance is:

$$M_{y,R} = min \begin{cases} \dfrac{F_{T,l,Rd} z}{z_{C,r}/e + 1} = 96{,}2\ KN.m \\ \dfrac{-F_{C,r,Rd} z}{z_{T,l}/e - 1} = 127{,}0\ KN.m \end{cases} = 96{,}2\ KN.m$$

COLUMN BASE UNDER WEAK AXIS BENDING

RESISTANCE OF COMPONENT BASE PLATE IN BENDING AND ANCHOR BOLTS IN TENSION

Effective lengths for the possible mechanism for the no-prying case (m_x=40,9mm):

$$l_{np,1} = 2\pi m = 257.3\ mm$$

$$l_{np,3} = \pi m + 4e = 468{,}6\ mm$$

$$l_{np,4} = 4m + 1{,}25e_x = 226{,}3\ mm$$

$$l_{np,6} = 2m + 0{,}625e_x + e = 198{,}1\ mm$$

Effective length of the T-stub:

$$l_{eff,1-2} = \min\left(l_{np,1}; l_{np,3}; l_{np,4}; l_{np,6}\right) = 198{,}1\ mm$$

Resistance of Mode 1-2 ($m_{pl,Rd}$=23,5KN.m)

$$F_{T,1-2,Rd} = \frac{2\ l_{eff\ ,1-2}\ m_{pl,Rd}}{m} = 227{,}4\ KN$$

Tension resistance of the bolts:

$$F_{t,Rd} = \frac{0{,}9\ f_{ub}\ A_s}{\gamma_{M2}} = 164{,}3\ KN$$

Resistance of failure Mode 3:

$$F_{T,3,Rd} = \sum B_{t,Rd} = 2BF_{t,Rd} = 328{,}7\ KN$$

Resistance of the tension T-stub:

$$F_{T,Rd} = min\left(F_{T,1-2,Rd}; F_{T,3,Rd}\right) = 227{,}4\ KN$$

And its lever arm:

$$z_t = \frac{p}{2} = 80\ mm$$

RESISTANCE OF COMPONENT BASE PLATE IN BENDING AND CONCRETE IN COMPRESSION

The bearing strength calculation is presented above (f_{jd}=30,962MPa), as well as the width of the strip (c=31,8 mm).

Effective area of the compressed T-stub:

$$A_{eff} = \frac{F_{T,Rd} - N_{Ed}}{f_{jd}} = 2{,}573 \times 10^3 mm^2$$

The effective width is:

$$b_{eff} = 2 \times \left(t_f + c + min\left\{c; \frac{a - h_c}{2}\right\}\right) = 161{,}2\ mm$$

And the effective length:

$$l_{eff} = \begin{cases} \dfrac{A_{eff}}{b_{eff}} = 125{,}7\ mm \\ {b_c}/{2} + c = 151{,}8mm \\ {b}/{2} = 165\ mm \end{cases} = 125{,}7mm$$

The component resistance is then:

$$F_{C,Rd} = b_{eff}\ l_{eff}\ f_{jd} = 683{,}1\ KN$$

And the lever arm of the compression force:

$$z_c = \ min\left(\frac{b_c}{2} + c; \frac{b}{2}\right) - \frac{l_{eff}}{2} = 83{,}4\ mm$$

ASSEMBLY

Since the eccentricity is $e = -250\ mm$, which corresponds to the case of a dominant bending moment with tension on the left side and compression in the right side ($N_{Ed} \leq 0$ and $e \leq -z_{C,l}$), the joint resistance is calculated by:

$$M_{z,R} = min \begin{cases} \dfrac{F_{T,l,Rd} z}{{z_{C,r}}/{e} + 1} = 59{,}7 KN.m \\ \dfrac{-F_{C,r,Rd} z}{{z_{T,l}}/{e} - 1} = 80{,}3\ KN.m \end{cases} = 59{,}7\ KN.m$$

MZ-MY INTERACTION CURVE

The interaction curve is defined by the following function (see Figure 1):

$$\left(\frac{M_z}{M_{z,R}}\right)^2 + \left(\frac{M_y}{M_{y,R}}\right)^2 = 1 \Leftrightarrow\ M_z = \sqrt{\left(1 - \left(\frac{M_y}{M_{y,R}}\right)^2\right) {M_{z,R}}^2}$$

Where:

$$M_{z,R} = 59{,}7\ KN.m$$
$$M_{y,R} = 96{,}2\ KN.m$$

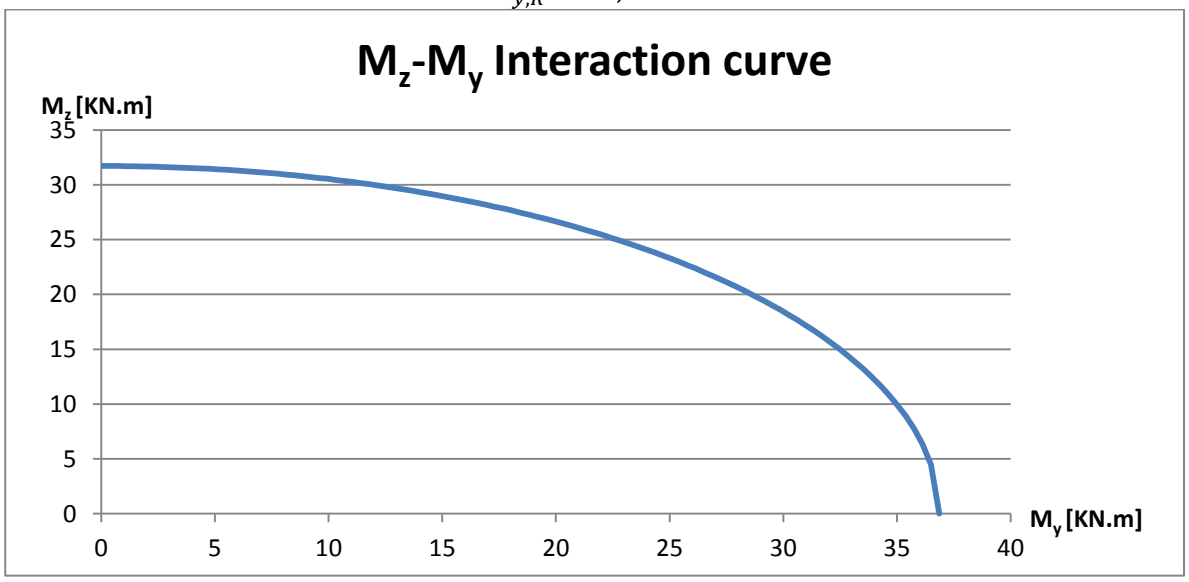


Figure 1 - M_z-M_y Interaction curve

ANNEX 2

CALCULATION FOR THE COMPARISON WITH THE NUMERICAL MODEL – e= +0,25m

The following table shows the data of the joint.

Table 2 - Data of the joint

	Column		Base plate		Concrete		Bolts	
Material Properties		Steel S235		Steel S235		C16/20		Grade 8.8
	f_y	235 MPa	f_y	235 MPa	f_{ck}	16 MPa	f_{ub}	830 MPa
	E	210 GPa	E	210 GPa	E_c	29 GPa		
Dimensions		HEB 240	a	440 mm	a_1	1500 mm		M20
	h_c	240 mm	b	330 mm	b_1	1000 mm	d	20 mm
	b_c	240 mm	t	20 mm	h	400 mm	A_s	220 mm^2
	t_w	10 mm	e_a	50 mm	$a_{r,l}$	380 mm	L	250 mm
	t_f	17 mm	e_b	85 mm	$a_{r,r}$	680 mm	h_{bh}	20 mm
	A	$1,06x10^6$ mm^2	e_c	50 mm	b_r	335 mm		
	$I_{c,y}$	$1,126x10^8$ mm^4	p	160 mm	t_{gr}	30 mm		
	$w_{y,pl}$	$1,053x10^6$ mm^3	a_{wf}	8mm				
	$I_{c,z}$	$3,923x10^7$ mm^4						
	$w_{z,pl}$	$4,984x10^5$ mm^3						

COLUMN BASE UNDER STRONG AXIS BENDING

RESISTANCE OF COMPONENT BASE PLATE IN BENDING AND ANCHOR BOLTS IN TENSION

Anchor bolt lever arm:

$$m = e_c - 0.8\, a_{wf}\sqrt{2} = 40.9mm$$

Verification of the prying effects:

$$L_{bf} = t + t_{gr} + h_{bh} = 60mm$$

$$L_{be} = 8d = 160\ mm$$

$$L_b = L_{bf} + L_{be} = 220\ mm$$

$$L_{b,min} = \frac{8.82\, m^3\, A_s}{l_{eff,1}\, t^3} = 100.9\ mm$$

$$L_b > L_{b,min} \Rightarrow No\ prying\ forces$$

Effective lengths for each mechanism:

$$l_{np,1} = 2\pi m = 257.3\ mm$$

$$l_{np,2} = 2\pi m + 2p = 577{,}3\ mm$$

$$l_{np,3} = \pi m + 4e = 468{,}6\ mm$$

$$l_{np,4} = 4m + 1{,}25e_x = 226{,}3\ mm$$

$$l_{np,5} = 2m + 0{,}625e_x + 0{,}5p = 193{,}1\ mm$$

$$l_{np,6} = 2m + 0{,}625e_x + e = 198{,}1\ mm$$

$$l_{np,7} = 0{,}5b = 165\ mm$$

Effective length of the T-stub:

$$l_{eff,1-2} = min\left(l_{np,1}; l_{np,2}; l_{np,3}; l_{np,4}; l_{np,5}; l_{np,6}; l_{np,7}\right) = 165mm$$

Plastic bending moment capacity of the base plate:

$$m_{pl,Rd} = \frac{1}{4} t^2 f_{yd} = 23{,}5\ KN.m/m$$

Resistance of failure Mode 1-2:

$$F_{T,1-2,Rd} = \frac{2\, l_{eff,1-2}\, m_{pl,Rd}}{m} = 189{,}4\ KN$$

Tension resistance of the bolts:

$$F_{t,Rd} = \frac{0{,}9\, f_{ub}\, A_s}{\gamma_{M2}} = 164{,}3\ KN$$

Resistance of failure Mode 3:

$$F_{T,3,Rd} = \sum B_{t,Rd} = 2BF_{t,Rd} = 328{,}7\ KN$$

Resistance of the tension T-stub:

$$F_{T,Rd} = min\left(F_{T,1-2,Rd}; F_{T,3,Rd}\right) = 189{,}4\ KN$$

Lever arm of the tension part:

$$z_t = \frac{h_c}{2} + e_c = 170\ mm$$

RESISTANCE OF COMPONENT BASE PLATE IN BENDING AND CONCRETE IN COMPRESSION

Loaded area, A_{C0}, and spread area, A_{C1}:

$$A_{c0} = a\ b = 1{,}452 \times 10^5\ mm^2$$

$$a_2 = min\begin{cases} a + h = 840\ mm \\ 3a = \ 1320\ mm \\ a_1 = 1500\ mm \end{cases} = 840\ mm$$

$$b_2 = min\begin{cases} b + h = 730\ mm \\ 3b = 990\ mm \\ b_1 = 1000\ mm \end{cases} = 730\ mm$$

$$A_{c1} = a_2\ b_2 = 6{,}132 \times 10^5\ mm^2$$

Checking the influence of the grout:

$$0{,}2\ \min(\ a; b) = 66mm > t = 20\ mm$$

Thus, the joint material coefficient β_j is 2/3 and the bearing strength is:

$$f_{jd} = \beta_j\ f_{cd}\ \sqrt{\frac{A_{c1}}{A_{c0}}} = 30{,}962\ MPa \leq 3\ f_{cd} = 67{,}8MPa$$

Width of the strip:

$$c = t\ \sqrt{\frac{f_{yk}}{3\ f_{jd}\ \gamma_{M0}}} = 31{,}8\ mm$$

Effective length:

$$l_{eff} = min\begin{cases} b_c + 2\ c = 332{,}6\ mm \\ b = 330\ mm \end{cases} = 303{,}6\ mm$$

Effective width:

$$b_{eff} = min\{c; (a - h_c)/2\} + t_f + c = 80{,}6mm$$

Effective area:

$$A_{eff} = b_{eff}\ l_{eff} = 2{,}447 \times 10^4\ mm^2$$

Lever arm of the compression force:

$$z_c = \frac{h_c}{2} - \frac{t_f}{2} = 111{,}5\ mm$$

Compressed part resistance:

$$F_{c,pl,Rd} = A_{eff}\ f_{jd} = 757{,}9\ KN$$

RESISTANCE OF THE COMPONENT COLUMN FLANGE AND WEB IN COMPRESSION

The component resistance depends on the plastic bending moment capacity of the column:

$$M_{c,Rd} = M_{pl,y,Rd} = \frac{W_{y,pl}\, f_{yk}}{\gamma_{M0}} = 247{,}5\ KN.m$$

Thus, the design compression resistance of the flange is:

$$F_{c,fc,Rd} = \frac{M_{c,Rd}}{\left(h_c - t_f\right)} = 1109{,}7\ KN$$

ASSEMBLY

For the calculation of the bending resistance, the load eccentricity needed:

$$e = +250\ mm$$

This corresponds to the case of a dominant bending moment with tension in one side and compression in the ohter side (N_{Ed}>0 and e>z_T).

The tension part resistance is:

$$F_{T,Rd} = 189{,}4\ KN$$

And its lever arm:

$$z_t = 170\ mm$$

The compression part resistance:

$$F_{C,Rd} = min\left(F_{c,pl,Rd}; F_{c,fc,Rd}\right) = 666{,}1\ KN$$

And the lever arm is:

$$z_c = 111{,}5\ mm$$

Thus, knowing that $z = z_t + z_c$, the joint resistance is (e= +0,25m):

$$M_{y,R} = min\begin{cases} \dfrac{F_{T,l,Rd}\, z}{z_{C,r}/e + 1} = 36{,}9\ KN.m \\ \dfrac{-F_{C,r,Rd}\, z}{z_{T,l}/e - 1} = 66{,}7\ KN.m \end{cases} = 36{,}9\ KN.m$$

COLUMN BASE UNDER WEAK AXIS BENDING

RESISTANCE OF COMPONENT BASE PLATE IN BENDING AND ANCHOR BOLTS IN TENSION

Effective lengths for the possible mechanism for the no-prying case (m_x=40,9mm):

$$l_{np,1} = 2\pi m = 257.3\ mm$$

$$l_{np,3} = \pi m + 4e = 468{,}6\ mm$$

$$l_{np,4} = 4m + 1{,}25e_x = 226{,}3\ mm$$

$$l_{np,6} = 2m + 0{,}625e_x + e = 198{,}1\ mm$$

Effective length of the T-stub:

$$l_{eff,1-2} = \min\left(l_{np,1}; l_{np,3}; l_{np,4}; l_{np,6}\right) = 198{,}1\ mm$$

Resistance of Mode 1-2 ($m_{pl,Rd}$=23,5KN.m)

$$F_{T,1-2,Rd} = \frac{2\ l_{eff\ ,1-2}\ m_{pl,Rd}}{m} = 227{,}4\ KN$$

Tension resistance of the bolts:

$$F_{t,Rd} = \frac{0{,}9\ f_{ub}\ A_s}{\gamma_{M2}} = 164{,}3\ KN$$

Resistance of failure Mode 3:

$$F_{T,3,Rd} = \sum B_{t,Rd} = 2BF_{t,Rd} = 328{,}7\ KN$$

Resistance of the tension T-stub:

$$F_{T,Rd} = min\left(F_{T,1-2,Rd}; F_{T,3,Rd}\right) = 227{,}4\ KN$$

And its lever arm:

$$z_t = \frac{p}{2} = 80\ mm$$

RESISTANCE OF COMPONENT BASE PLATE IN BENDING AND CONCRETE IN COMPRESSION

The bearing strength calculation is presented above (f_{jd}=30,962MPa), as well as the width of the strip (c=31,8 mm).

Effective area of the compressed T-stub:

$$A_{eff} = \frac{F_{T,Rd} - N_{Ed}}{f_{jd}} = 5{,}573 \times 10^3 mm^2$$

The effective width is:

$$b_{eff} = 2 \times \left(t_f + c + min\left\{c; \frac{a - h_c}{2}\right\}\right) = 161{,}2\ mm$$

And the effective length:

$$l_{eff} = \begin{cases} \dfrac{A_{eff}}{b_{eff}} = 34{,}6\ mm \\ b_c/_2 + c = 151{,}8mm \\ b/_2 = 165\ mm \end{cases} = 34{,}6mm$$

The component resistance is then:

$$F_{C,Rd} = b_{eff}\ l_{eff}\ f_{jd} = 172{,}6\ KN$$

And the lever arm of the compression force:

$$z_c = \ min\left(\frac{b_c}{2} + c; \frac{b}{2}\right) - \frac{l_{eff}}{2} = 134{,}6\ mm$$

ASSEMBLY

Since the eccentricity is $e = +250\ mm$, which corresponds to the case of a dominant bending moment with tension in one side and compression in the other side (N_{Ed}>0 and e>-z_T), the joint resistance is calculated by:

$$M_{z,R} = min\begin{cases} \dfrac{F_{T,l,Rd}z}{z_{C,r}/_e + 1} = 31{,}7KN.m \\ \dfrac{-F_{C,r,Rd}z}{z_{T,l}/_e - 1} = 54{,}4\ KN.m \end{cases} = 31{,}7\ KN.m$$

MZ-MY INTERACTION CURVE

The interaction curve is defined by the following function (see Figure 2):

$$\left(\frac{M_z}{M_{z,R}}\right)^2 + \left(\frac{M_y}{M_{y,R}}\right)^2 = 1 \Leftrightarrow\ M_z = \sqrt{\left(1 - \left(\frac{M_y}{M_{y,R}}\right)^2\right) {M_{z,R}}^2}$$

Where:

$$M_{z,R} = 31{,}7\ KN.m$$

$$M_{y,R} = 36{,}9\ KN.m$$

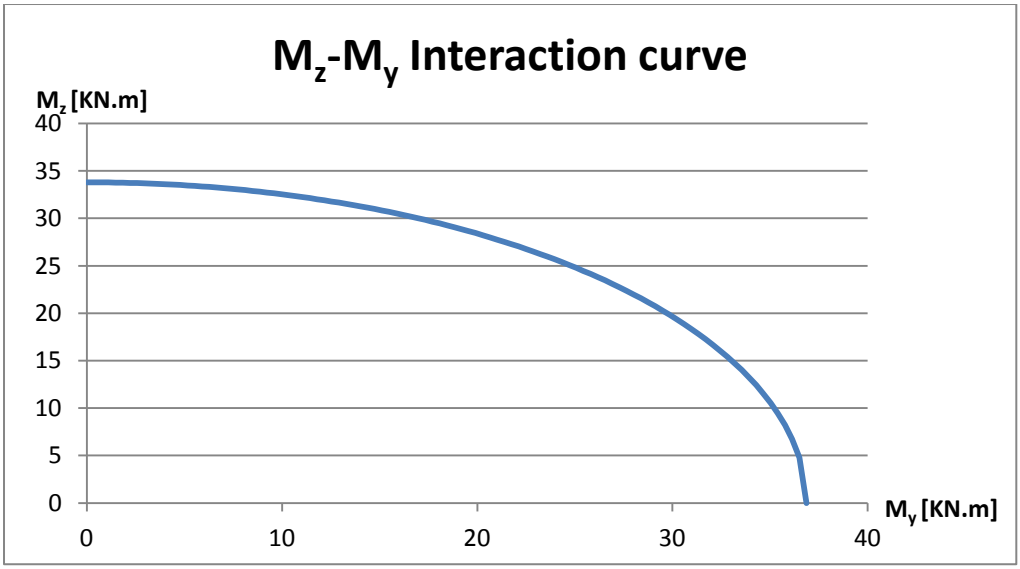


Figure 2 - M_z-M_y Interaction curve

ANNEX 3

CALCULATION FOR THE COMPARISON WITH THE NUMERICAL MODEL – e=infinite

The following table shows the data of the joint.

Table 3 - Data of the joint

	Column		Base plate		Concrete		Bolts	
Material Properties		Steel S235		Steel S235		C16/20		Grade 8.8
	f_y	235 MPa	f_y	235 MPa	f_{ck}	16 MPa	f_{ub}	830 MPa
	E	210 GPa	E	210 GPa	E_c	29 GPa		
Dimensions		HEB 240	a	440 mm	a_1	1500 mm		M20
	h_c	240 mm	b	330 mm	b_1	1000 mm	d	20 mm
	b_c	240 mm	t	20 mm	h	400 mm	A_s	220 mm^2
	t_w	10 mm	e_a	50 mm	$a_{r,l}$	380 mm	L	250 mm
	t_f	17 mm	e_b	85 mm	$a_{r,r}$	680 mm	h_{bh}	20 mm
	A	1,06x10^6 mm^2	e_c	50 mm	b_r	335 mm		
	$I_{c,y}$	1,126x10^8 mm^4	p	160 mm	t_{gr}	30 mm		
	$w_{y,pl}$	1,053x10^6 mm^3	a_{wf}	8mm				
	$I_{c,z}$	3,923x10^7 mm^4						
	$w_{z,pl}$	4,984x10^5 mm^3						

COLUMN BASE UNDER STRONG AXIS BENDING

RESISTANCE OF COMPONENT BASE PLATE IN BENDING AND ANCHOR BOLTS IN TENSION

Anchor bolt lever arm:

$$m = e_c - 0.8\, a_{wf}\sqrt{2} = 40.9mm$$

Verification of the prying effects:

$$L_{bf} = t + t_{gr} + h_{bh} = 60mm$$

$$L_{be} = 8d = 160\ mm$$

$$L_b = L_{bf} + L_{be} = 220\ mm$$

$$L_{b,min} = \frac{8.82\, m^3\, A_s}{l_{eff,1}\, t^3} = 100.9\ mm$$

$$L_b > L_{b,min} \Rightarrow No\ prying\ forces$$

Effective lengths for each mechanism:

$$l_{np,1} = 2\pi m = 257.3\ mm$$

$$l_{np,2} = 2\pi m + 2p = 577{,}3\ mm$$

$$l_{np,3} = \pi m + 4e = 468{,}6\ mm$$

$$l_{np,4} = 4m + 1{,}25e_x = 226{,}3\ mm$$

$$l_{np,5} = 2m + 0{,}625e_x + 0{,}5p = 193{,}1\ mm$$

$$l_{np,6} = 2m + 0{,}625e_x + e = 198{,}1\ mm$$

$$l_{np,7} = 0{,}5b = 165\ mm$$

Effective length of the T-stub:

$$l_{eff,1-2} = min\left(l_{np,1}; l_{np,2}; l_{np,3}; l_{np,4}; l_{np,5}; l_{np,6}; l_{np,7}\right) = 165mm$$

Plastic bending moment capacity of the base plate:

$$m_{pl,Rd} = \frac{1}{4}t^2 f_{yd} = 23{,}5\ KN.m/m$$

Resistance of failure Mode 1-2:

$$F_{T,1-2,Rd} = \frac{2\, l_{eff,1-2}\, m_{pl,Rd}}{m} = 189{,}4\ KN$$

Tension resistance of the bolts:

$$F_{t,Rd} = \frac{0{,}9\, f_{ub}\, A_s}{\gamma_{M2}} = 164{,}3\ KN$$

Resistance of failure Mode 3:

$$F_{T,3,Rd} = \sum B_{t,Rd} = 2BF_{t,Rd} = 328{,}7\ KN$$

Resistance of the tension T-stub:

$$F_{T,Rd} = min\left(F_{T,1-2,Rd}; F_{T,3,Rd}\right) = 189{,}4\ KN$$

Lever arm of the tension part:

$$z_t = \frac{h_c}{2} + e_c = 170\ mm$$

RESISTANCE OF COMPONENT BASE PLATE IN BENDING AND CONCRETE IN COMPRESSION

Loaded area, A_{C0}, and spread area, A_{C1}:

$$A_{c0} = a\ b = 1{,}452 \times 10^5\ mm^2$$

$$a_2 = min\begin{cases} a + h = 840\ mm \\ 3a = \ 1320\ mm \\ a_1 = 1500\ mm \end{cases} = 840\ mm$$

$$b_2 = min\begin{cases} b + h = 730\ mm \\ 3b = 990\ mm \\ b_1 = 1000\ mm \end{cases} = 730\ mm$$

$$A_{c1} = a_2\ b_2 = 6{,}132 \times 10^5\ mm^2$$

Checking the influence of the grout:

$$0{,}2\ \min(\ a; b) = 66mm > t = 20\ mm$$

Thus, the joint material coefficient β_j is 2/3 and the bearing strength is:

$$f_{jd} = \beta_j\ f_{cd}\ \sqrt{\frac{A_{c1}}{A_{c0}}} = 30{,}962\ MPa \leq 3\ f_{cd} = 67{,}8MPa$$

Width of the strip:

$$c = t\ \sqrt{\frac{f_{yk}}{3\ f_{jd}\ \gamma_{M0}}} = 31{,}8\ mm$$

Effective length:

$$l_{eff} = min\begin{cases} b_c + 2\ c = 332{,}6\ mm \\ b = 330\ mm \end{cases} = 303{,}6\ mm$$

Effective width:

$$b_{eff} = min\{c; (a - h_c)/2\} + t_f + c = 80{,}6mm$$

Effective area:

$$A_{eff} = b_{eff}\ l_{eff} = 2{,}447 \times 10^4\ mm^2$$

Lever arm of the compression force:

$$z_c = \frac{h_c}{2} - \frac{t_f}{2} = 111{,}5\ mm$$

Compressed part resistance:

$$F_{c,pl,Rd} = A_{eff}\ f_{jd} = 757{,}9\ KN$$

RESISTANCE OF THE COMPONENT COLUMN FLANGE AND WEB IN COMPRESSION

The component resistance depends on the plastic bending moment capacity of the column:

$$M_{c,Rd} = M_{pl,y,Rd} = \frac{W_{y,pl}\, f_{yk}}{\gamma_{M0}} = 247{,}5\ KN.m$$

Thus, the design compression resistance of the flange is:

$$F_{c,fc,Rd} = \frac{M_{c,Rd}}{\left(h_c - t_f\right)} = 1109{,}7\ KN$$

ASSEMBLY

For the calculation of the bending resistance, the load eccentricity needed:

$$e = \infty$$

This corresponds to the case of a bending without axial force.

The tension part resistance is:

$$F_{T,Rd} = 189{,}4\ KN$$

And its lever arm:

$$z_t = 170\ mm$$

The compression part resistance:

$$F_{C,Rd} = min\left(F_{c,pl,Rd}; F_{c,fc,Rd}\right) = 666{,}1\ KN$$

And the lever arm is:

$$z_c = 111{,}5\ mm$$

Thus, knowing that $z = z_t + z_c$, the joint resistance is ($e = \infty$):

$$M_{y,R} = min\begin{cases} \dfrac{F_{T,l,Rd} z}{z_{C,r}/e + 1} = 53{,}3\ KN.m \\ \dfrac{-F_{C,r,Rd} z}{z_{T,l}/e - 1} = 213{,}4\ KN.m \end{cases} = 53{,}3\ KN.m$$

COLUMN BASE UNDER WEAK AXIS BENDING

RESISTANCE OF COMPONENT BASE PLATE IN BENDING AND ANCHOR BOLTS IN TENSION

Effective lengths for the possible mechanism for the no-prying case (m_x=40,9mm):

$$l_{np,1} = 2\pi m = 257.3\ mm$$

$$l_{np,3} = \pi m + 4e = 468{,}6\ mm$$

$$l_{np,4} = 4m + 1{,}25e_x = 226{,}3\ mm$$

$$l_{np,6} = 2m + 0{,}625e_x + e = 198{,}1\ mm$$

Effective length of the T-stub:

$$l_{eff,1-2} = \min\left(l_{np,1}; l_{np,3}; l_{np,4}; l_{np,6}\right) = 198{,}1\ mm$$

Resistance of Mode 1-2 ($m_{pl,Rd}$=23,5KN.m)

$$F_{T,1-2,Rd} = \frac{2\ l_{eff\ ,1-2}\ m_{pl,Rd}}{m} = 227{,}4\ KN$$

Tension resistance of the bolts:

$$F_{t,Rd} = \frac{0{,}9\ f_{ub}\ A_s}{\gamma_{M2}} = 164{,}3\ KN$$

Resistance of failure Mode 3:

$$F_{T,3,Rd} = \sum B_{t,Rd} = 2BF_{t,Rd} = 328{,}7\ KN$$

Resistance of the tension T-stub:

$$F_{T,Rd} = min\left(F_{T,1-2,Rd}; F_{T,3,Rd}\right) = 227{,}4\ KN$$

And its lever arm:

$$z_t = \frac{p}{2} = 80\ mm$$

RESISTANCE OF COMPONENT BASE PLATE IN BENDING AND CONCRETE IN COMPRESSION

The bearing strength calculation is presented above (f_{jd}=30,962MPa), as well as the width of the strip (c=31,8 mm).

Effective area of the compressed T-stub:

$$A_{eff} = \frac{F_{T,Rd} - N_{Ed}}{f_{jd}} = 7{,}345 \times 10^3 mm^2$$

The effective width is:

$$b_{eff} = 2 \times \left(t_f + c + min\left\{c; \frac{a - h_c}{2}\right\}\right) = 161{,}2\ mm$$

And the effective length:

$$l_{eff} = \begin{cases} \frac{A_{eff}}{b_{eff}} = 45{,}6\ mm \\ b_c/_2 + c = 151{,}8mm \\ b/_2 = 165\ mm \end{cases} = 45{,}6mm$$

The component resistance is then:

$$F_{C,Rd} = b_{eff}\ l_{eff}\ f_{jd} = 227{,}4\ KN$$

And the lever arm of the compression force:

$$z_c = \ min\left(\frac{b_c}{2} + c; \frac{b}{2}\right) - \frac{l_{eff}}{2} = 129{,}0\ mm$$

ASSEMBLY

Since the eccentricity is $e = \infty$, which corresponds to the case of bending moment without axial force (N_{Ed}=0), the joint resistance is calculated by:

$$M_{z,R} = min\begin{cases} \frac{F_{T,l,Rd}z}{z_{C,r}/_e + 1} = 47{,}5KN.m \\ \frac{-F_{C,r,Rd}z}{z_{T,l}/_e - 1} = 47{,}5KN.m \end{cases} = 47{,}5\ KN.m$$

MZ-MY INTERACTION CURVE

The interaction curve is defined by the following function (see Figure 3):

$$\left(\frac{M_z}{M_{z,R}}\right)^2 + \left(\frac{M_y}{M_{y,R}}\right)^2 = 1 \Leftrightarrow\ M_z = \sqrt{\left(1 - \left(\frac{M_y}{M_{y,R}}\right)^2\right) {M_{z,R}}^2}$$

Where:

$$M_{z,R} = 47{,}5\ KN.m$$

$$M_{y,R} = 53{,}3\ KN.m$$

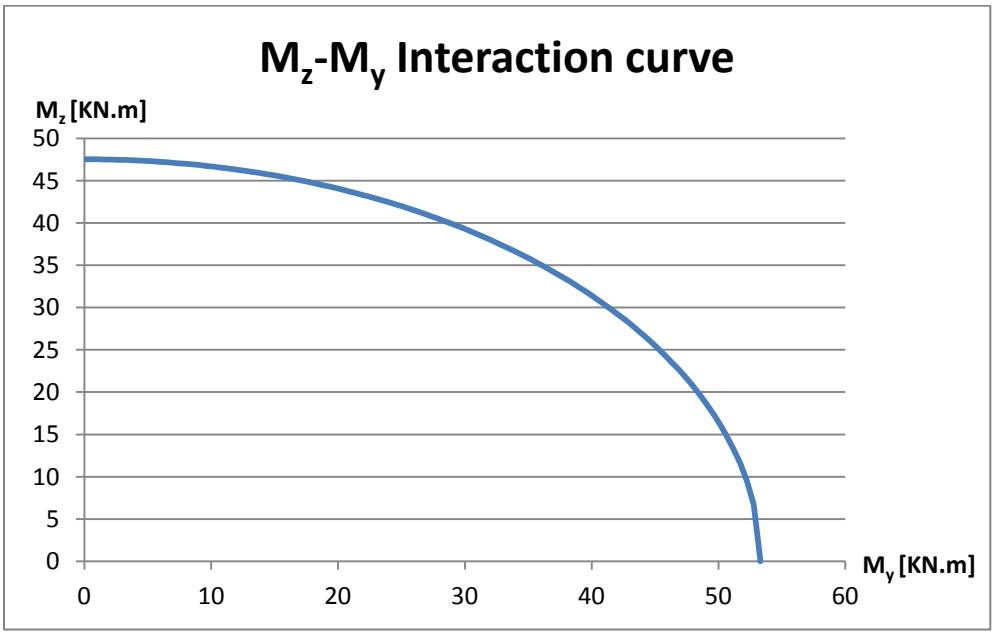


Figure 3 - M_z-M_y Interaction curve